Anisotropic physical properties of rocks
Single to Polycrystals
2010

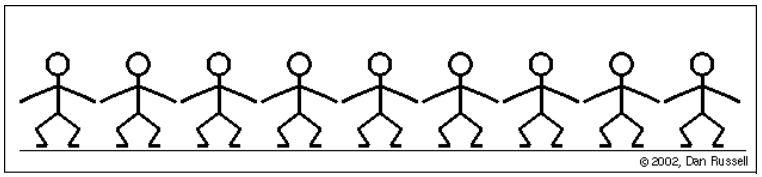

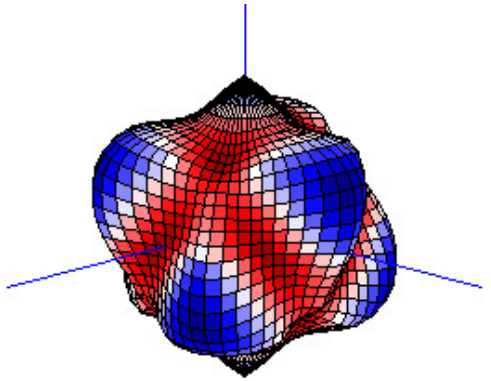

David Mainprice
UMR Géosciences, Université Montpellier 2
France

Number of students falling a sleep

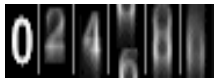

Plan of this Talk

Introduction

2nd Rank Tensors - Thermal Conductivity, Thermal Diffusivity and Thermal expansion

4th Rank Tensors - Elasticity, Seismic Velocity

Introduction

Why are we interested in Single Crystals ?

- To understand the anisotropic physical properties of poly-crystalline rocks caused by **crystal preferred orientation** (**CPO**) it is important to know the about the simplest case, the single crystal. CPO not **lattice** preferred orientation LPO !
- The single orientation (single crystal), has a perfectly defined ODF (orientation distribution function), PFs (pole figure) or IPFs (inverse pole figure).
- To understand the how crystal symmetry, sample symmetry, CPO and single crystal properties combined to produce anisotropic rock properties …

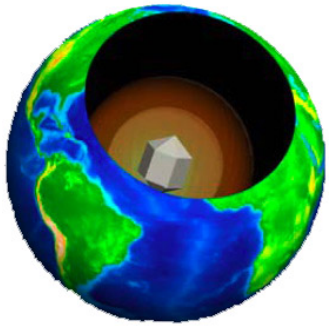

Physical properties of crystals

- Thermal conductivity and diffusivity (2^{th} rank tensor) → can be calculated from CPO
- Thermal expansion (2^{th} rank tensor) → can be calculated from CPO
- Electrical conductivity, electrical polarization and dielectric properties) → can be calculated from CPO, BUT may not be relevant if conductivity controlled by high conductivity phases in the grain boundaries (e.g. water, graphite or carbon)
- Piezoelectricity (3^{rd} rank tensor) → can be calculated from CPO, if we can determine the CPO of the Left- and Right-handed crystals…

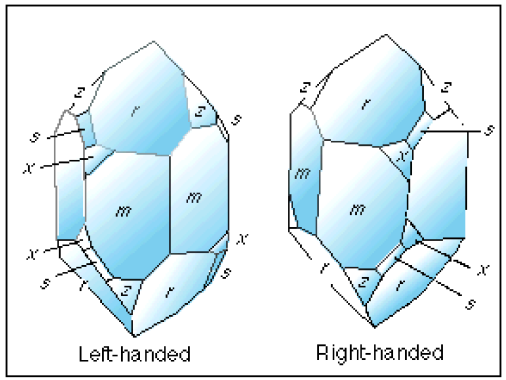

- Elasticity (4^{th} rank tensor) → seismic (elastic) properties, can be calculated from CPO

Anisotropic Properties

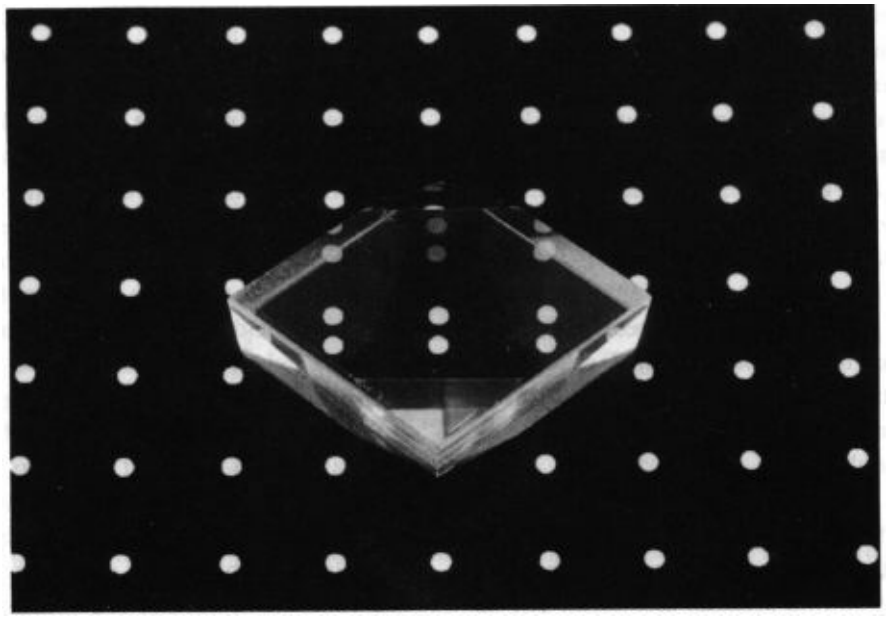

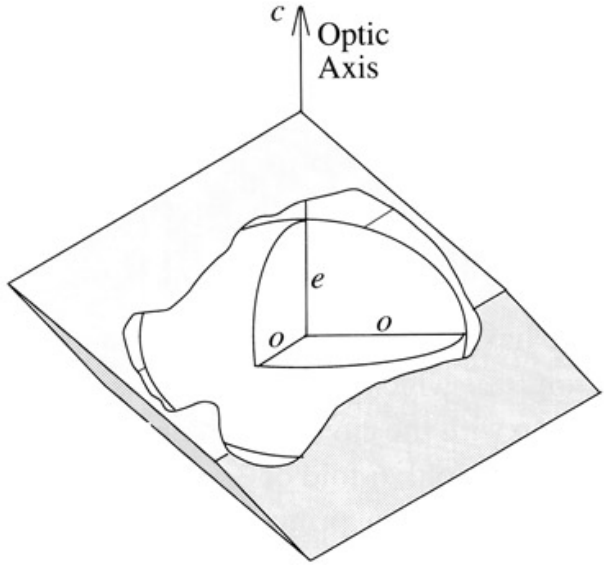

Calcite optical properties : 2nd Rank Tensor

Tensor rank of physical properties

Physical Property (rank)	**Driving Force (rank)**	**Response (rank)**
Density (0)	Mass (0)	Volume (0)
Pyroelectricity (1)	Temperature (0)	Electric Field (1)
Electric conductivity (2)	Electric Field (1)	Electric Current Density (1)
Electric Permitivity (2)	Electric Field (1)	Dielectric Displacement (1)
Dielectric Susceptibility (2)	Electric Field (1)	Polarization (1)
Chemical Diffusivity (2)	Potential Gradient –ve (1)	Chemical Flux (1)
Thermal Conductivity (2)	Temperature Gradient -ve (1)	Heat Flux (1)
Thermal Expansion (2)	Temperature (0)	Strain (2)
Magnetic Susceptibility (2)	Magnetic Field (1)	Magnetisation Intensity (1)
Magnetic Permeability (2)	Magnetic Field (1)	Magnetic Induction (1)
Piezolectricity (3)	Electric Field (1)	Strain (2)
Elastic Compliance (4)	Stress (2)	Strain (2)
Elastic Stiffness (4)	Strain (2)	Stress (2)

Transformation of axes

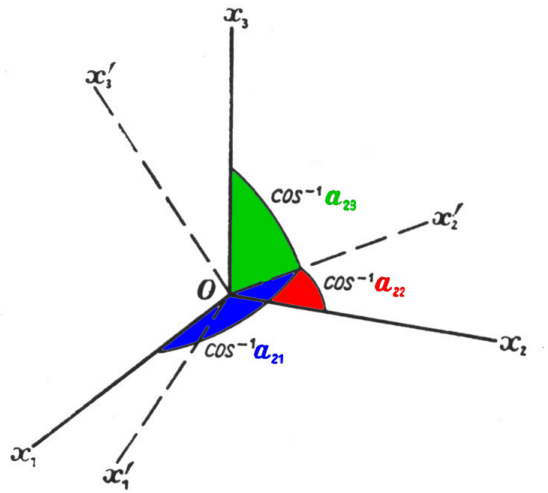

Transformation of axes.

		"old" axes	
	x1	x2	x3
x'1	a11	a12	a13
"new" x'2	a21	a22	a23
x'3	a31	a32	a33

a_{ij} is a 3 by 3 transformation matrix relating two orthogonal reference axes (x and x').

A major concept in defining the properties of tensors.

Cartesian Reference Frame for Tensors I

- Measurement of anisotropic physical properties are reported in the literature as components of tensors, typically as tabulated values. The reference frame most commonly used is a **right-handed Cartesian** (also called orthonormal) system.
- For cubic, tetragonal and orthorhombic the obvious choice is to use the orthogonal lattice basis vectors **a**[100], **b**[010] and **c**[001] of the crystal axes. However, for most general case of triclinic crystal symmetry where **a**, **b**, and **c** are not orthogonal, there are many possible choices and no general convention.
- The choice of a specific reference frame is often guided by presence of cleavage or well developed crystal faces that allow for an easy determination of the crystal orientation.

Cartesian Reference Frame for Tensors II

- Here are 3 common choices, for the tensor Cartesian reference frame (X1,X2,X3) ;
- a) X3 = **c**[001], X2= **b*** ⊥(010) and hence for a right-handed system X1 = X2 **x** X3
- b) X3 = **c**[001] , X1= **a*** ⊥(100) and X2 = X3 **x** X1
- c) X3 = **c***⊥ (001) , X1= **a**[100] and X2=X3 **x** X1

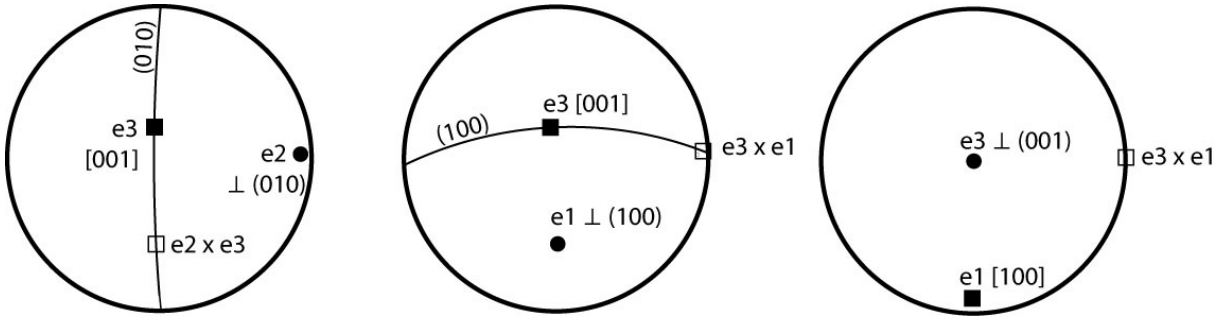

Reference Frames a), b) and c) for triclinic plagioclase Labradorite An66 (**a**=0.817 nm **b**=1.287 nm **c**=1.420 nm α=93.46° β=116.09° γ=90.51°)

Cubic crystal

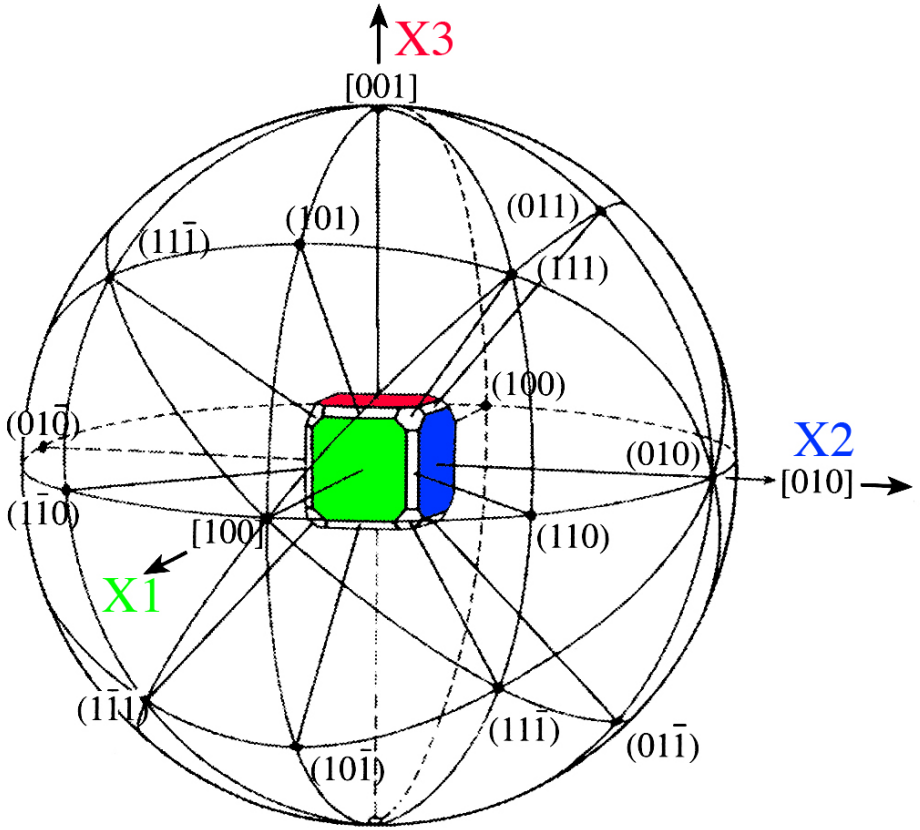

Hexagonal and trigonal symmetries

6/mmm

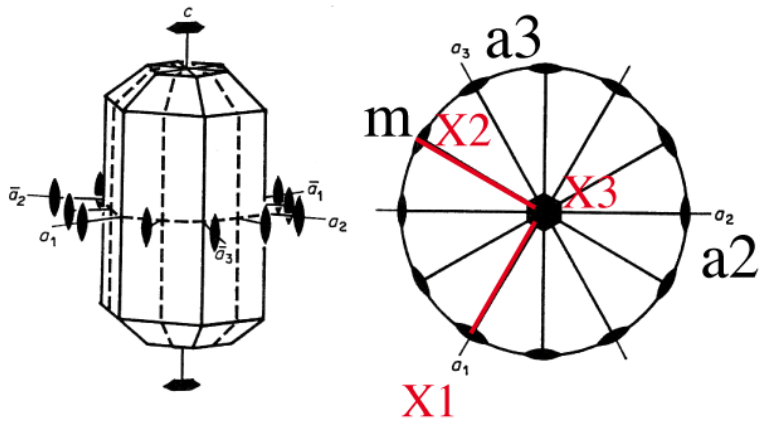

$\bar{3}$m

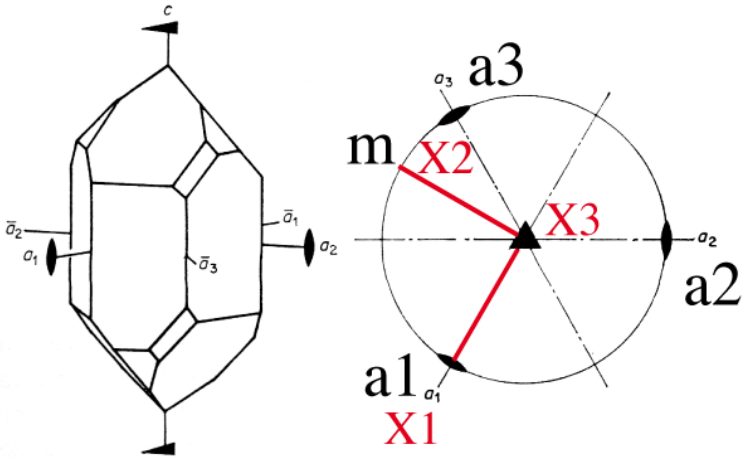

X2 = m = c x a1

Tensor reference frames for all Laüe classes

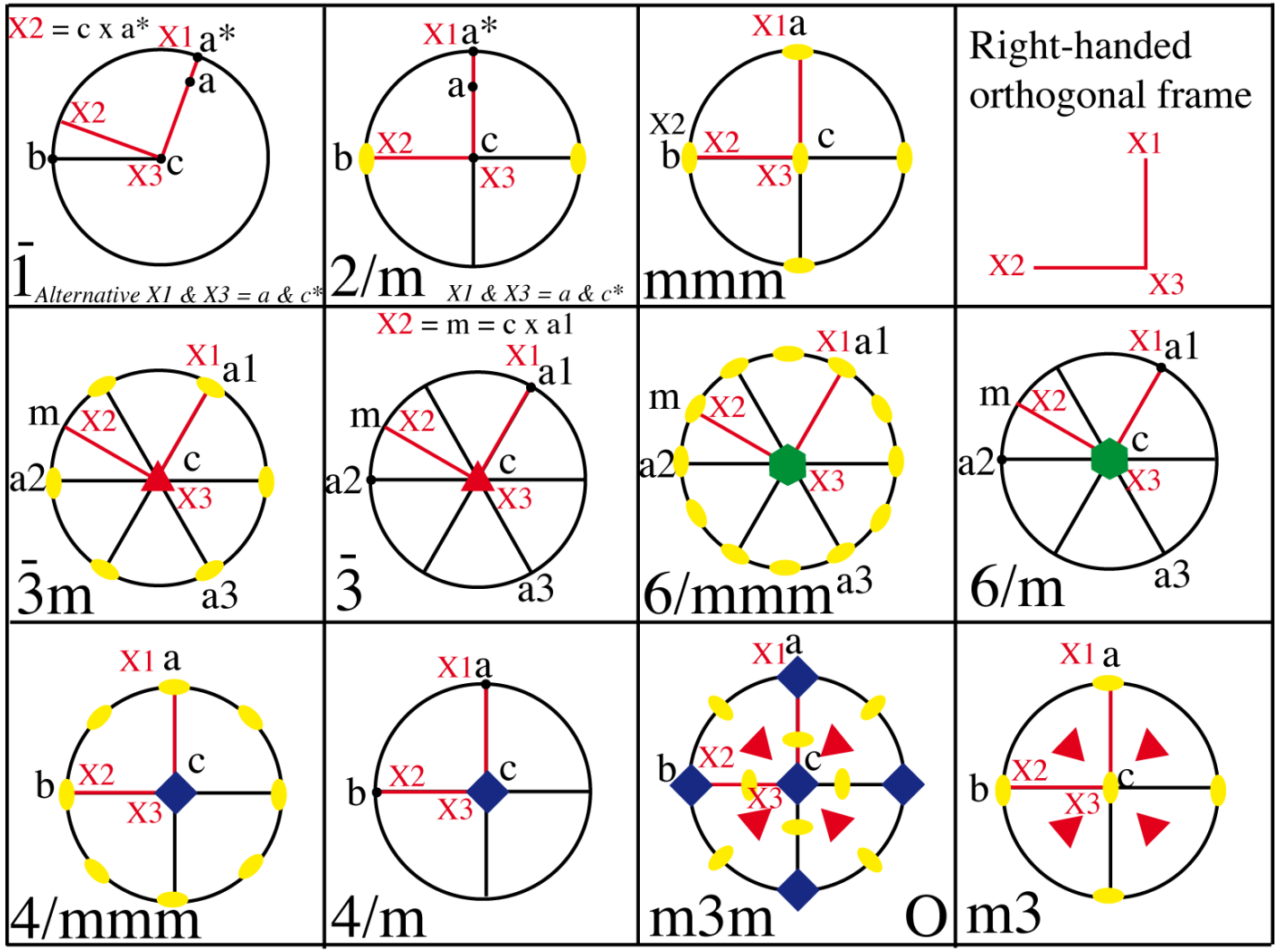

a =[100] a*= ⊥(100) etc

Cartesian Reference Frame for Tensors III

- Examples of reference frames for elastic constants, **but check for yourself !**

a,b/b*,c* (monoclinic alkali feldspar)

a*,b/b*,c (monoclinic diopside,augite,hornblende,muscovite, antigorite)

a,(c* x a),c* (triclinic plagioclase, antigorite)

Tensor and Euler frames

- You should also be aware that the tensor Cartesian reference frame (X1, X2, X3) used for a tensor may not be the same as the reference frame with respect to the crystal axes used for the Euler angles (Xc, Yc, Zc) to define your orientation data.
- For example the commonly used BearTex Texture package uses Yc = b* ⊥(010), Zc = c[001] and Xc= Yc x Zc and the EBSD software from Oxford HKL uses Xc = a* ⊥ (100), Yc= Zc x X, Zc = c[001], and the TSL EBSD package uses different axes for each crystal symmetry !
- In general a rotation (or transformation) matrix (Rij) will be needed to bring the tensor reference frame into the correct orientation for a specific Euler angle frame. For example g'(i,j)=g(k,i)*R(k,j) where g(k,i) =g(ϕ1φ ϕ 2) is Euler angle matrix, g'(i,j) is orientation matrix of the tensor and R(k,j) the rotation matrix.

Rules for selecting a crystallophysical coordinate sytem

Syngony	Orientation with respect to crystallographic axes	Orientation with respect to symmetry elements of crystal
Triclinic	$X_3 \parallel c$, or $X_2 \parallel b$, or $X_1 \parallel a$	
Monoclinic	$X_2 \parallel b$ and $X_1 \parallel a$ (or $X_3 \parallel c$) Sometimes $X_3 \parallel b$ and $X_1 \parallel a$ (or $X_2 \parallel c$)	$X_2 \parallel$ to axis 2 or $\perp$ to plane m. Sometimes $X_3 \parallel$ to axis 2 or $\perp$ to plane m
Orthorhombic	$X_3 \parallel c$, $X_2 \parallel b$, $X_1 \parallel a$	$X_3 \parallel$ to axis 2; X_1, $X_2 \parallel$ to other axes 2 or $\perp$ to planes m
Tetragonal	$X_3 \parallel c$, $X_2 \parallel b$, $X_1 \parallel a$	$X_3 \parallel$ to axis 4 (or $\bar{4}$); X_1, $X_2 \parallel$ to axes 2 or $\perp$ to planes m (if they exist); for class $\bar{4}2m$ usually X_1, $X_2 \parallel$ to axes 2
Trigonal and hexagonal	$X_3 \parallel c$, $X_1 \parallel a$. For classes $3m$ and $\bar{6}m2$ sometimes $X_2 \parallel b$	$X_3 \parallel$ to axis 3, $\bar{3}$, 6 or $\bar{6}$; $X_1 \parallel$ to axis 2 (if they exist, except class $\bar{6}m2$); for classes $3m$ and $\bar{6}m2$ usually $X_1 \perp$ to plane m, but sometimes $X_2 \perp m$
Cubic	$X_3 \parallel c$, $X_2 \parallel b$, $X_1 \parallel a$	X_1, X_2, $X_3 \parallel$ to three mutually perpendicular axes 4 (or $\bar{4}$), and if they do not exist, then to similar axes 2

Euler reference frames for all Laüe classes

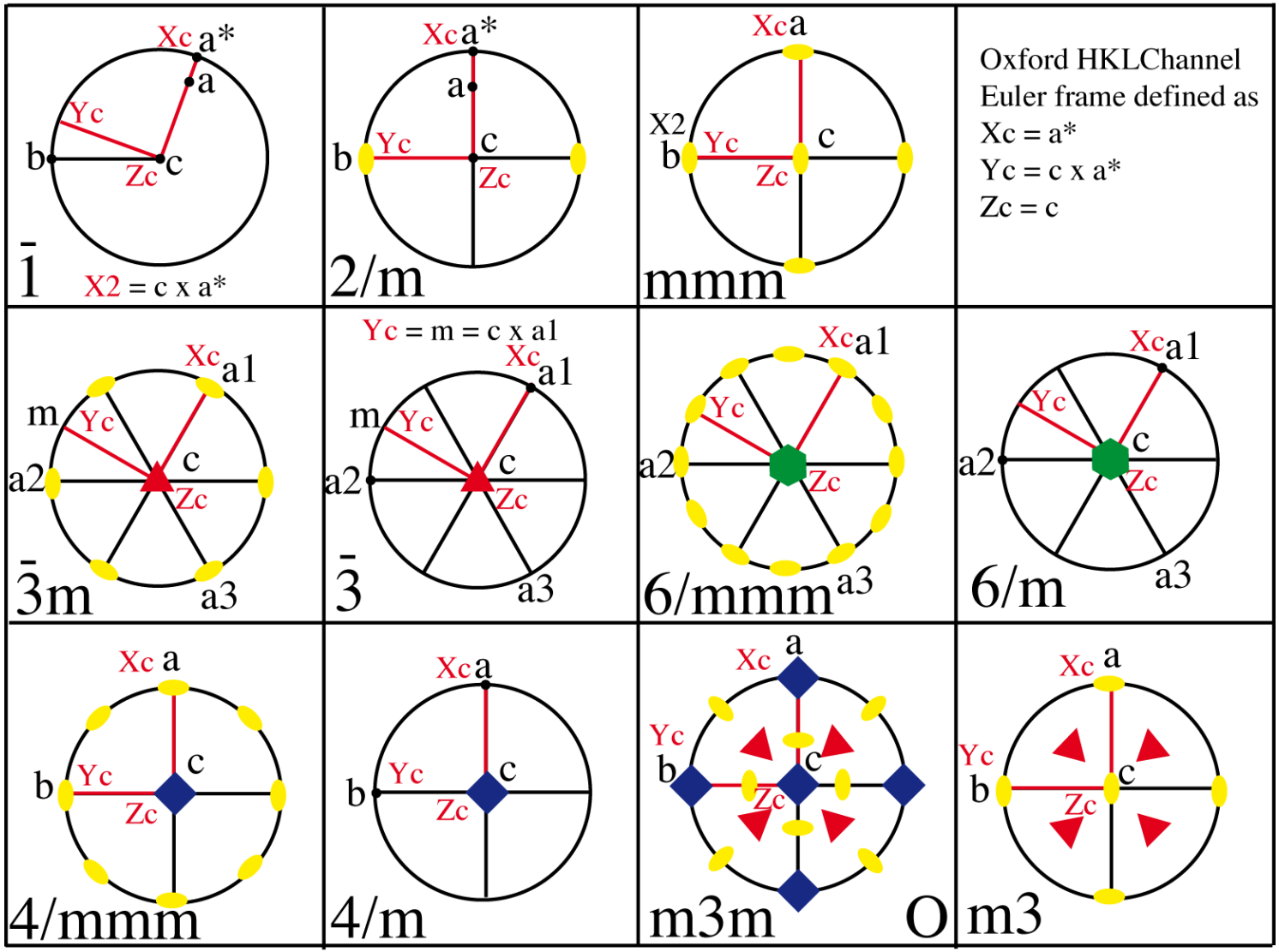

Transformation laws for tensors

	Rank of		
Name	Tensor	New in terms of old	Old in terms of new
Scalar	0	X'=X	X'=X
Vector	1	P'i=AijPj	Pi=AjiP'j
2nd Rank	2	T'ij=AikAjlTkl	Tij=AkiAljT'kl
3rd Rank	3	T'ijk=AilAjmAknTlmn	Tijk=AliAmjAnkT'lmn
4th Rank	4	T'ijkl= AimAjnAkoAlpTmnop	Tijkl= AimAnjAokAplT'mnop

Difference between a transformation matrix (A_{ij}) and a 2nd rank tensor (T_{ij})

Aij is an 3 by 3 matrix relating two (right-handed) reference frames [orthogonal matrix $A^t.A=A.A^t = I$, $A^t=A^{-1}$ and Det(A)=+1 where the rows and columns are orthogonal (orthonormal) unit vectors.] (e.g. rotation or orientation matrix) N.B. when Aij is relating right-handed to left-handed reference frames Det(A)=-1.

Tij is a physical quantity (e.g. 2nd rank tensor) that for a given set of reference axes is represented by 9 numbers (a 3 by 3 table).

Zero and First Rank Tensors

- **Zero Rank Tensor (1 component)**

Scalars – example density (kg/m3)

- **First Rank Tensor (3 components)**

Vectors – example electric field E = [E1 E2 E3] = E_i

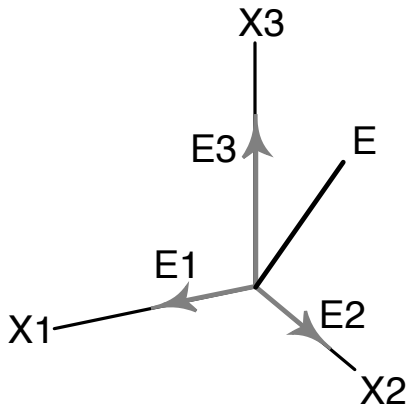

2^{nd} Rank Tensors

2nd Rank Tensors - important for geophysics

- Typically relates 2 vectors – for example thermal conductivity : applied vector (negative) temperature gradient and resulting vector heat flow density, exception thermal expansion relates temperature (0) and strain (2).

$$T_{ij} = \begin{vmatrix} T_{11} & T_{12} & T_{13} \\ T_{21} & T_{22} & T_{23} \\ T_{31} & T_{32} & T_{33} \end{vmatrix}$$

9 components

- The generic 2nd rank tensor **T** is the relation between an applied vector **p** and resultant vector **q**. We can write relation between **p** and **q** as a tensor equation

$$\mathbf{p} = \mathbf{T}\,\mathbf{q} \quad \text{or} \quad p_i = T_{ij}\, q_j \;\; (i=1,2,3 \; ; \; j=1,2,3)$$

- In general the vectors **p** and **q** are not parallel.

Thermal Expansion

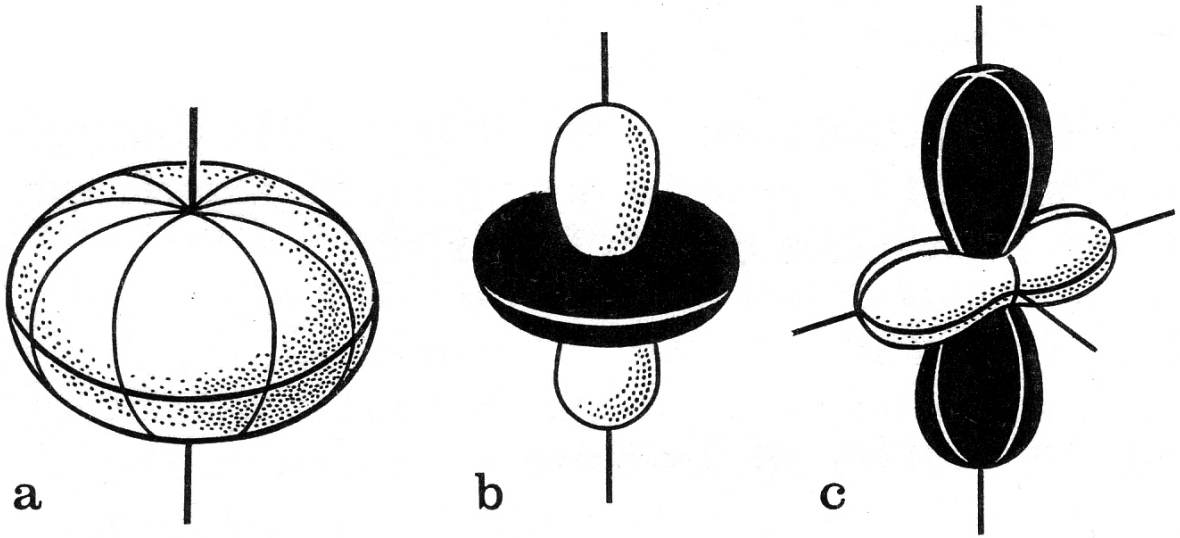

Examples of indicatrice surfaces of the tensor of thermal expansion α_{ij} at various relationships among the signs of the main components of the tensor α_1, α_2, and α_3: **(a)** uniaxial crystals with $\alpha_3 > 0$ and $\alpha_1 > 0$, surface symmetry ∞/mmm; **(b)** uniaxial crystals with $\alpha_3 > 0$ and $\alpha_1 < 0$, surface symmetry ∞/mmm; **(c)** biaxial crystals with $\alpha_1 \neq \alpha_2 \neq \alpha_3$; α_1, $\alpha_2 > 0$, while $\alpha_3 < 0$; surface symmetry mmm. The regions corresponding to $\alpha > 0$ are white, and those corresponding to $\alpha < 0$ are black

Single Crystal Thermal Expansion

Quartz

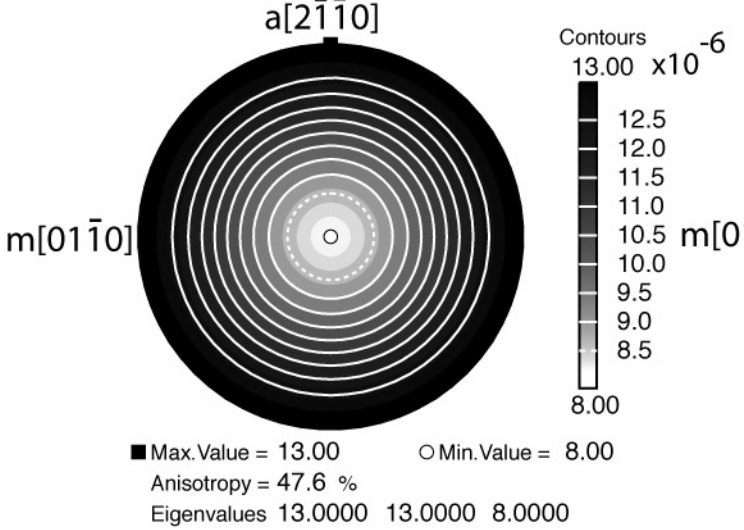

Calcite

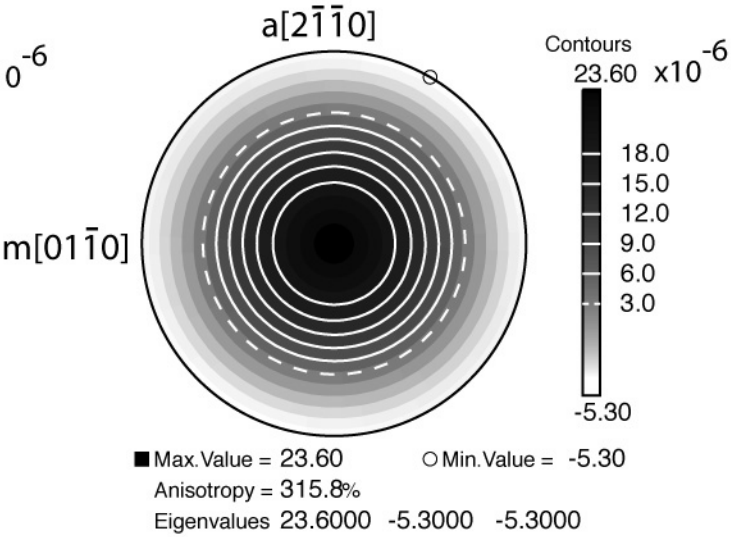

Plagioclase An76

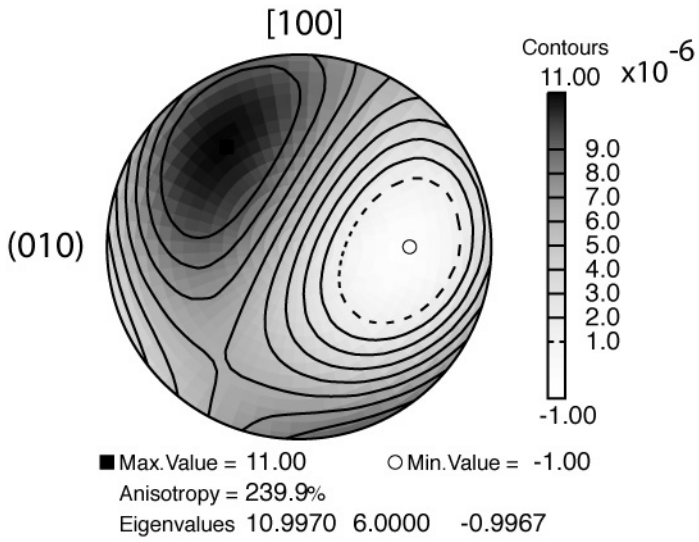

Olivine

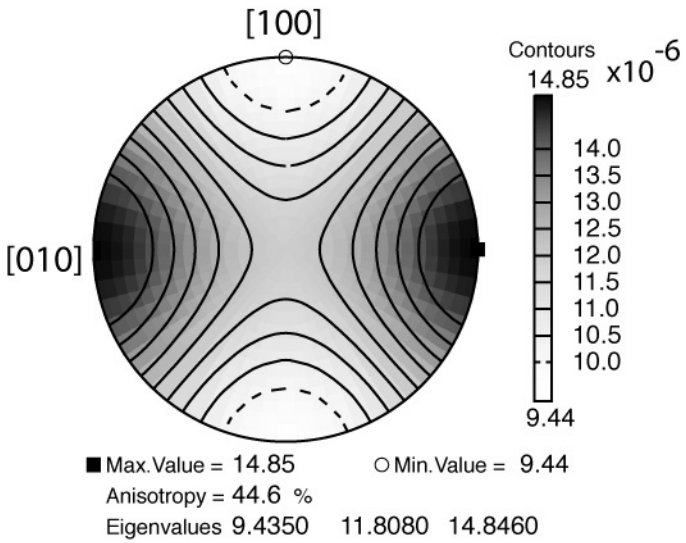

Thermal diffusivity of Olivine

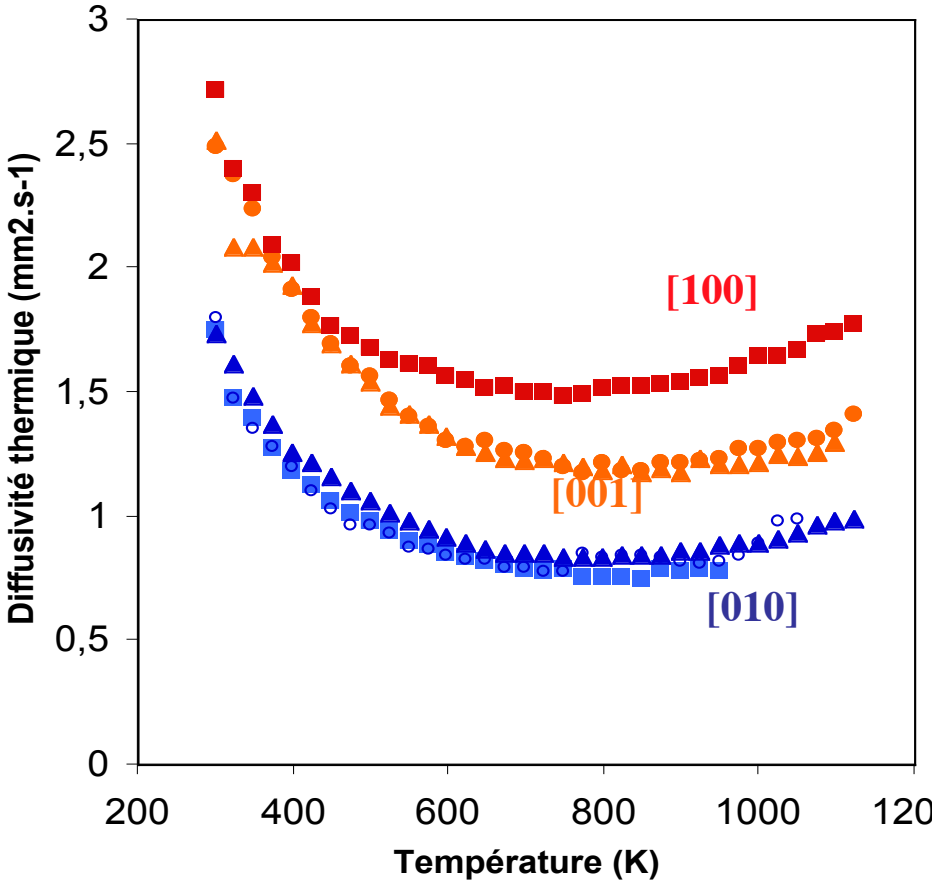

2^{nd} order Tensor

$$\begin{vmatrix} 2.73 & 0 & 0 \\ 0 & 1.70 & 0 \\ 0 & 0 & 2.49 \end{vmatrix}$$

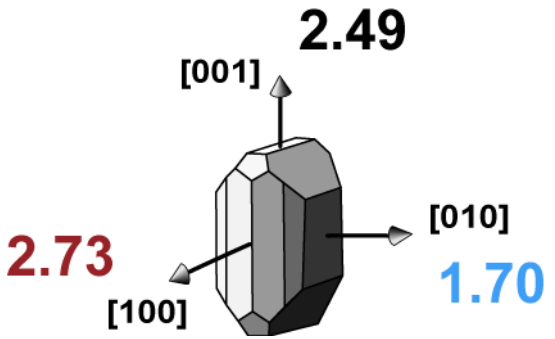

Gibert et al, *GRL*, 2003

Anisotropie des propriétés thermiques dans le manteau supérieur

Modélisation pétrophysique et mesure en laboratoire de l'anisotropie de diffusivité thermique des roches mantelliques

Thèse B. Gibert (2001-2003)

Prix Hauy-Lacroix 2004 SFMC
coll. U. Seipold & F. Schilling, GFZ Postsdam

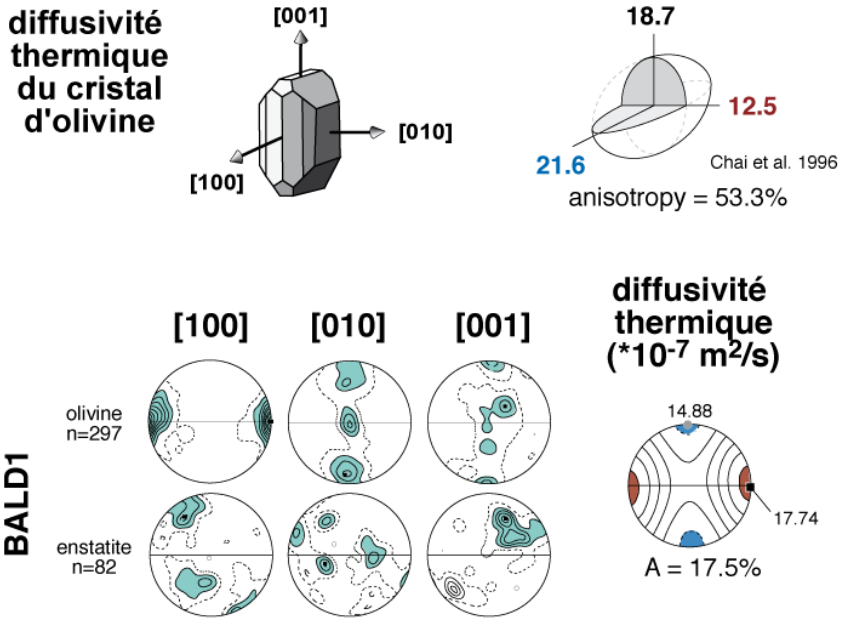

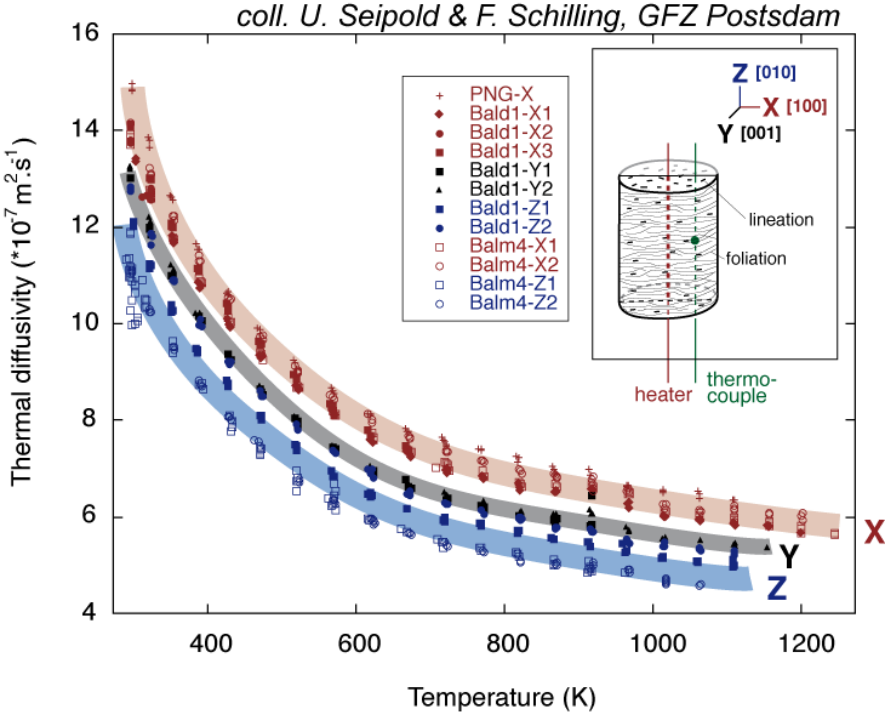

Tommasi, Gibert, Seipold & Mainprice, Nature 2001
Gibert, Seipold, Tommasi & Mainprice, JGR 2003
Gibert, Schilling, Tommasi & Mainprice, GRL 2003
Gibert, Schilling, Gratz &Tommasi, PEPI 2005

Radius-normal property and melting wax experiment

- Consider a red hot arrow touching the second order prism plane of a single crystal of quartz and creating a point heat source. A (negative) thermal gradient will result in heat flow away from the hot heat source (arrow tip) to the colder regions of the crystal. As the thermal resistivity (reciprocal of thermal conductivity) varies with direction the heat flow will not be equal in all radial directions, i.e. heat flow is anisotropic.

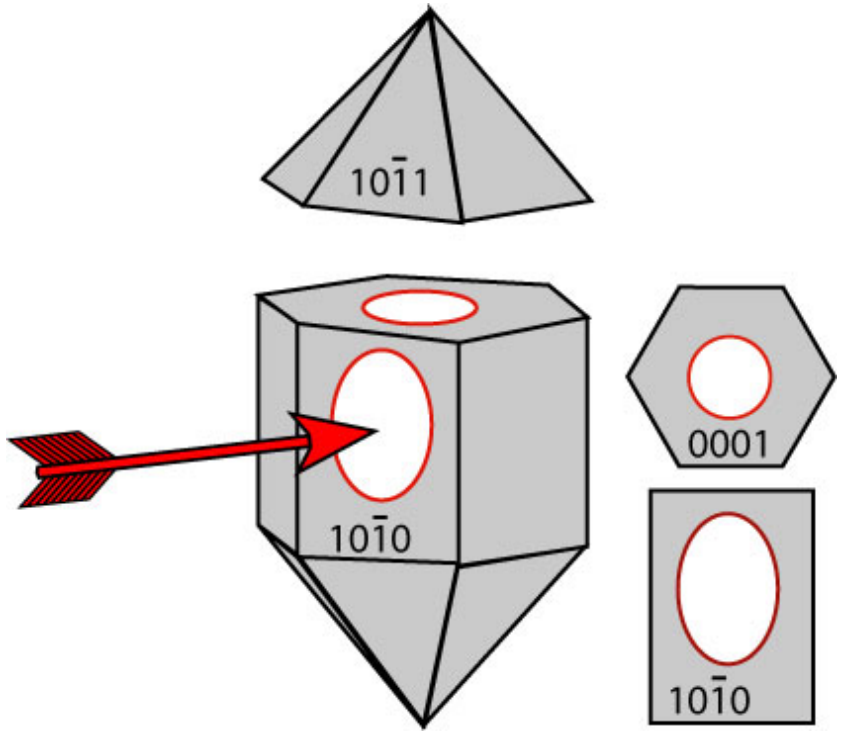

Radius-normal property of the representation quadric

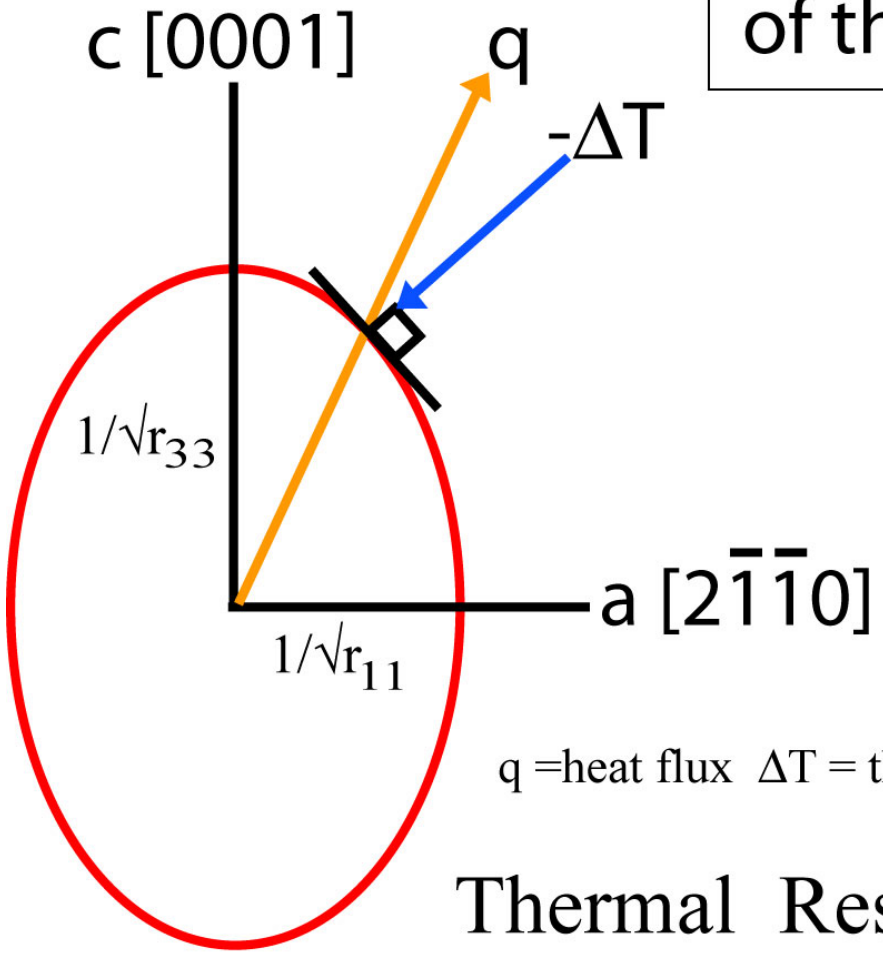

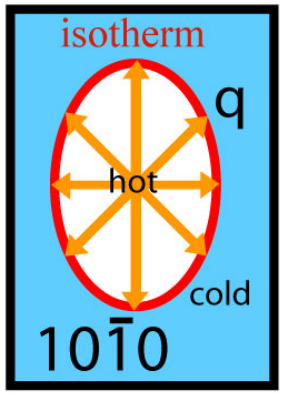

Radial heat flux (q) (controlled by crystal properties not boundary conditions)

q =heat flux ΔT = thermal gradient

Thermal Resistivity (r)

$\Delta T_i = - r_{ij} q_j$ where $r_{11} = 1/k_{11}$ etc

Thermal Conductivity (k)

$q_i = - k_{ij} \Delta T_i$

The stimulus vector and response vectors for 2nd rank tensors

In general in anisotropic crystals the stimulus vector (e.g. ΔT) is not parallel to the response vector (e.g. q)

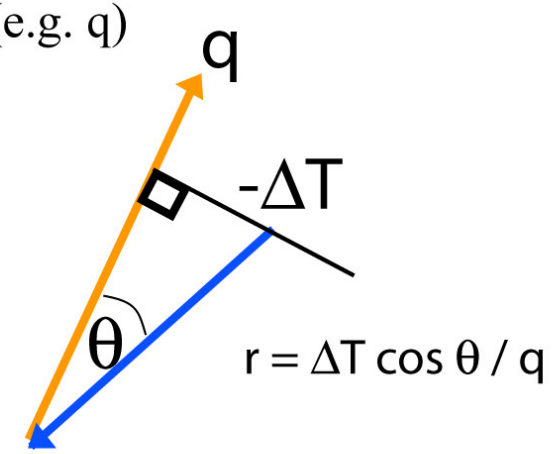

In certain directions (e.g. principal axes) the stimulus vectors and the response vectors may be parallel in anisotropic crystals. It is always the case for isotropic crystals (e.g. 2nd rank tensors of cubic crystals)

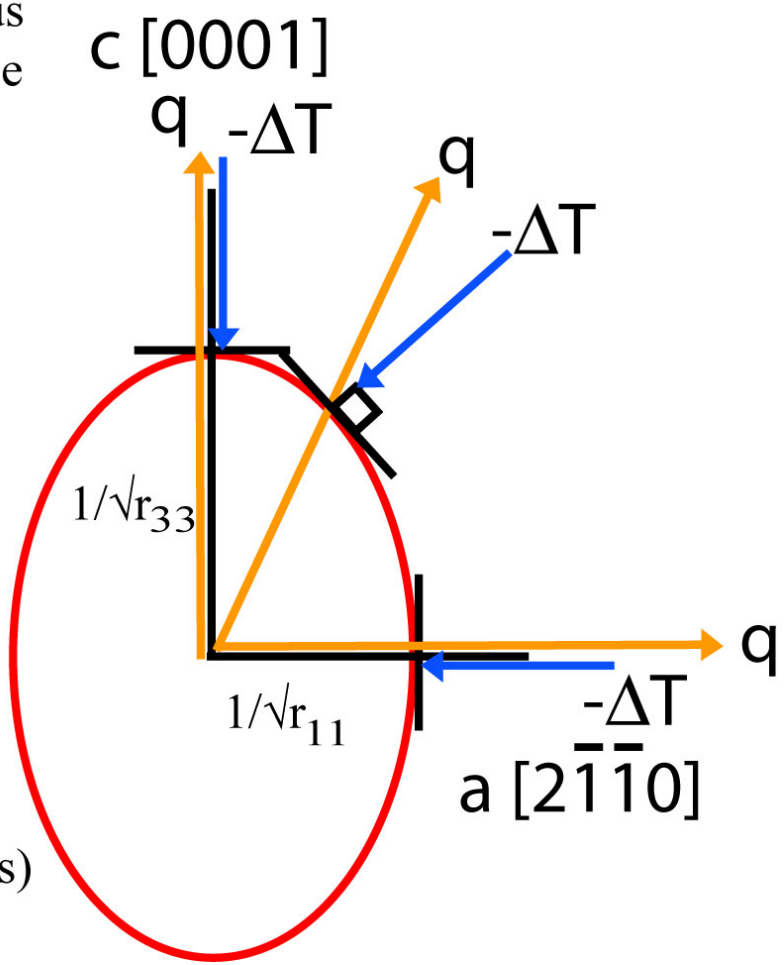

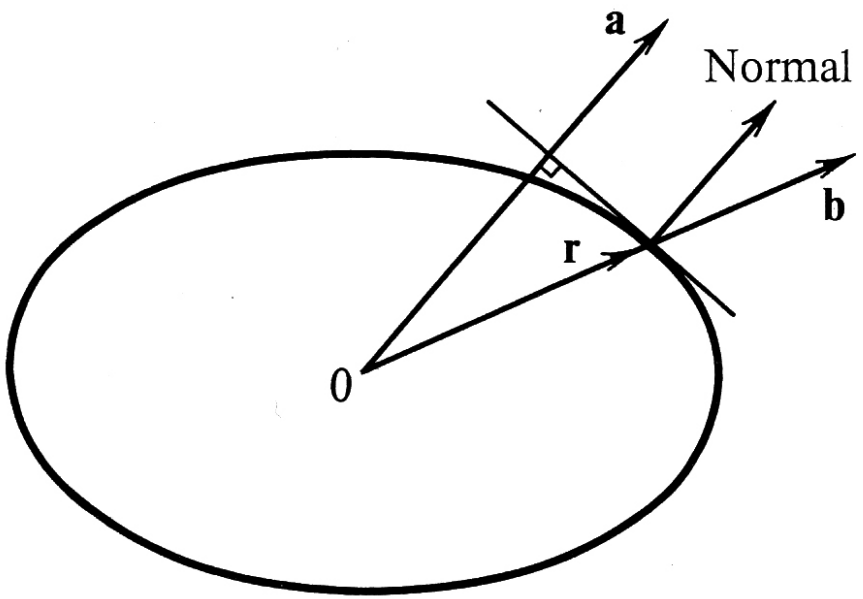

Diagram explaining the properties of a radius vector and normal of the characteristic surface of a symmetric second-rank tensor

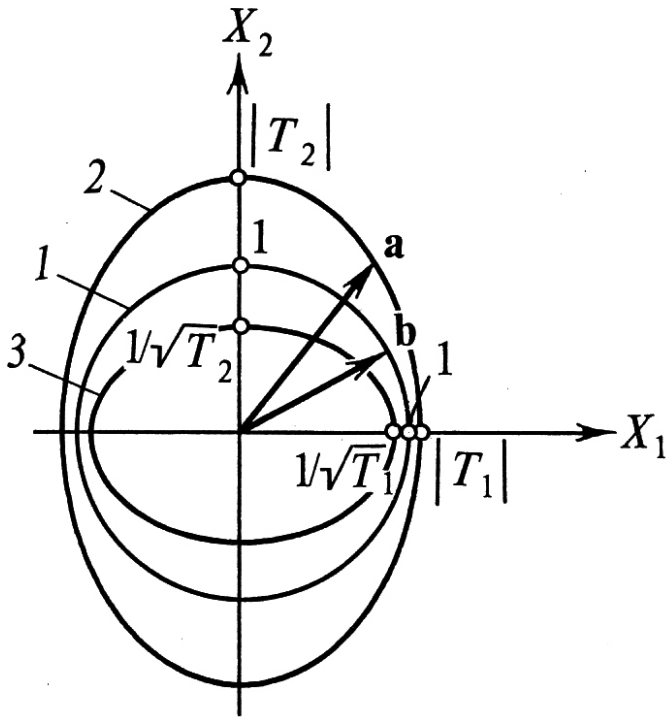

Central sections of a sphere (*1*) described by a unit vector $\boldsymbol{b}$, the ellipsoid of the values of a symmetric tensor (*2*) given by the equation $a_i = T_{ij} b_j$ and of the characteristic surface of this tensor (*3*)

The effect of symmetry on symmetric 2nd rank tensors

Cubic
(Sphere)

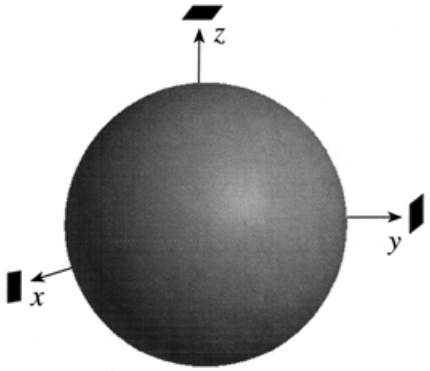

Tetragonal, Hexagonal, Trigonal
(Uniaxial Ellipsoid)

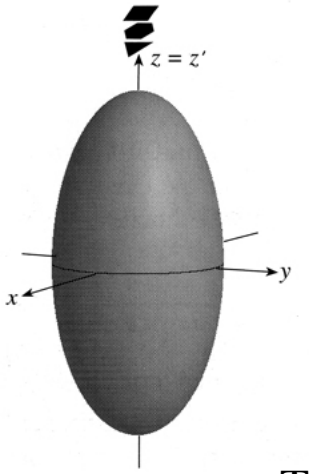

Orthorhombic | Monoclinic | Triclinic

<---------- Triaxial Ellipsoids ---------->

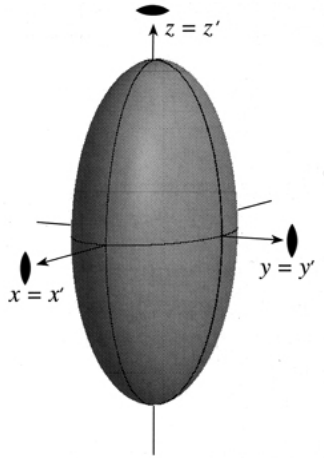

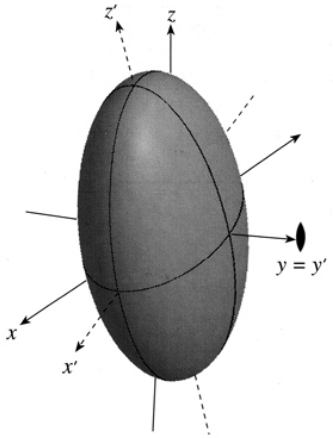

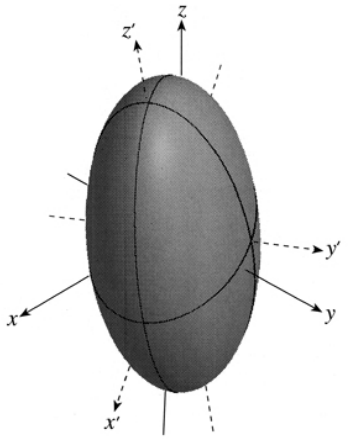

Effect of symmetry on Physical Properties : Neumann's Principle

F.E. Neumann's principle (1885) states that "symmetry elements of any physical property of a crystal must include ALL the symmetry elements of the point group of the crystal". This implies that that a given physical property may possess a **higher** symmetry than that possessed by the crystal and it cannot be of a **lower** symmetry than that of the crystal. Some physical properties are inherently centrosymmetric (all symmetric second order tensors and elasticity) which will add a center of symmetry in many minerals (e.g. quartz) and result in a **higher** symmetry than the possessed by the crystal.

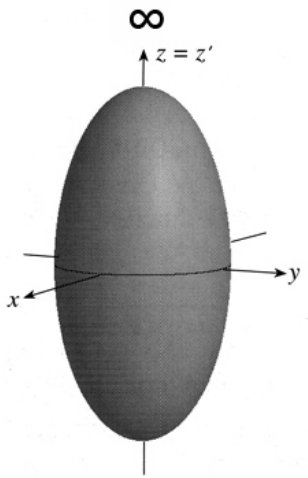

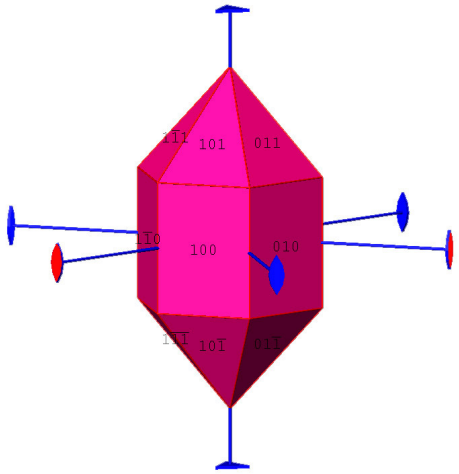

Table 4.2 Number of independent components of physical properties represented by second rank (order) tensors

Crystal system	Orientation of principal axes with respect to the crystal axes	Form of tensor	Number of independent components
Cubic	Any. Representation quadric is a sphere	$\begin{bmatrix} S & 0 & 0 \\ 0 & S & 0 \\ 0 & 0 & S \end{bmatrix}$	1
Tetragonal Hexagonal Trigonal*	x_3 parallel to 4, 6, 3 or $\bar{3}$	$\begin{bmatrix} S_1 & 0 & 0 \\ 0 & S_1 & 0 \\ 0 & 0 & S_3 \end{bmatrix}$	2
Orthorhombic	x_1, x_2, x_3 parallel to the diads along x-, y-, z-axes	$\begin{bmatrix} S_1 & 0 & 0 \\ 0 & S_2 & 0 \\ 0 & 0 & S_3 \end{bmatrix}$	3
Monoclinic	x_2 parallel to the diad along y-axis	$\begin{bmatrix} S_{11} & 0 & S_{13} \\ 0 & S_{22} & 0 \\ S_{13} & 0 & S_{33} \end{bmatrix}$	4
Triclinic	Not fixed	$\begin{bmatrix} S_{11} & S_{12} & S_{13} \\ S_{12} & S_{22} & S_{23} \\ S_{13} & S_{23} & S_{33} \end{bmatrix}$	6

*A hexagonal cell is used.

The magnitude of a 2nd rank property in a given direction

- Let a given direction (**x**) be specified by the direction cosines (x_1,x_2,x_3). Referred to general axes

  $T(\mathbf{x}) = T_{ij}\, x_i x_j$

- From the magnitude T(**x**) in a given direction one can calculate the radius vector r(**x**) of the representation quadric. When T(**x**) is negative, which occurs for example for thermal expansion in calcite, radius vector $1/\sqrt{T(\mathbf{x})}$, is an imaginary value.

  $R(\mathbf{x}) = 1/\sqrt{T(\mathbf{x})}$

- Although the quadric representation is a hyperboloid when one or more principal axes are negative, the representation is quite straight forward as a contoured equal area projection (pole figure).

Non-polar and Polar properties

Non-polar case:

centro-symmetric
symmetry
property the same value
in +ve and -ve direction

Example elasticity

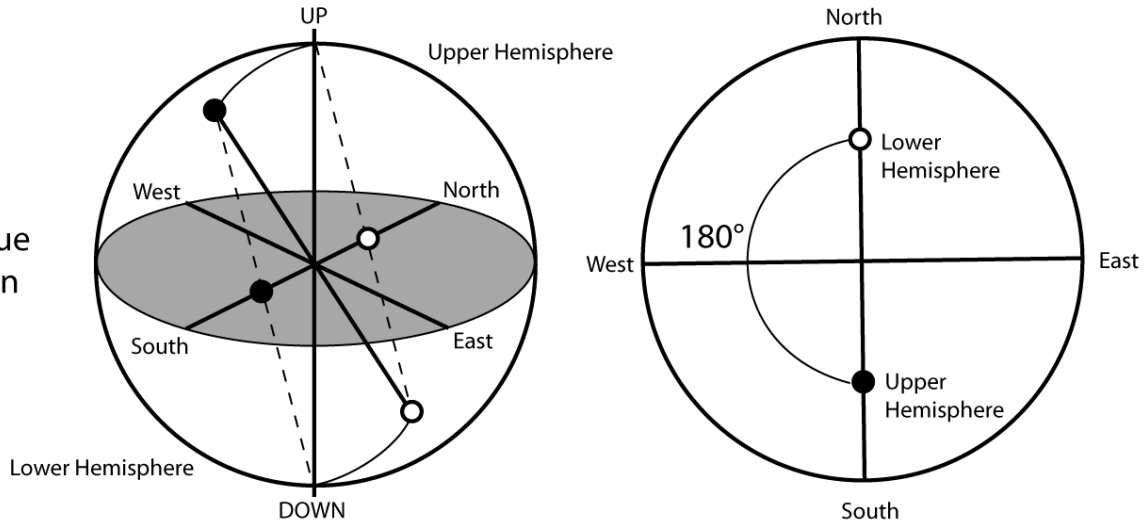

Polar case:

no centre of symmetry
property has different values
in +ve and -ve direction

Example piezoelectricity
in quartz along a-axes

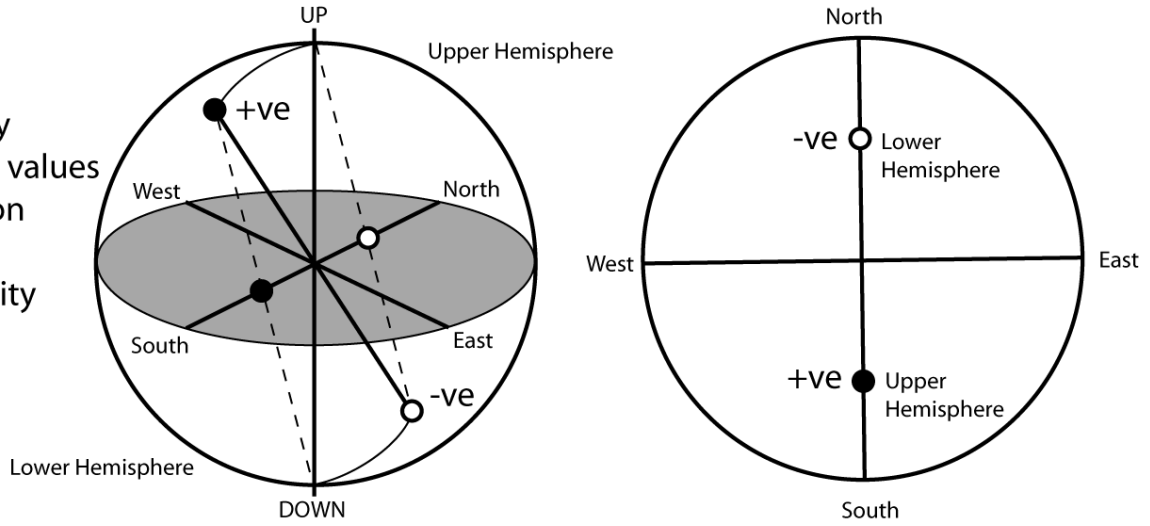

Piezoelectricity – 3rd Order Tensor

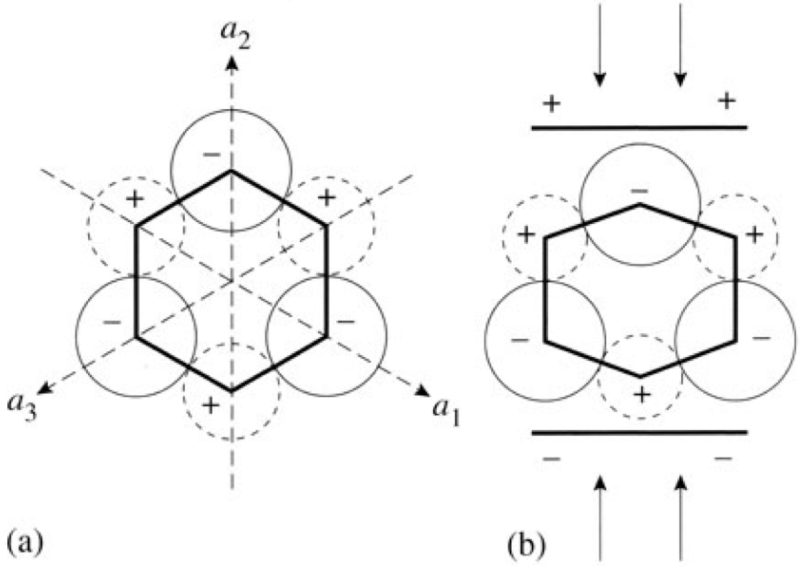

Fig. 8.16 Piezoelectricity in quartz. (a) In an undeformed quartz crystal charges of cations (Si^{4+}) and anions (O^{2-}) are balanced. (b) Compression parallel or perpendicular to an a-axis produces a shift of charges and induces an electric field.

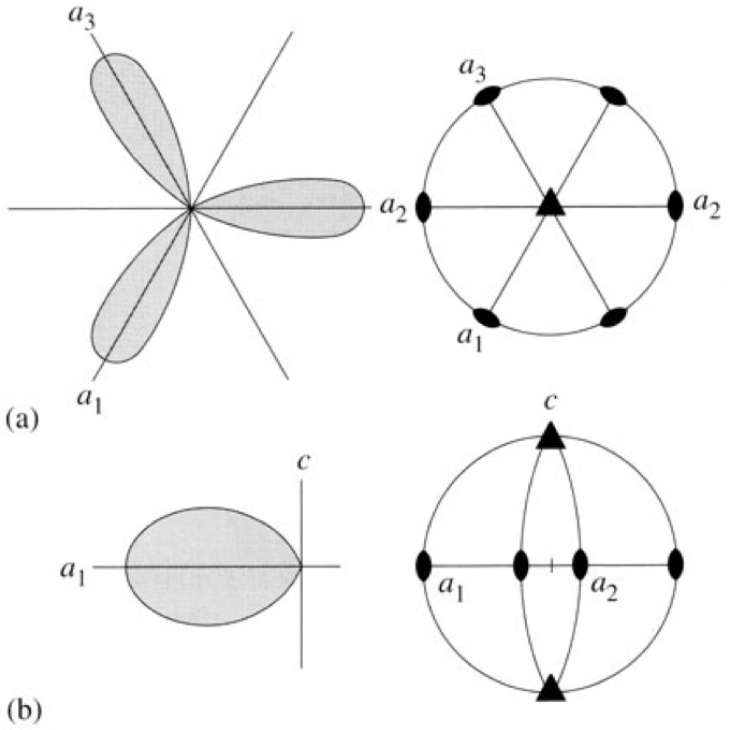

Fig. 8.17 The representation quadric of the piezoelectric tensor of quartz consists of three lobes that extend parallel to the positive a-axes.

4^{th} Rank Tensors

4^{th} Rank Tensors - important for geophysics

- In any crystalline material there is balance between Coulomb attractive forces between oppositely charge ions and Born repulsive forces due to the overlap of electron shells. At any given thermodynamic state the crystal will tend toward an equilibrium structure.

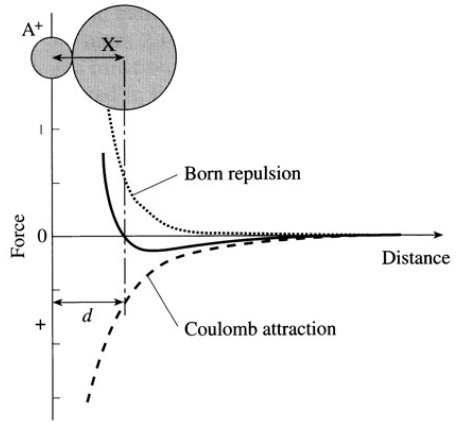

- For a change in hydrostatic or non-hydrostatic stress, the crystal structure will adjust at the atomic level to the new thermodynamic state.
- The fundamental nature of atomic forces in the determination of elastic properties has been illustrated by the emergence of first principles atomic modeling to predict single crystal elastic tensors of geophysical importance at lower mantle PT conditions.

Hooke's Law

$$\sigma = c\,\varepsilon \quad \text{and} \quad \varepsilon = s\sigma$$

where c = stiffness coefficients (dimensions of stress)

s = compliance coefficients (dimensions of 1/stress)

σ = stress tensor (2nd order tensor)

ε = deformation tensor (2nd order tensor)

$$\sigma_{ij} = c_{ijkl}\,\varepsilon_{kl}$$

or

$$\varepsilon_{ij} = S_{ijkl}\,\sigma_{kl}$$

i,j,k,l can have the values 1,2 or 3

so 3 x 3 x 3 x 3 = 3^4 = 81 coefficients.

But due to the symmetry of the deformation and stress tensors the 81 coefficients are not independent. In Voigt notation we can write the Cijkl tensor as 6 by 6 symmetric tensor Cnm with 21 independent values for a triclinic crystal where n,m can have the values 1, 2, 3, 4, 5 or 6.

32 Crystal symmetry classes and their Elastic tensors

Cubic (3) 23, $m3$, 432, $\bar{4}3m$, $m3m$

$$\begin{bmatrix} c_{11} & c_{12} & c_{12} & 0 & 0 & 0 \\ c_{12} & c_{11} & c_{12} & 0 & 0 & 0 \\ c_{12} & c_{12} & c_{11} & 0 & 0 & 0 \\ 0 & 0 & 0 & c_{44} & 0 & 0 \\ 0 & 0 & 0 & 0 & c_{44} & 0 \\ 0 & 0 & 0 & 0 & 0 & c_{44} \end{bmatrix}$$

Hexagonal (5) 6, $\bar{6}$, 6/m, 622, 6mmm, $\bar{6}$2m, 6/mmm

$$\begin{bmatrix} c_{11} & c_{12} & c_{13} & 0 & 0 & 0 \\ c_{12} & c_{11} & c_{13} & 0 & 0 & 0 \\ c_{13} & c_{13} & c_{33} & 0 & 0 & 0 \\ 0 & 0 & 0 & c_{44} & 0 & 0 \\ 0 & 0 & 0 & 0 & c_{44} & 0 \\ 0 & 0 & 0 & 0 & 0 & \frac{1}{2}(c_{11}-c_{12}) \end{bmatrix}$$

Trigonal (6) 32, 3m, $\bar{3}m$

$$\begin{bmatrix} c_{11} & c_{12} & c_{13} & c_{14} & 0 & 0 \\ c_{12} & c_{11} & c_{13} & -c_{14} & 0 & 0 \\ c_{13} & c_{13} & c_{33} & 0 & 0 & 0 \\ c_{14} & -c_{14} & 0 & c_{44} & 0 & 0 \\ 0 & 0 & 0 & 0 & c_{44} & c_{14} \\ 0 & 0 & 0 & 0 & c_{14} & \frac{1}{2}(c_{11}-c_{12}) \end{bmatrix}$$

Trigonal (7) 3, $\bar{3}$

$$\begin{bmatrix} c_{11} & c_{12} & c_{13} & c_{14} & -c_{25} & 0 \\ c_{12} & c_{11} & c_{13} & -c_{14} & c_{25} & 0 \\ c_{13} & c_{13} & c_{33} & 0 & 0 & 0 \\ c_{14} & -c_{14} & 0 & c_{44} & 0 & c_{25} \\ -c_{25} & c_{25} & 0 & 0 & c_{44} & c_{14} \\ 0 & 0 & 0 & c_{25} & c_{14} & \frac{1}{2}(c_{11}-c_{12}) \end{bmatrix}$$

Tetragonal (6) 422, 4mm, $\bar{4}2m$, 4/mmm

$$\begin{bmatrix} c_{11} & c_{12} & c_{13} & 0 & 0 & 0 \\ c_{12} & c_{11} & c_{13} & 0 & 0 & 0 \\ c_{13} & c_{13} & c_{33} & 0 & 0 & 0 \\ 0 & 0 & 0 & c_{44} & 0 & 0 \\ 0 & 0 & 0 & 0 & c_{44} & 0 \\ 0 & 0 & 0 & 0 & 0 & c_{66} \end{bmatrix}$$

Tetragonal (7), 4, $\bar{4}$ 4/m

$$\begin{bmatrix} c_{11} & c_{12} & c_{13} & 0 & 0 & c_{16} \\ c_{12} & c_{11} & c_{13} & 0 & 0 & -c_{16} \\ c_{13} & c_{13} & c_{33} & 0 & 0 & 0 \\ 0 & 0 & 0 & c_{44} & 0 & 0 \\ 0 & 0 & 0 & 0 & c_{44} & 0 \\ c_{16} & -c_{16} & 0 & 0 & 0 & c_{66} \end{bmatrix}$$

Orthorhombic (9) 222, $mm2$, mmm

$$\begin{bmatrix} c_{11} & c_{12} & c_{13} & 0 & 0 & 0 \\ c_{12} & c_{22} & c_{23} & 0 & 0 & 0 \\ c_{13} & c_{23} & c_{33} & 0 & 0 & 0 \\ 0 & 0 & 0 & c_{44} & 0 & 0 \\ 0 & 0 & 0 & 0 & c_{55} & 0 \\ 0 & 0 & 0 & 0 & 0 & c_{66} \end{bmatrix}$$

Mononclinic (13) 2, m, 2/m

$$\begin{bmatrix} c_{11} & c_{12} & c_{13} & 0 & c_{15} & 0 \\ c_{12} & c_{22} & c_{23} & 0 & c_{25} & 0 \\ c_{13} & c_{23} & c_{33} & 0 & c_{35} & 0 \\ 0 & 0 & 0 & c_{44} & 0 & c_{46} \\ c_{14} & c_{25} & c_{35} & 0 & c_{55} & 0 \\ 0 & 0 & 0 & c_{46} & 0 & c_{66} \end{bmatrix}$$

Triclinic (21) 1, $\bar{1}$

$$\begin{bmatrix} c_{11} & c_{12} & c_{13} & c_{14} & c_{15} & c_{16} \\ c_{12} & c_{22} & c_{23} & c_{24} & c_{25} & c_{26} \\ c_{13} & c_{23} & c_{33} & c_{34} & c_{35} & c_{36} \\ c_{14} & c_{24} & c_{34} & c_{44} & c_{45} & c_{46} \\ c_{15} & c_{25} & c_{35} & c_{45} & c_{55} & c_{56} \\ c_{16} & c_{26} & c_{36} & c_{46} & c_{56} & c_{66} \end{bmatrix}$$

Constants Elastique

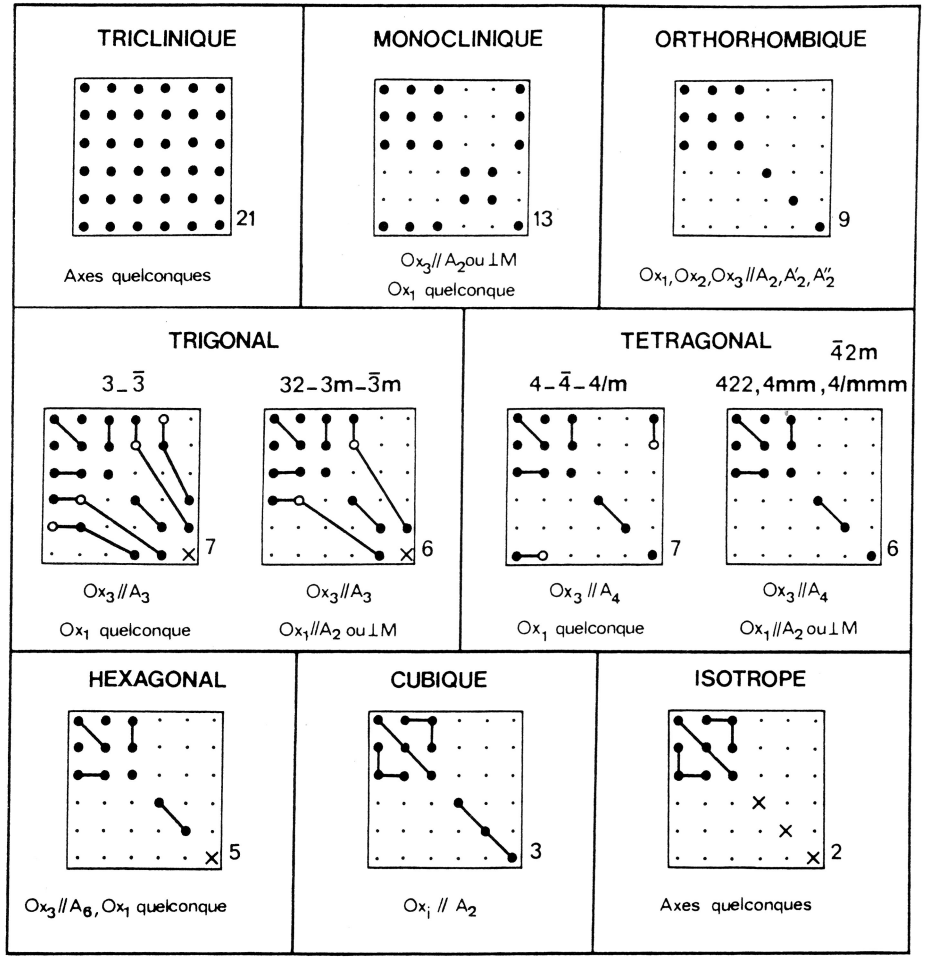

Composantes $c_{\alpha\beta}$ du tenseurs des rigidités élastiques suivant les systèmes de symétrie avec les axes de référence de la figure 2. 22.

composante – *non nulle* : ● ○ – *nulle* : •
composantes – *égales* : ●—● – *opposées* : ●—○
– *égales à* $(c_{11} - c_{12})/2$: ×

La symétrie par rapport à la diagonale principale n'est pas mentionnée. Le nombre de composantes indépendantes est indiqué, en bas, à droite de chaque ensemble.

What can you do with Cij ?

- Elastic wave velocity - Vp,Vs,(slowness - 1/V) polarization, wavefront velocity
- Moduli - Young's modulus
- Linear compressiblity in any direction
- Volume compressbility or Bulk modulus
- Mechanical instability analysis - softening of acoustic modes
- Isotropic moduli and velocities
- Debye temperature & mean sound (phono) velocity
- Elastic energy

Young's Modulus

No single surface can represent the elastic behaviour of a single crystal. The surface of the Young's modulus is often used. Young's modulus for a given direction is defined as the ratio of the longitudinal stress to the longitudinal elastic strain.

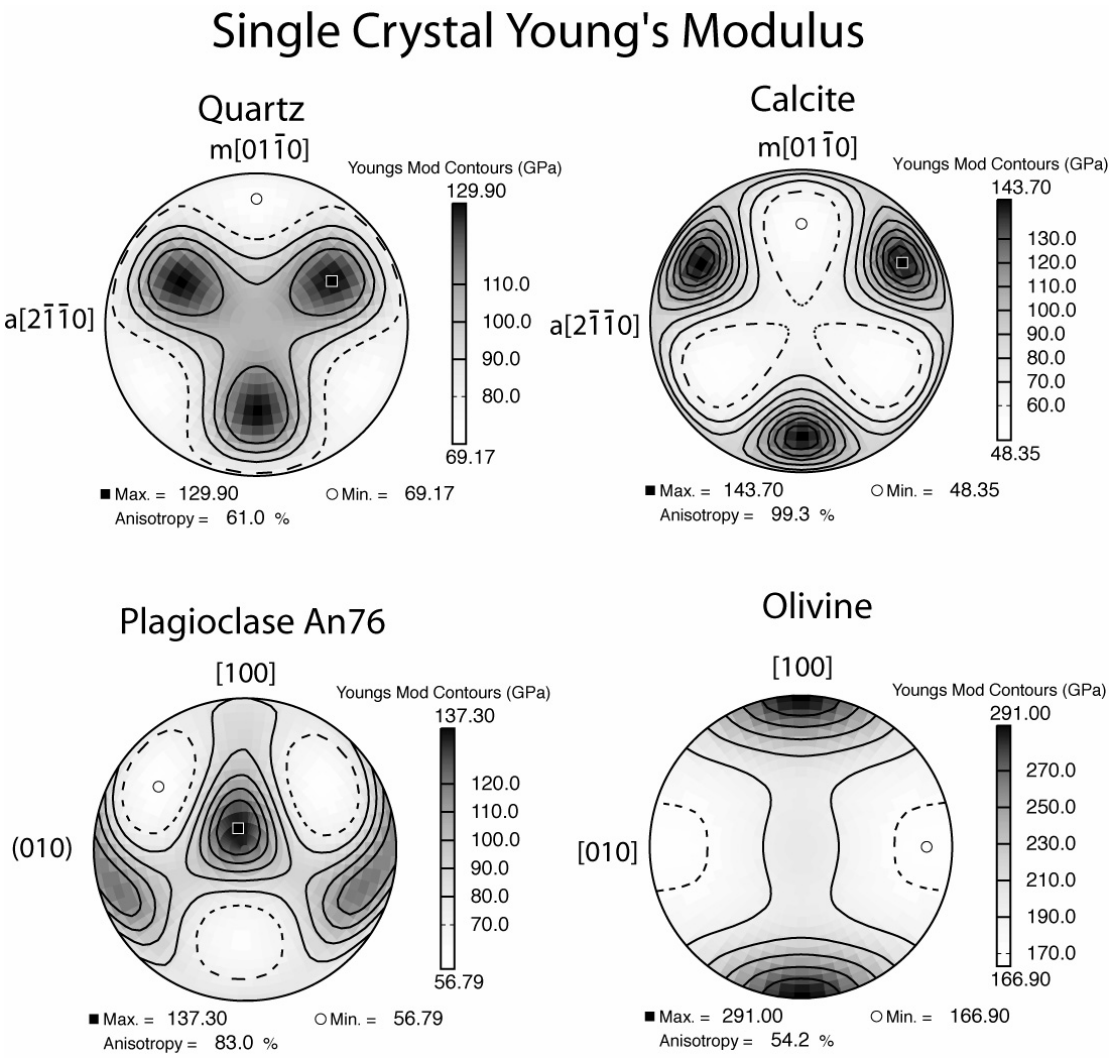

Talc – Poisson's ratio

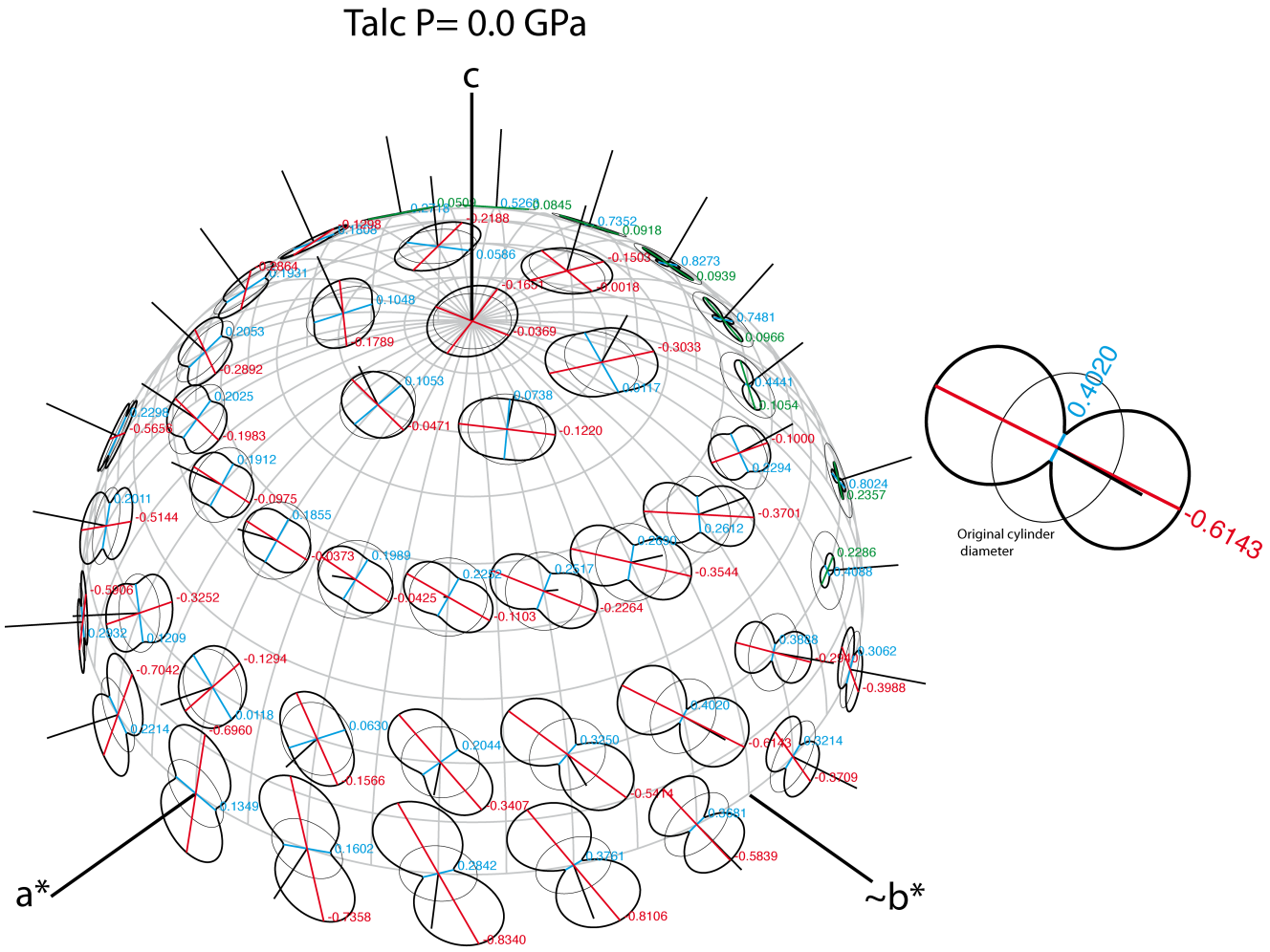

Isotropic moduli

$$K_R = [S_{11} + S_{22} + S_{33} + 2(S_{12} + S_{13} + S_{23})]^{-1} = \frac{1}{\beta},$$

$$G_R = 15[4(S_{11} + S_{22} + S_{33}) - 4(S_{12} + S_{13} + S_{23}) + 3(S_{44} + S_{55} + S_{66})]^{-1}$$

$$K_V = \frac{1}{9}\,[C_{11} + C_{22} + C_{33} + 2(C_{12} + C_{13} + C_{23})],$$

$$G_V = \frac{1}{15}\,[C_{11} + C_{22} + C_{33} - (C_{12} + C_{13} + C_{23}) + 3(C_{44} + C_{55} + C_{66})]$$

$$K_{VRH} = \frac{1}{2}\,(K_V + K_R);\;\; G_{VRH} = \frac{1}{2}\,(G_V + G_R)$$

Typical Cij data set

Table 5. Elastic Moduli of Tetragonal Crystals (6 Moduli) at Room P & T

Material	ρ Mg/m^3	Subscript ij in modulus c_{ij} (GPa) 11	33	44	66	12	13	K_S GPa	G GPa	References
Rutile-Structured										
SiO_2, Stishovite	4.290	453	776	252	302	211	203	316	220	143
SiO_2, α-Cristobalite	2.335	59.4	42.4	67.2	25.7	3.8	−4.4	16.4	39.1	151
SnO_2, Cassiterite	6.975	261.7	449.6	103.1	207.4	177.2	155.5	212.3	101.8	22
TeO_2,	6.02	55.7	105.8	26.5	65.9	51.2	21.8	45.0	20.4	93
Paratellurite	5.99	53.2	108.5	24.4	55.2	48.6	21.2	43.7	19.0	122
TiO_2, Rutile	4.260	269	480	124	192	177	146	215.5	112.4	47
GeO_2	6.279	337.2	599.4	161.5	258.4	188.2	187.4	257.6	150.8	131
Other Minerals										
$Ba_2Si_2TiO_8$,		140	83	33	59	36	24	56.9	42.1	46
Fresnoite (c^E)		166	100	31.7	69.4	58	44	77.6	43.3	46
Scapolite,		99	113	15.6	22.9	35.1	35.4	58.0	23.1	47
$(Na,Ca,K)_4Al_3(Al,Si)_3$		102	140	23.0	30.4	38.9	43.3	65.3	29.1	47
$Si_6O_{24}(Cl,SO_4,CO_3)$		102	140	23.0	30.4	38.9	43.3	65.3	29.1	47
Vesuvianite		153	166	55.8	54.0	48	44	82.6	55.5	47
$Ca_{10}Mg_2Al_4(SiO_4)_5(Si_2O_7)_2(OH)_4$										
$ZrSiO_4$[a],	4.675	424.3	489.3	131.1	48.3	69.7	149	227.9	109.0	88
Zircon	4.70	256	372	73.5	116	175	214	223.9	66.6	47

[a] nonmetamict.

From J.D.Bass (1995) Elasticity of Minerals, Glasses and Melts
Mineral Physics and Crystallography A Handbook of Physical Constants
AGU Reference Shelf 2 pp 45-63.
http://www.agu.org/reference/minphys.html

The origin of seismic anisotropy

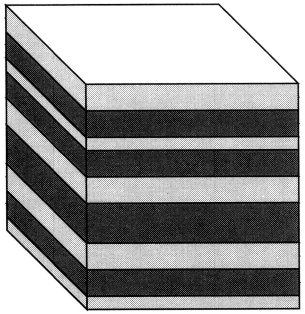

Horizontal layering - sediments, metamorphic layering..
Upper and lower crust, transition zone, D ”

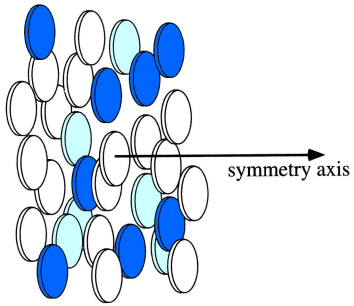

Vertically aligned cracks in the crust……
filled with gas, liquid or solid

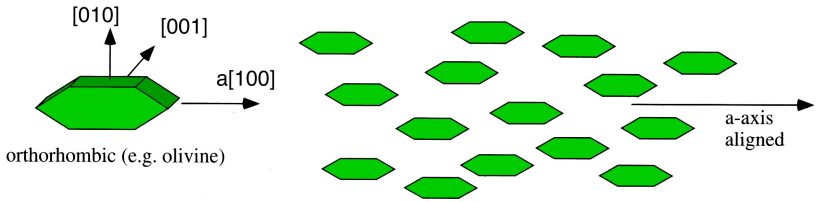

CPO in lower crust, upper mantle
& inner core

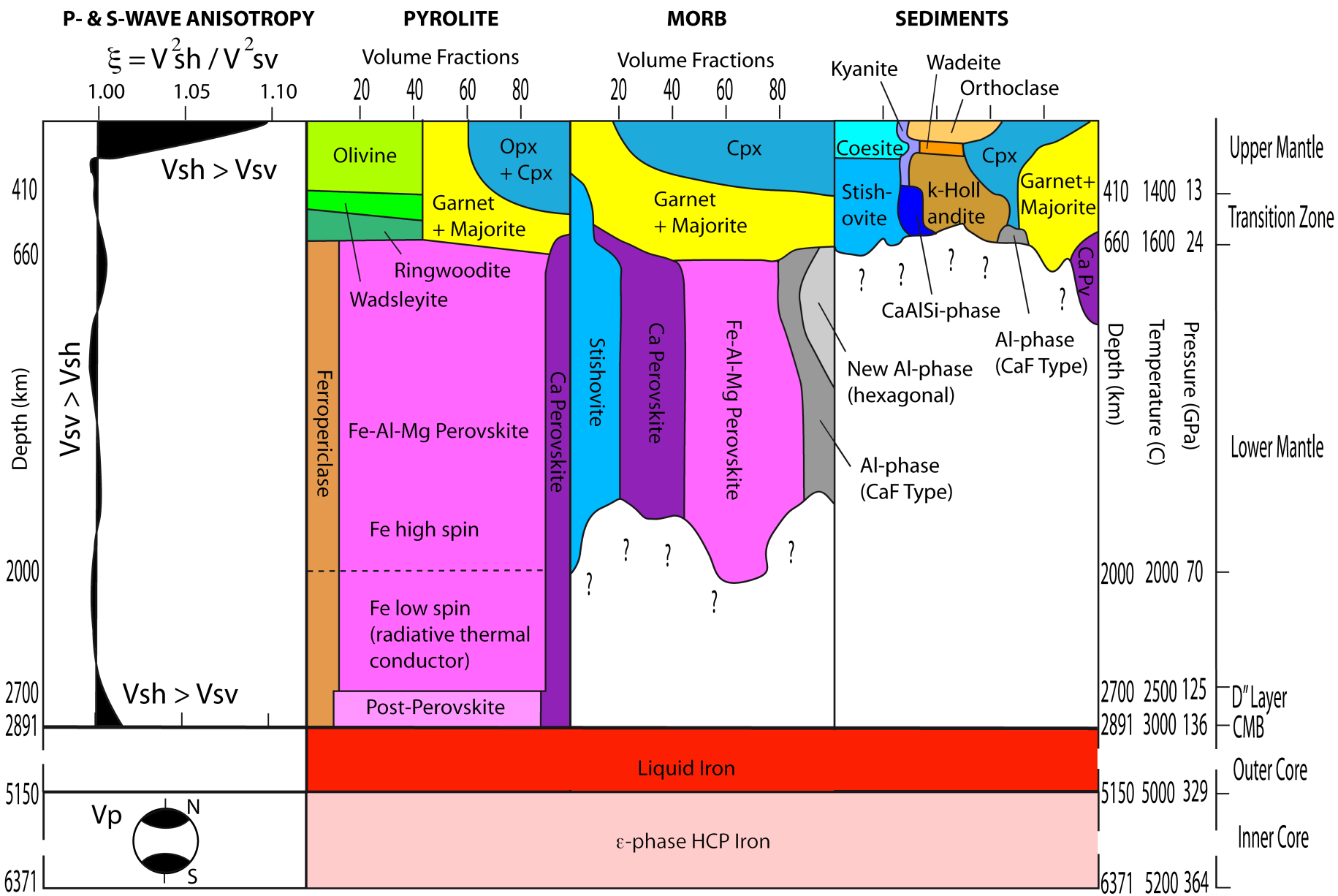
P- & S-WAVE ANISOTROPY
ξ = V²sh / V²sv
1.00
1.05
1.10
Vsh > Vsv
Vsv > Vsh
Vsh > Vsv
Depth (km)
410
660
2000
2700
2891
5150
6371
Vp
N
S
PYROLITE
Volume Fractions
20
40
60
80
Olivine
Opx + Cpx
Garnet + Majorite
Ringwoodite
Wadsleyite
Fe-Al-Mg Perovskite
Fe high spin
Fe low spin (radiative thermal conductor)
Post-Perovskite
Ferropericlase
Ca Perovskite
MORB
Volume Fractions
20
40
60
80
Cpx
Garnet + Majorite
Stishovite
Ca Perovskite
Fe-Al-Mg Perovskite
SEDIMENTS
Kyanite
Wadeite
Orthoclase
Coesite
Cpx
Stish-ovite
k-Holl andite
Garnet+ Majorite
Ca Pv
CaAlSi-phase
Al-phase (CaF Type)
New Al-phase (hexagonal)
Al-phase (CaF Type)
Liquid Iron
ε-phase HCP Iron
Depth (km)
Temperature (C)
Pressure (GPa)
410 1400 13
660 1600 24
2000 2000 70
2700 2500 125
2891 3000 136
5150 5000 329
6371 5200 364
Upper Mantle
Transition Zone
Lower Mantle
D" Layer
CMB
Outer Core
Inner Core

Christoffel Tensor T_{ik}

The calculation of the three seismic phase velocities from the Christoffel tensor

$$T_{ik} = C_{ijkl}\, n_j n_l$$

where **n** is the plane wave propagation direction and C_{ijkl} the elastic constants of the crystal. The three eigenvalues E_i of the symmetric Christoffel tensor (T_{ik}) are related to three seismic phase velocities V_i (qP,qS1,qS2) by $V_i = (E_i/\rho)^{1/2}$,

where ρ is the density and qS1 > qS2.

The three eigenvectors of Christoffel tensor are the particle motion vectors of qP,qS1,qS2.

Why qP and not Vp ?

For a triclinic elastic body the plane wave propagation direction (**n**) is not *parallel* to the particle motion vector for P, hence it is called quasi-P or qP. Similarly the **n** is not *perpendicular* to particle motion vector for S1 and S2, hence qS1,qS2.

Wavefronts

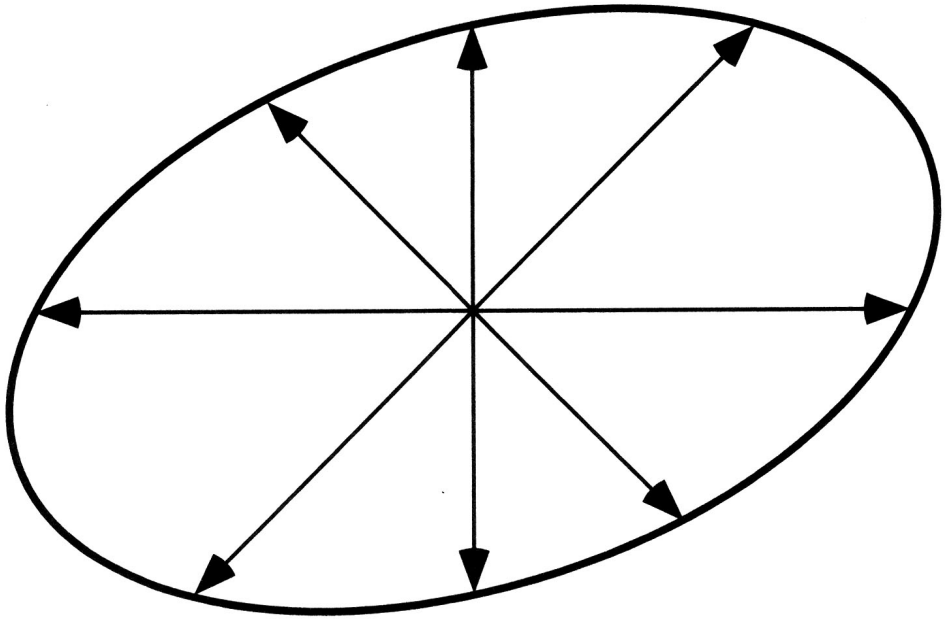

The wavefront generated by a point source in an anisotropic material.

Group and phase velocity

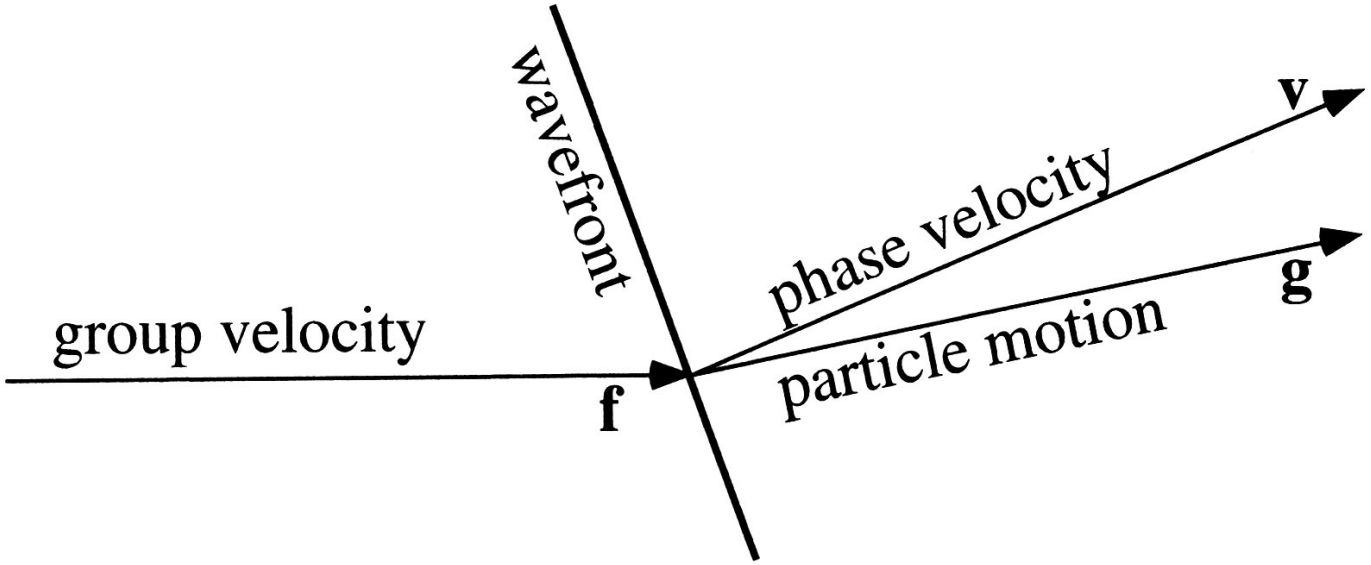

The phase velocity, group velocity, and particle motion vectors point in different directions for a quasi-compressional wave propagating in anisotropic material (except along a symmetry plane of the anisotropy where they will coincide). The phase velocity vector **v** points in the same direction as the slowness vector **s**

Deflected beam trajectory in an anisotropic solid

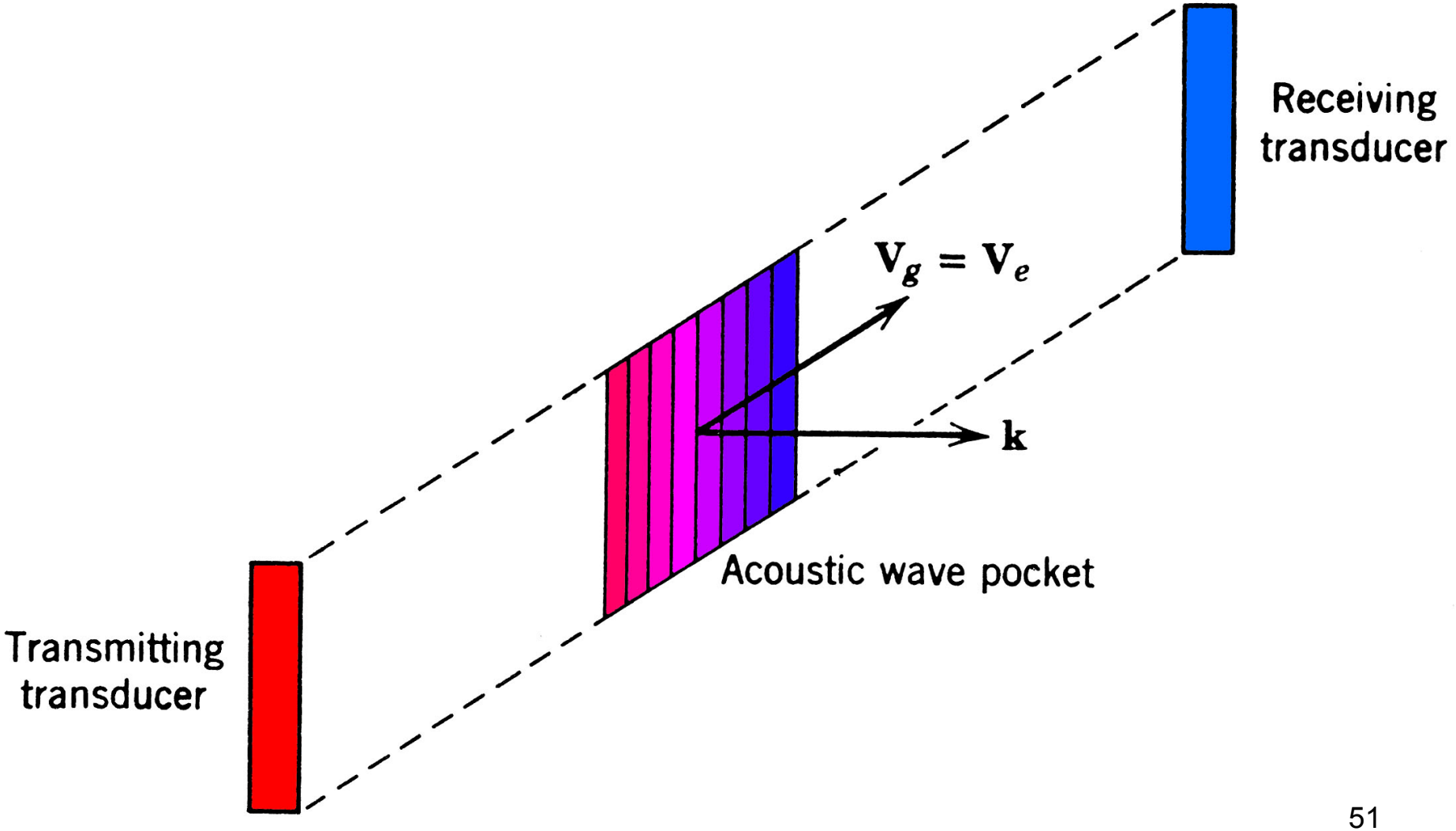

Deflected trajectory in Quartz crystal

Quasi-Vp

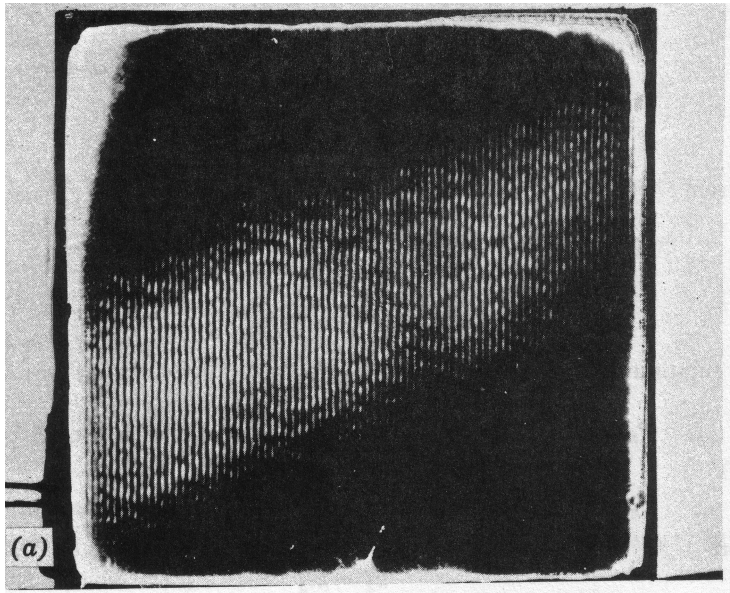

Quasi-Vs

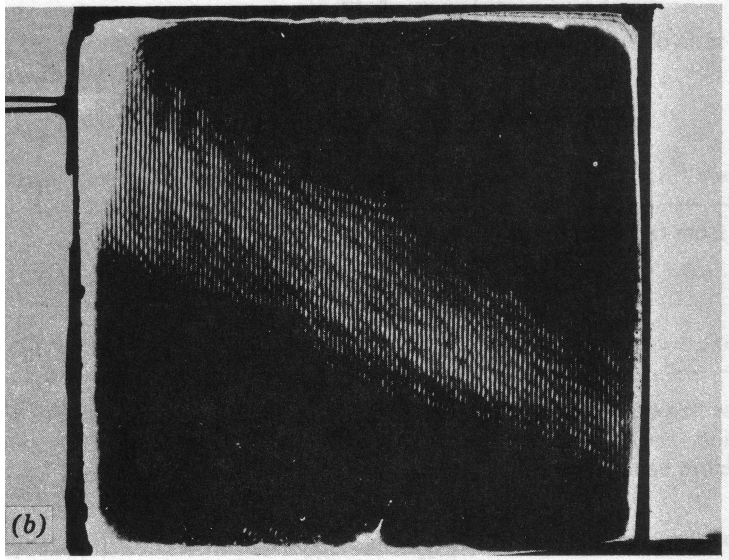

Staudt & Cook (1967)

Group velocity and slowness surfaces

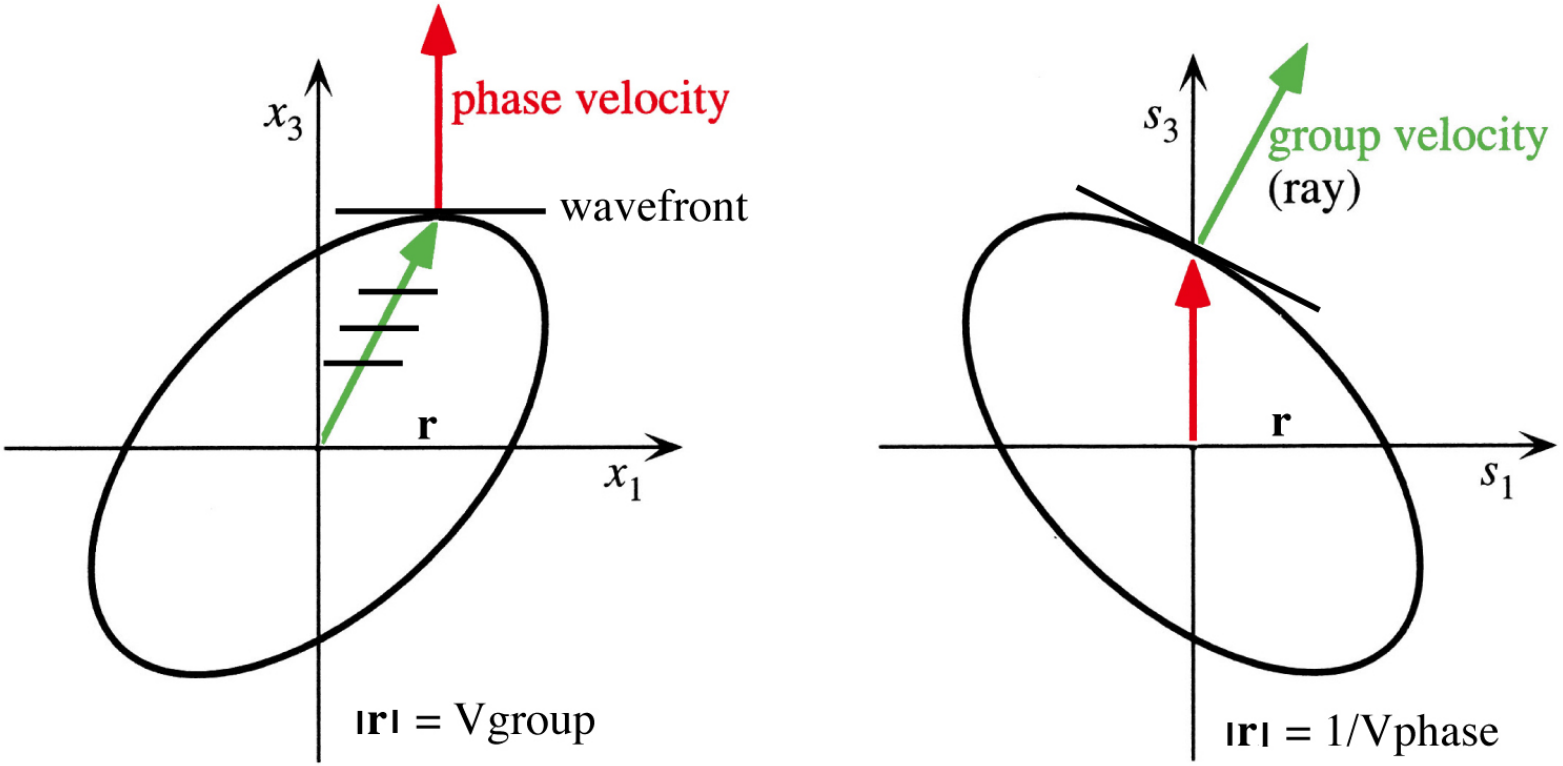

wavefront
(group velocity)

slowness surface
(inverse phase velocity)

The relationship between the wavefront and slowness surface for anisotropic material.

N.B. These surfaces are not generally an ellipse !

SH-wave surfaces of ε-phase iron at a pressure of 211 GPa

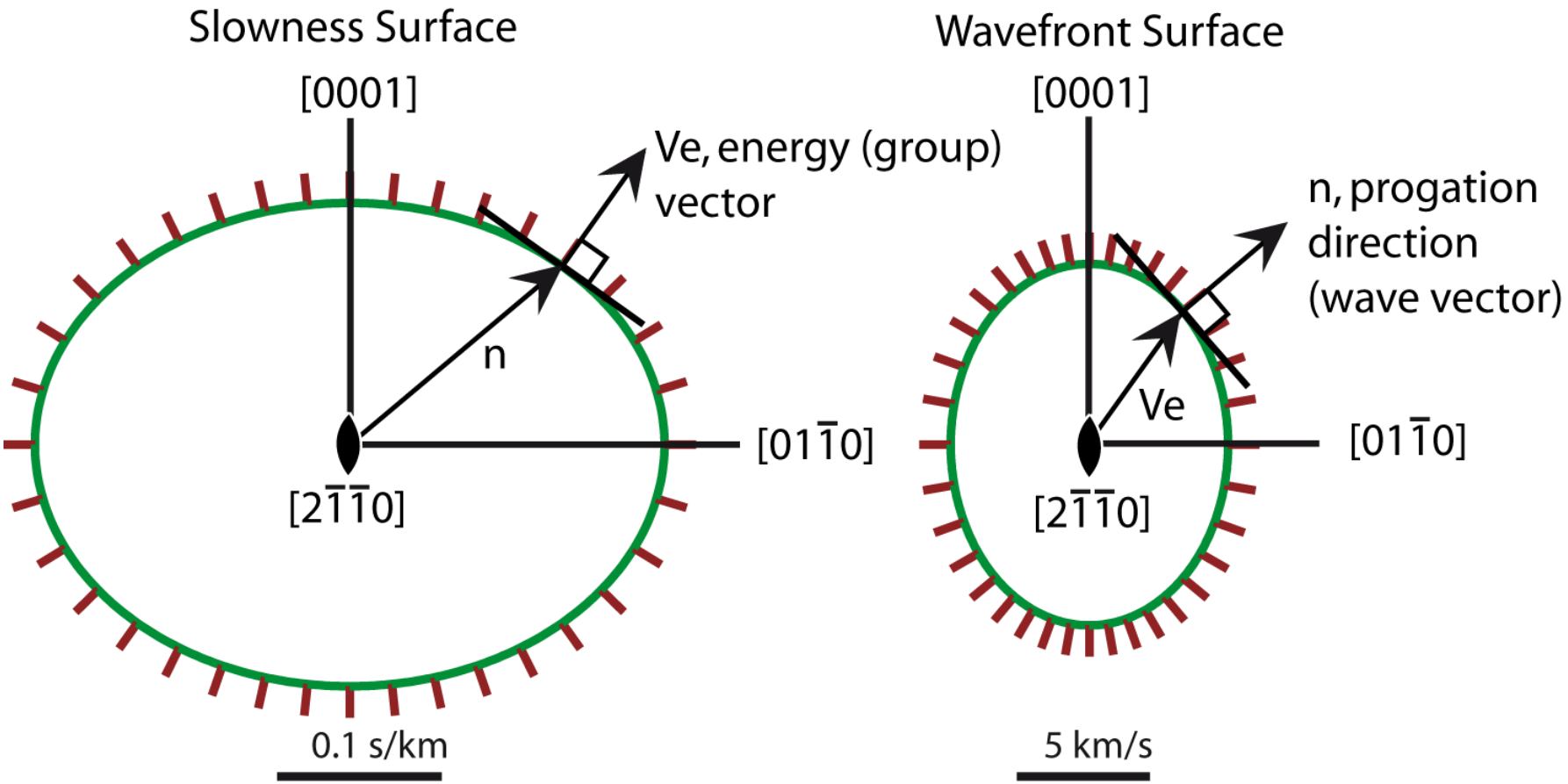

Stishovite surfaces in the (001) plane

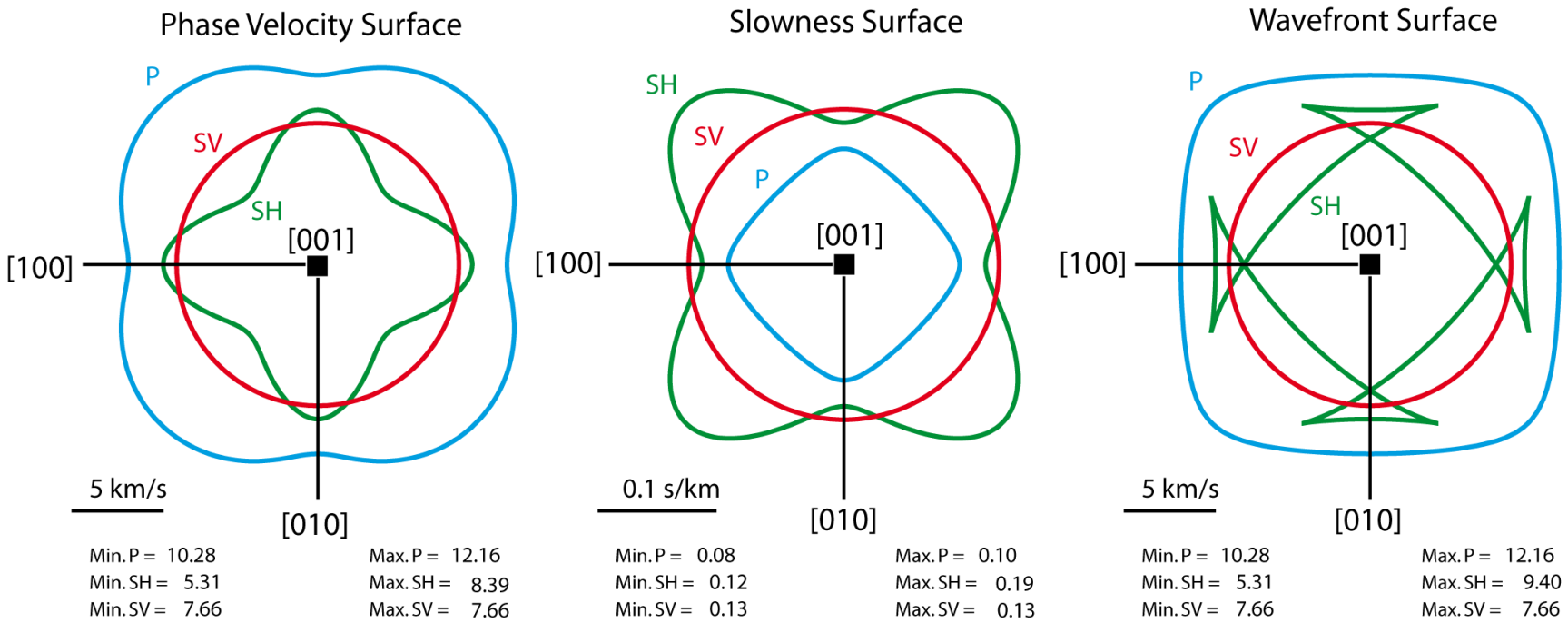

Wavefront cusps on SH-waves in Stishovite in the (001) plane

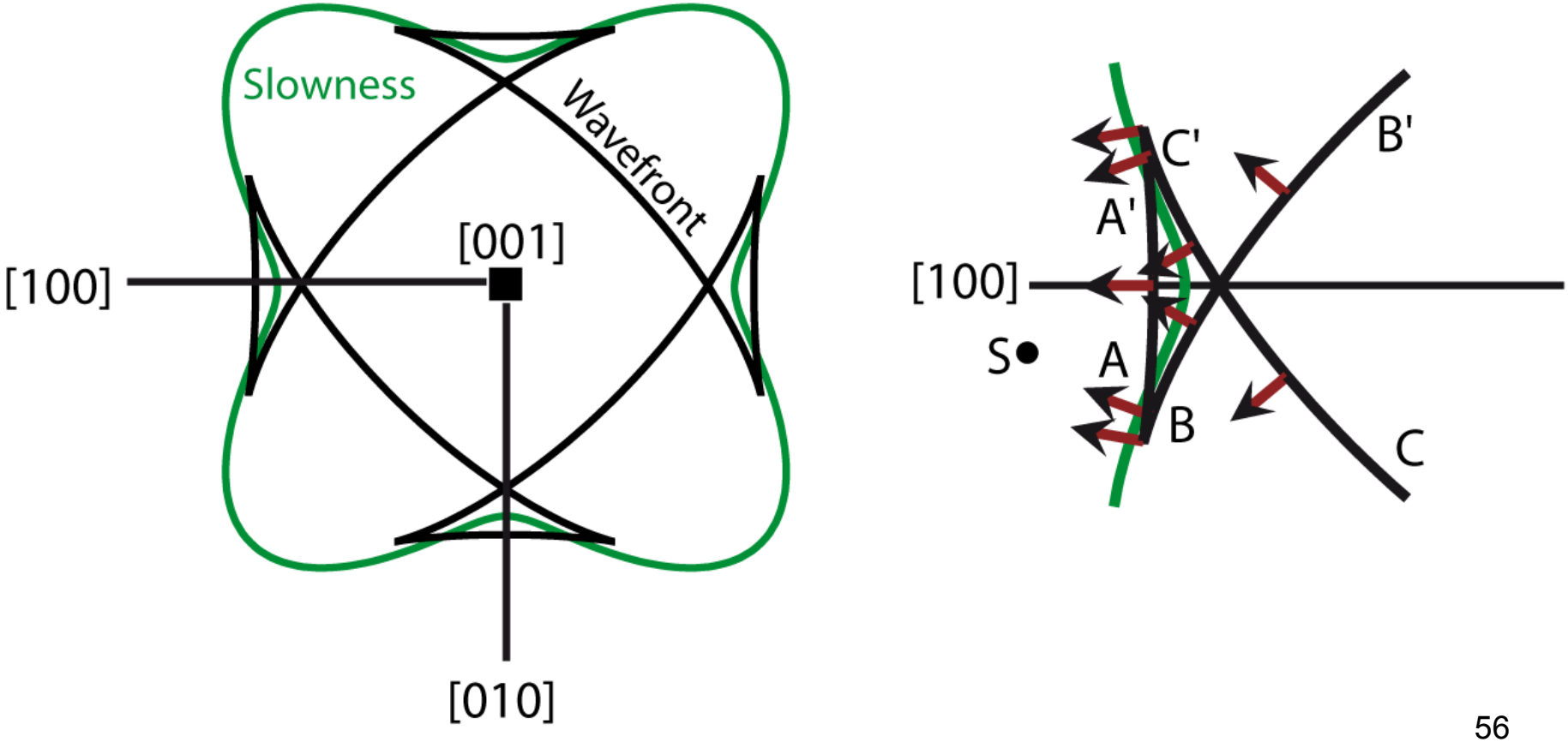

ε-phase iron (hexagonal) surfaces in the (100) and (001) planes

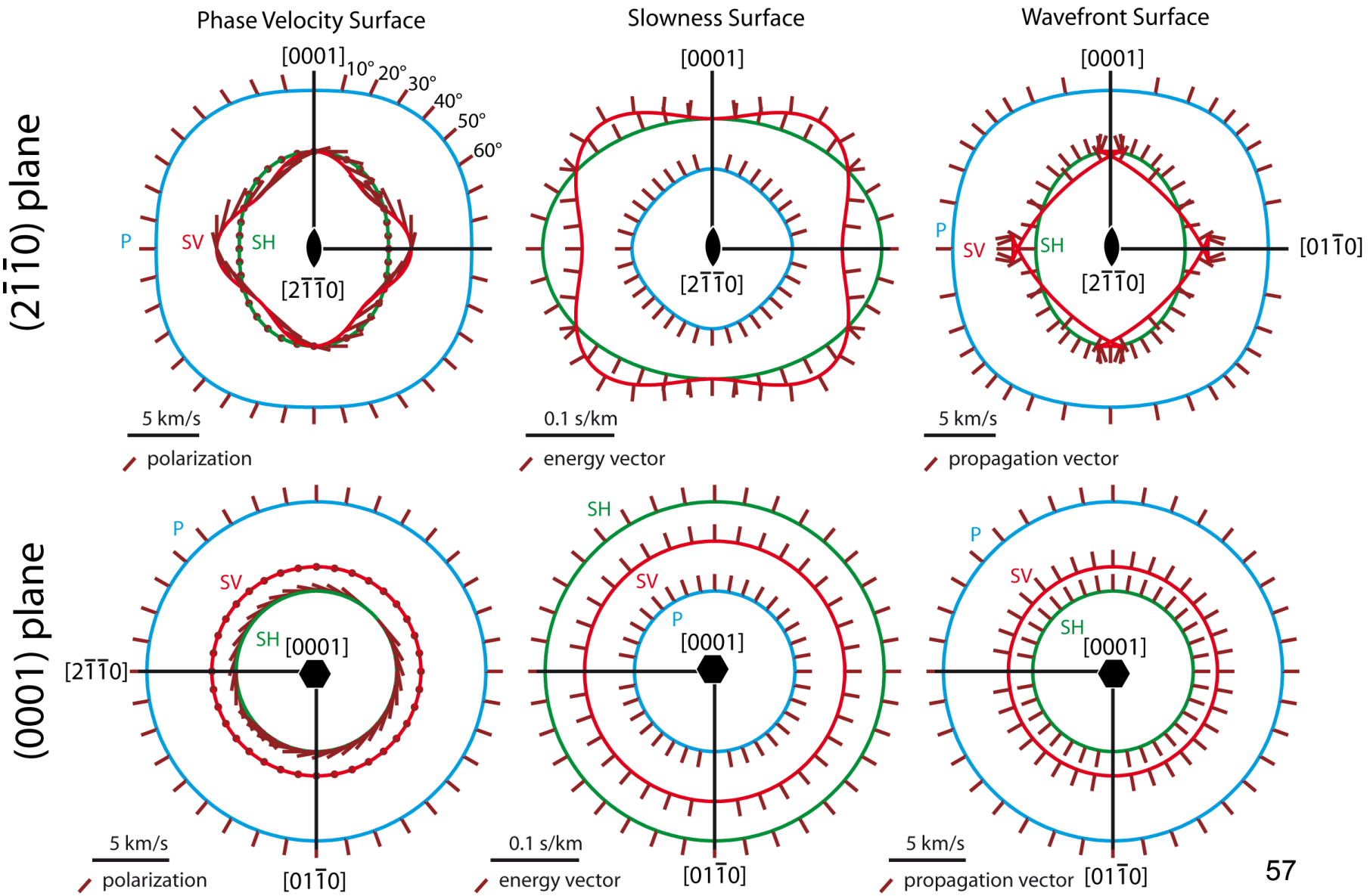

ε-phase iron (hexagonal)

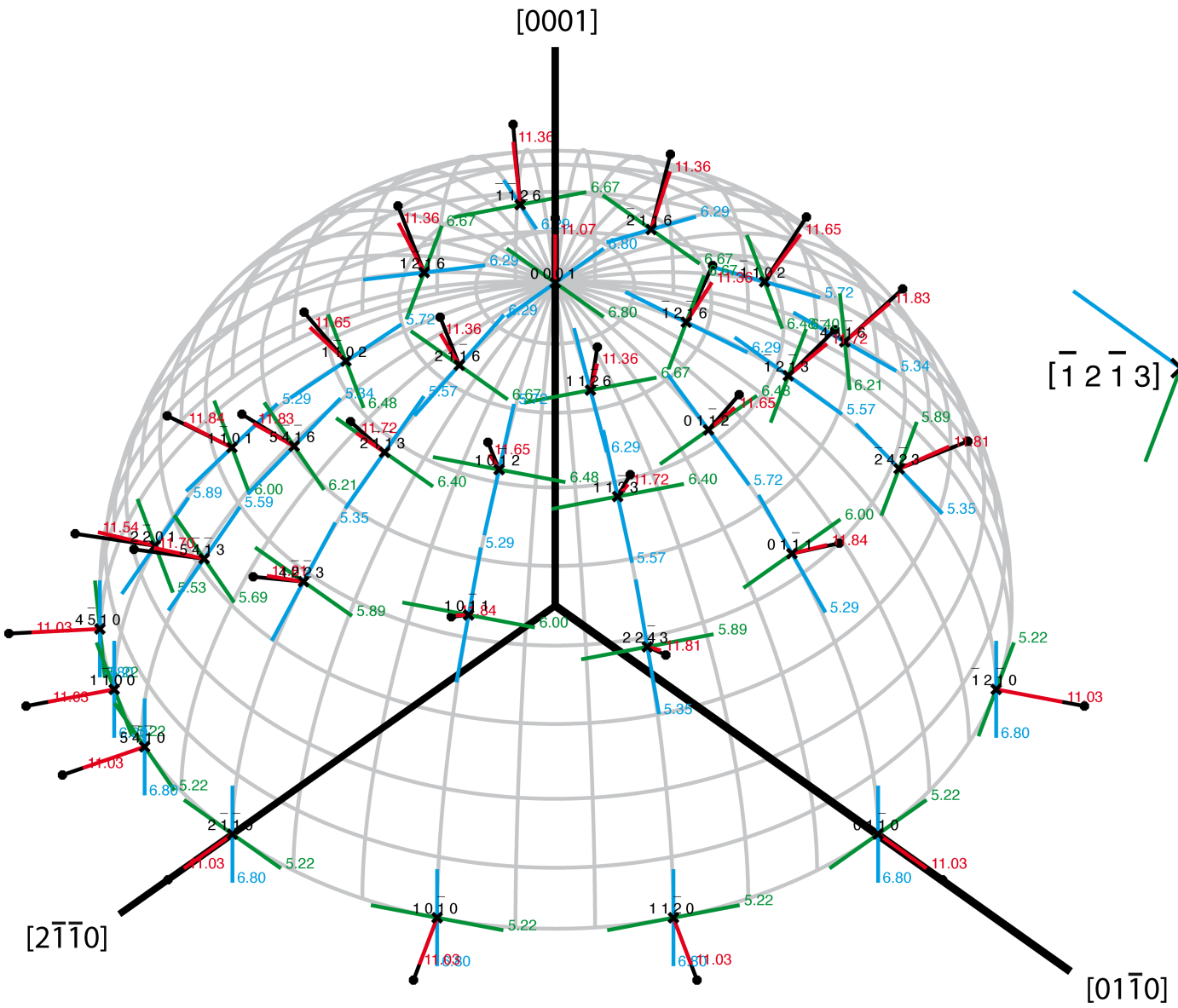

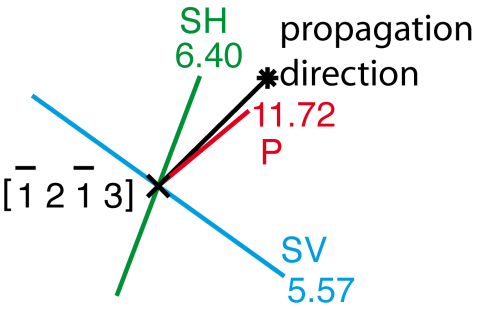

ε-phase iron (hexagonal)

P velocity

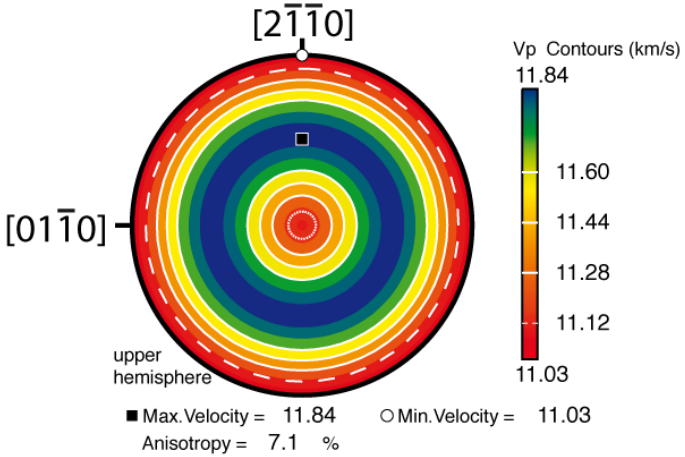

■ Max. Velocity = 11.84 ○ Min. Velocity = 11.03
Anisotropy = 7.1 %

SH velocity

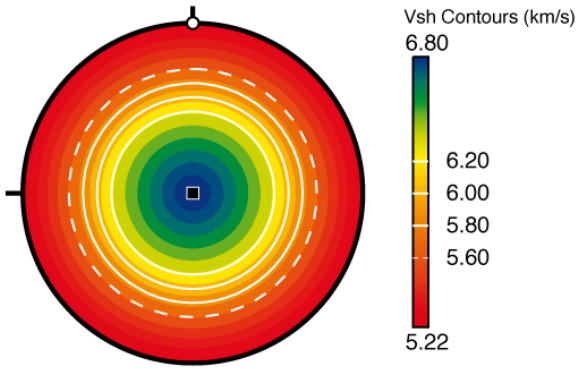

■ Max. Velocity = 6.80 ○ Min. Velocity = 5.22
Anisotropy = 26.3 %

SV velocity

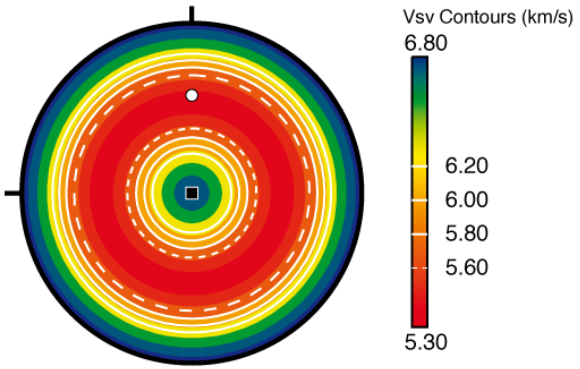

■ Max. Velocity = 6.80 ○ Min. Velocity = 5.30
Anisotropy = 24.8 %

dVs anisotropy

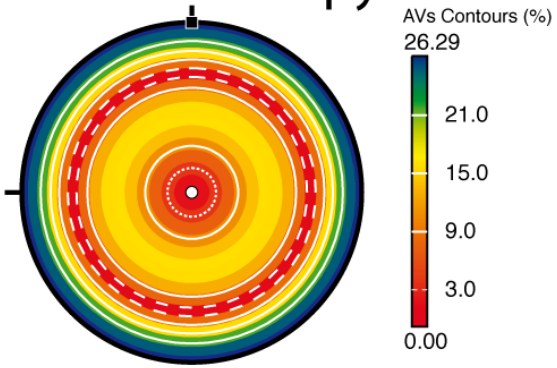

■ Max. Anisotropy = 26.29 ○ Min. Anisotropy = 0.00

SH polarisation

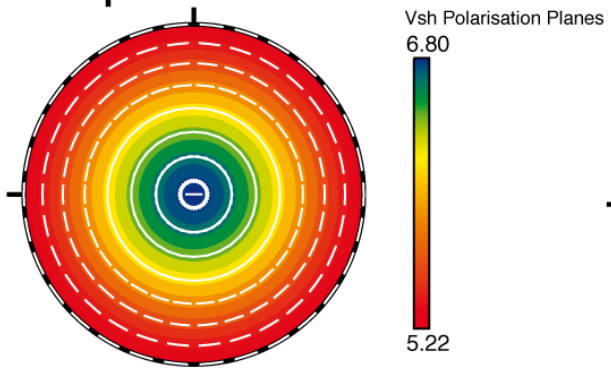

SV polarisation

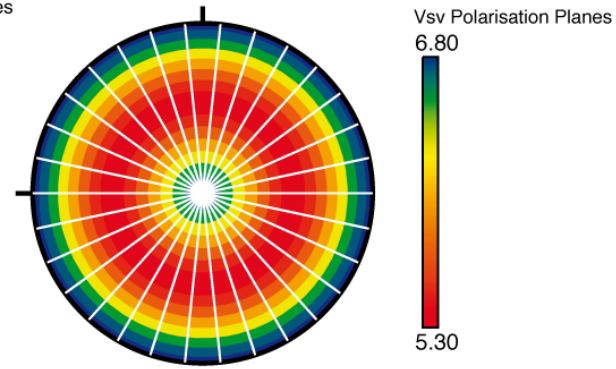

Isotropic case :

propagation direction // polarization Vp

in general Vp > Vs1 = Vs2

polarization Vs1 & Vs2 ⊥ propagation direction

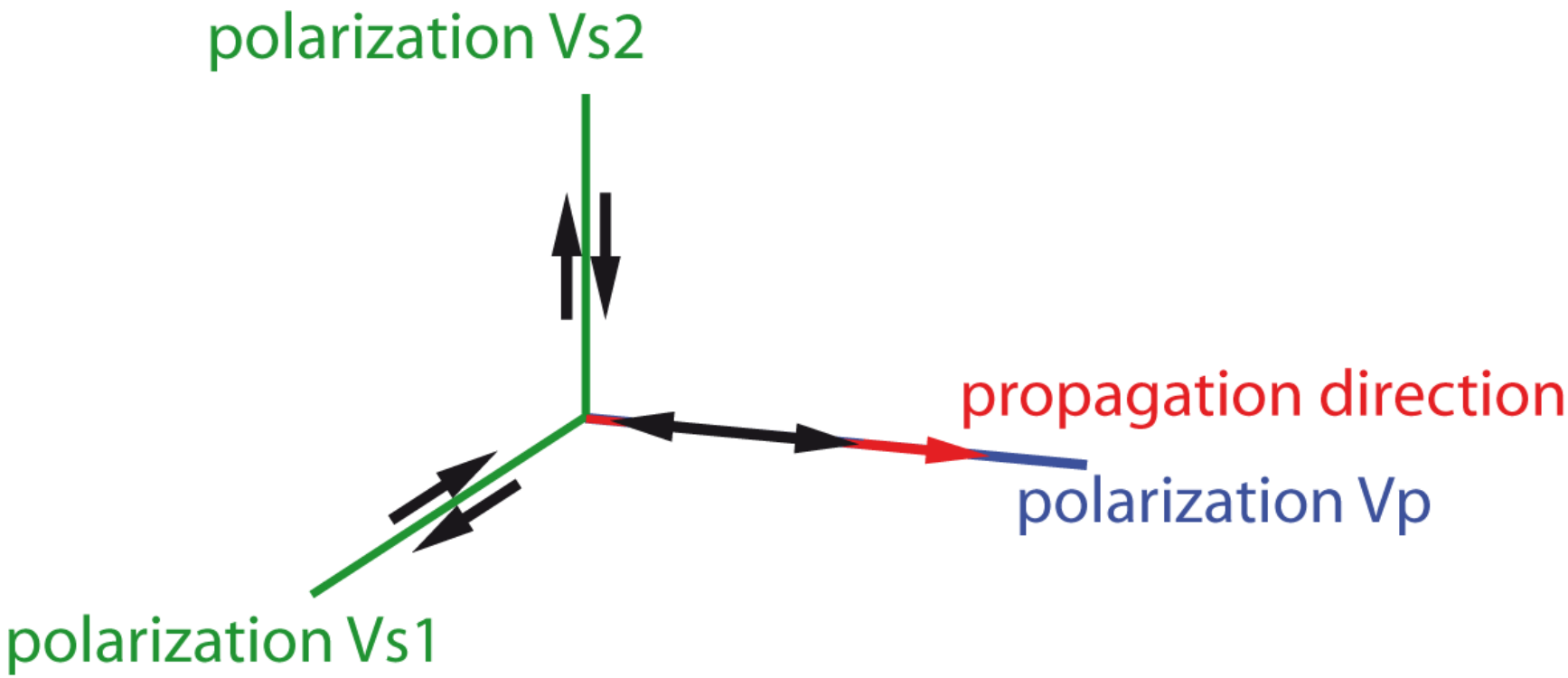

Anisotropic case :

polarisation of quasi-Vp closest to propagation direction

in general quasi-Vp > quasi-Vs1> quasi-Vs2

polarizations are mutually perpendicular

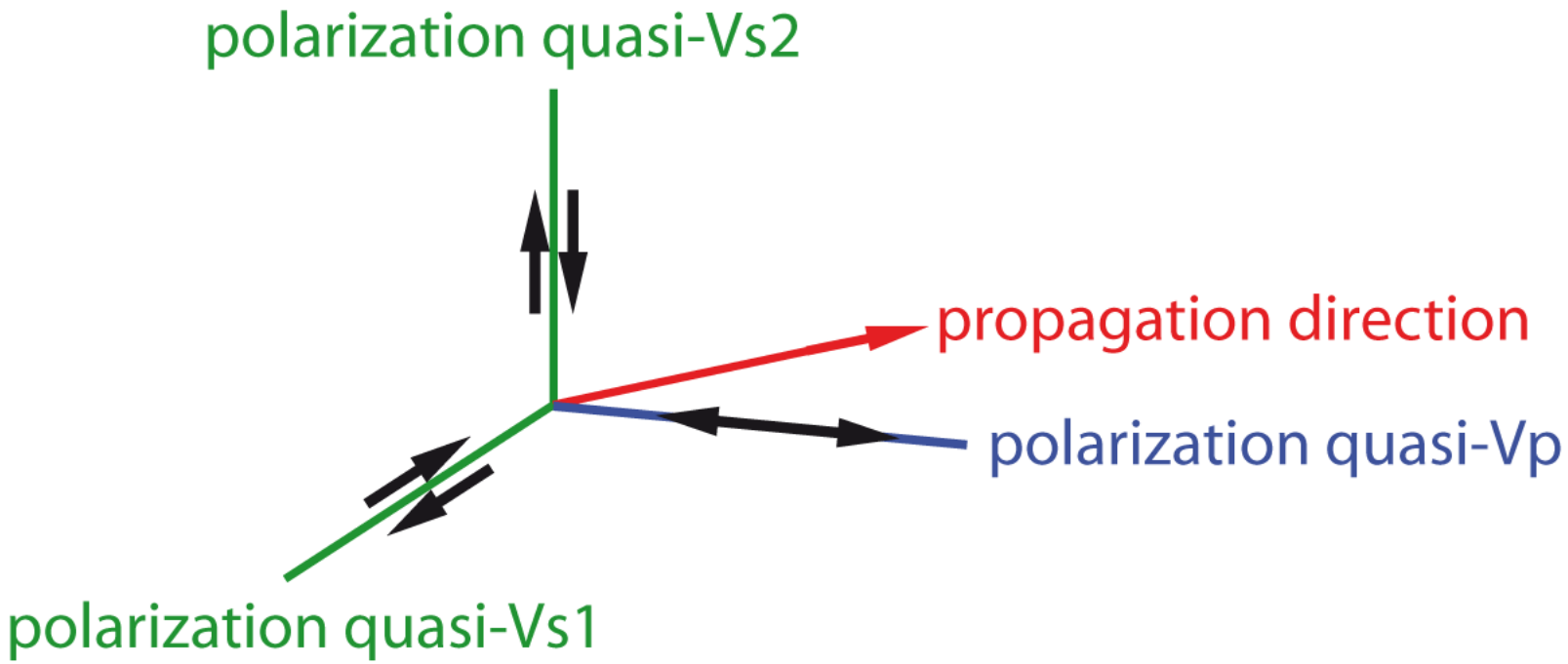

Olivine Single Crystal - quasi-P, S1 & S2

General case : particale motion not parallel to propagation direction long [112]

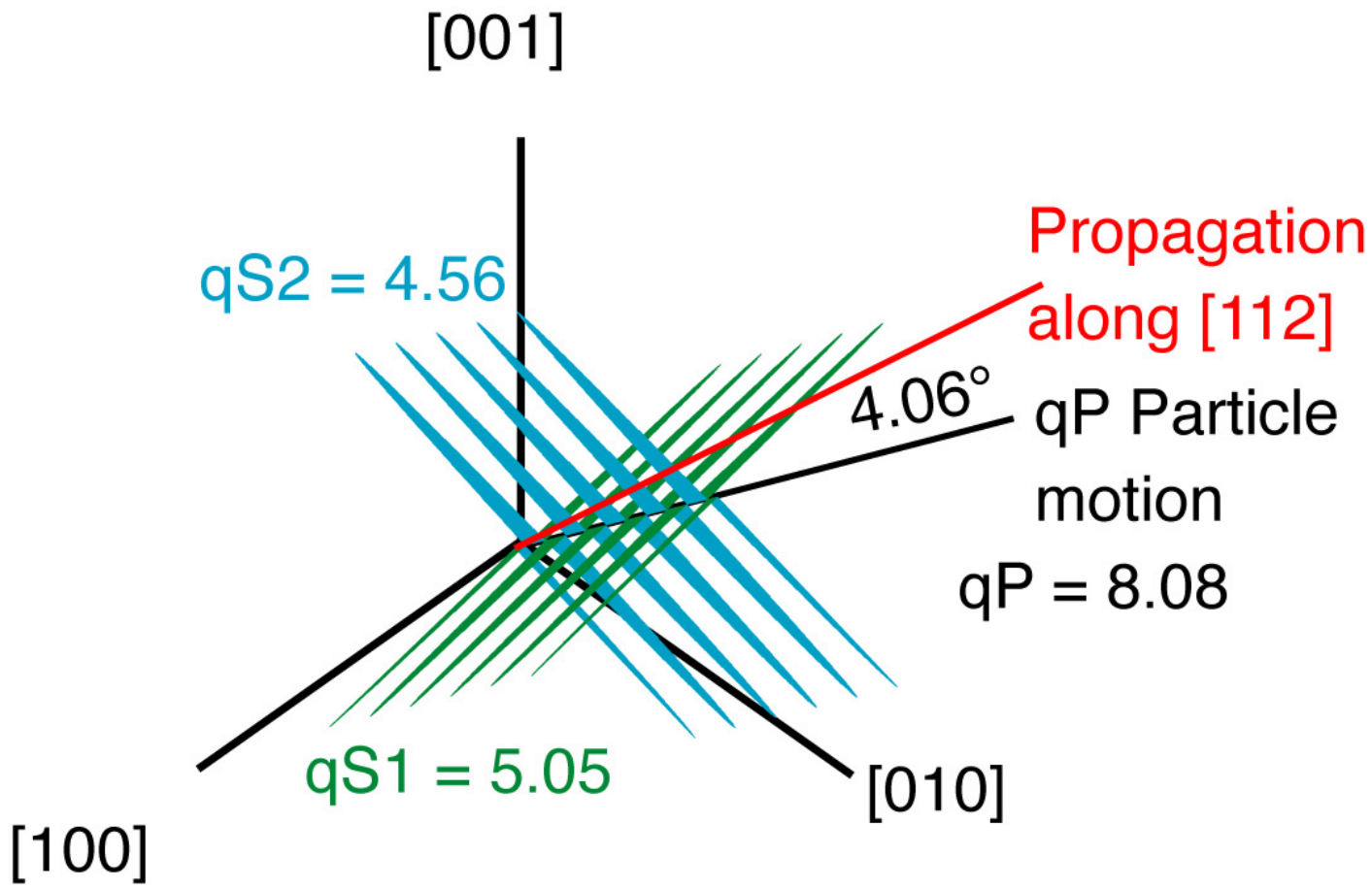

Olivine Single Crystal

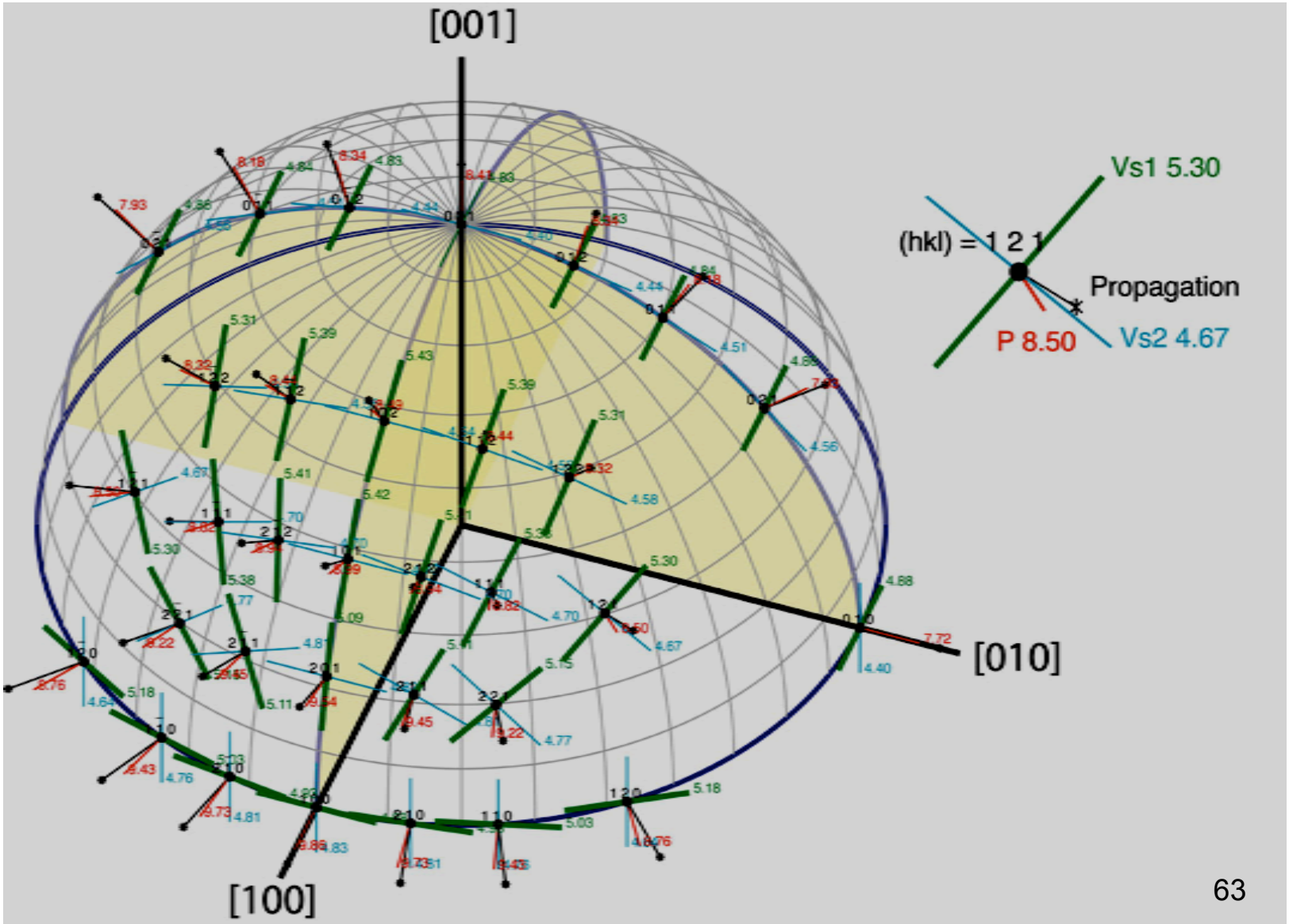

Olivine Single Crystal

qP Propagation to Polarisation

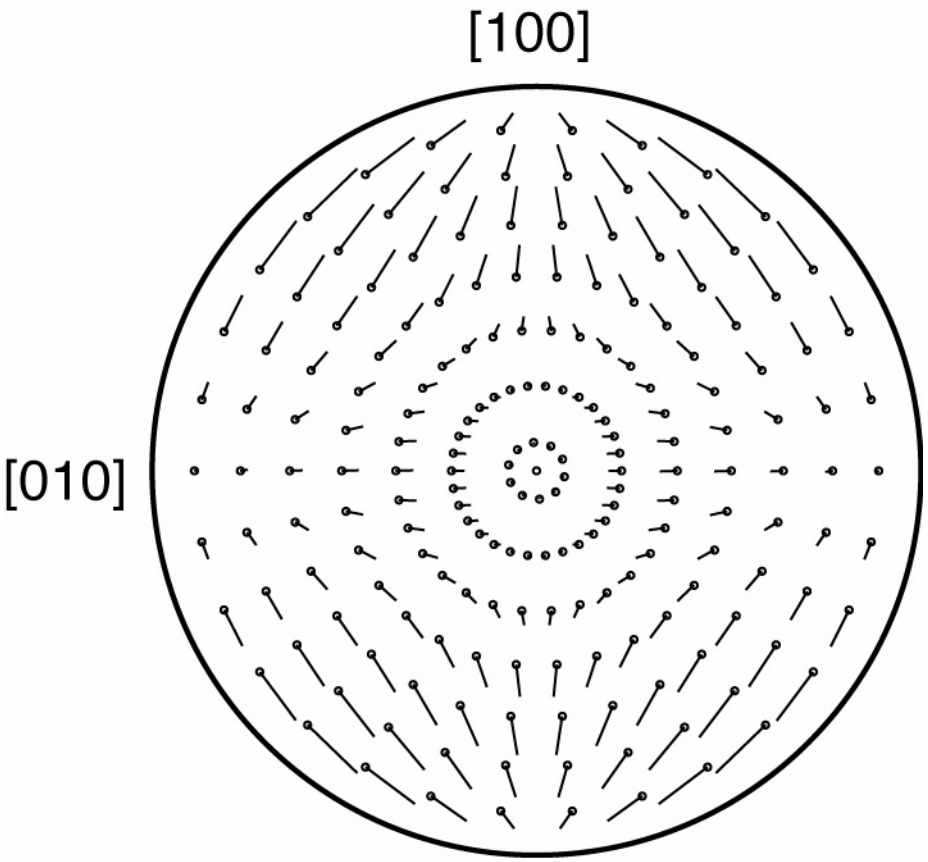

- Propagation vector upper hemisphere

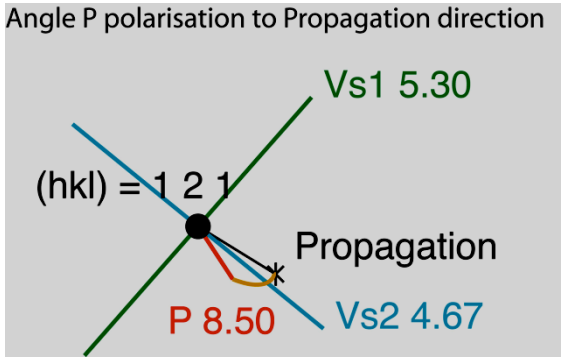

Olivine

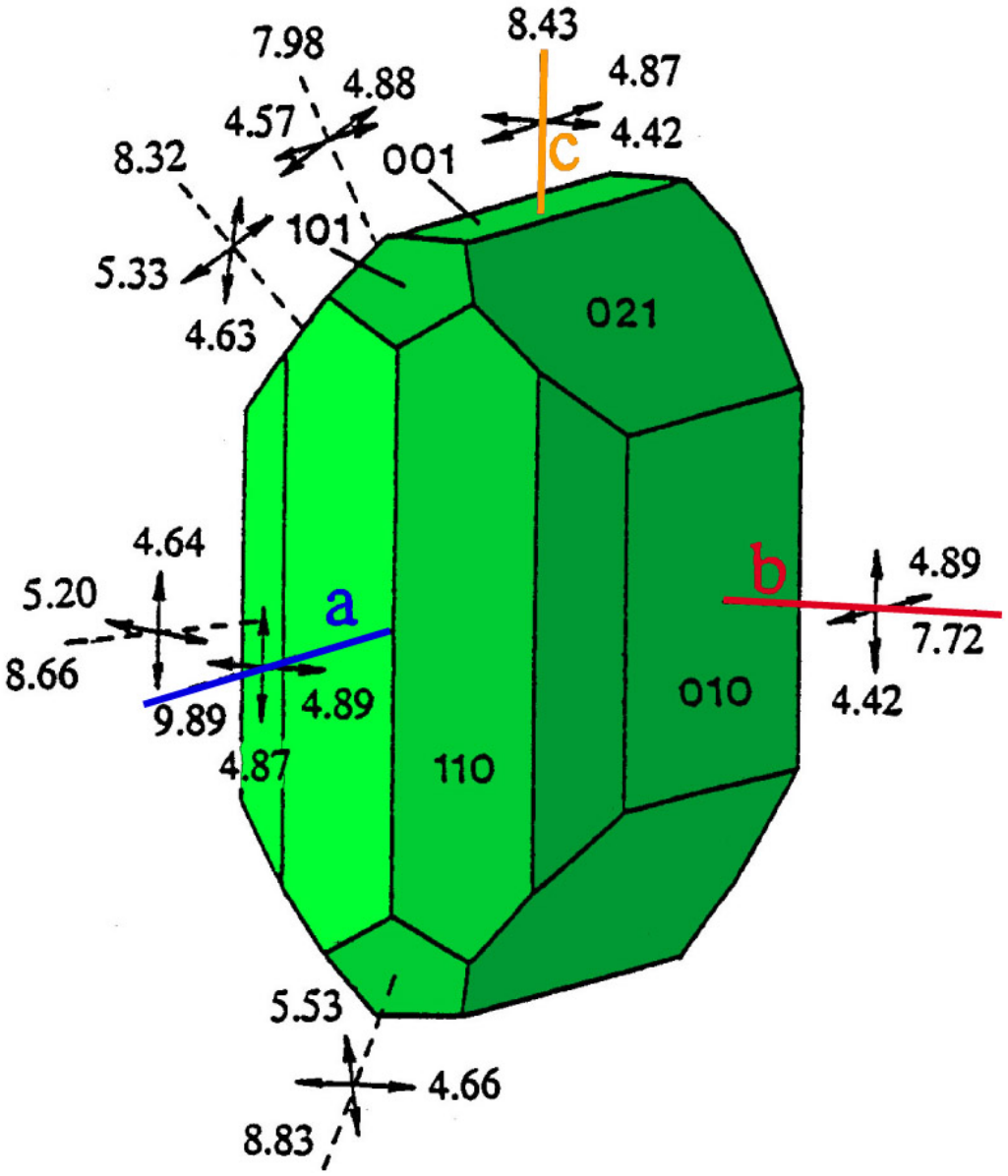
7.98
4.88
4.57
8.32
5.33
4.63
8.43
4.87
4.42
c
001
101
021
4.64
5.20
8.66
a
9.89
4.89
4.87
110
b
4.89
7.72
4.42
010
5.53
4.66
8.83

Olivine 3D to 2D projection

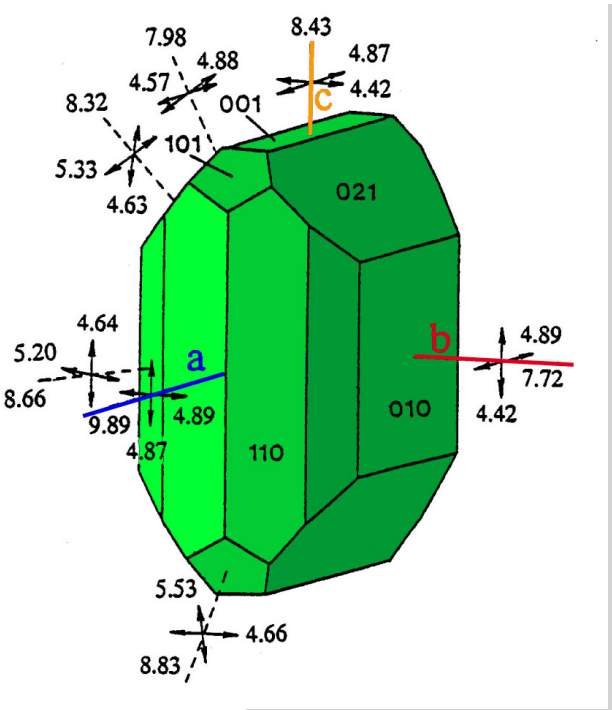

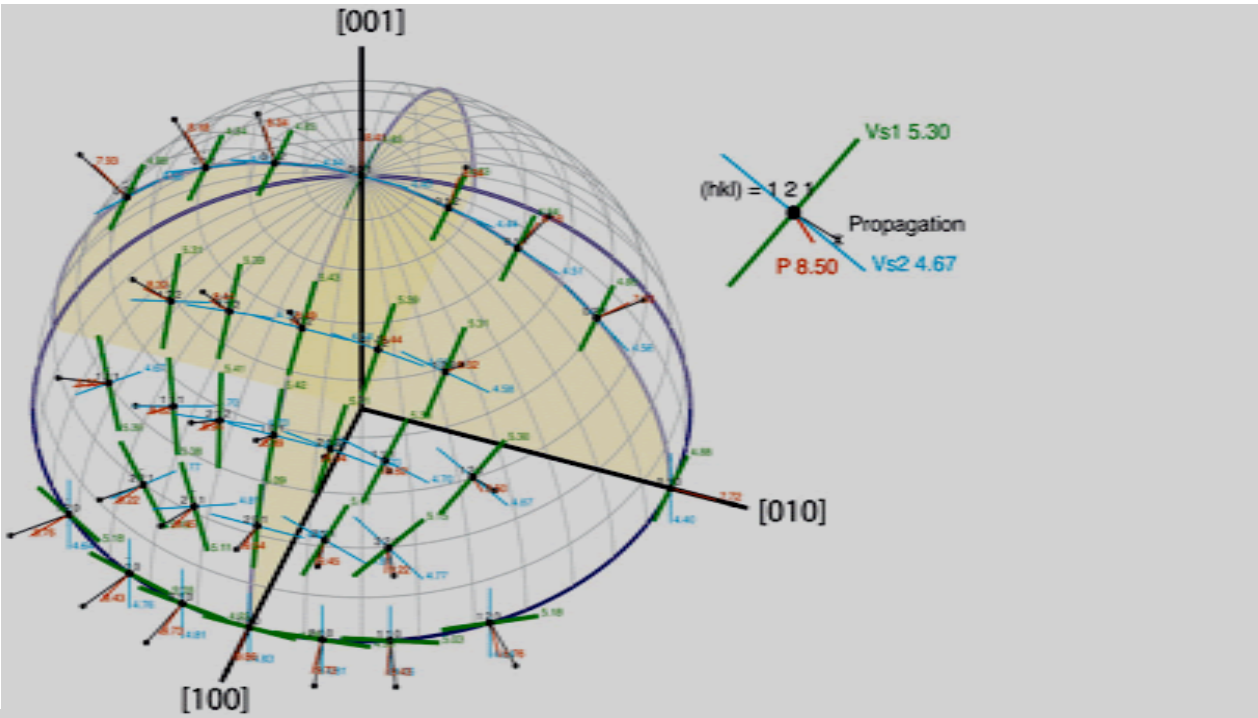

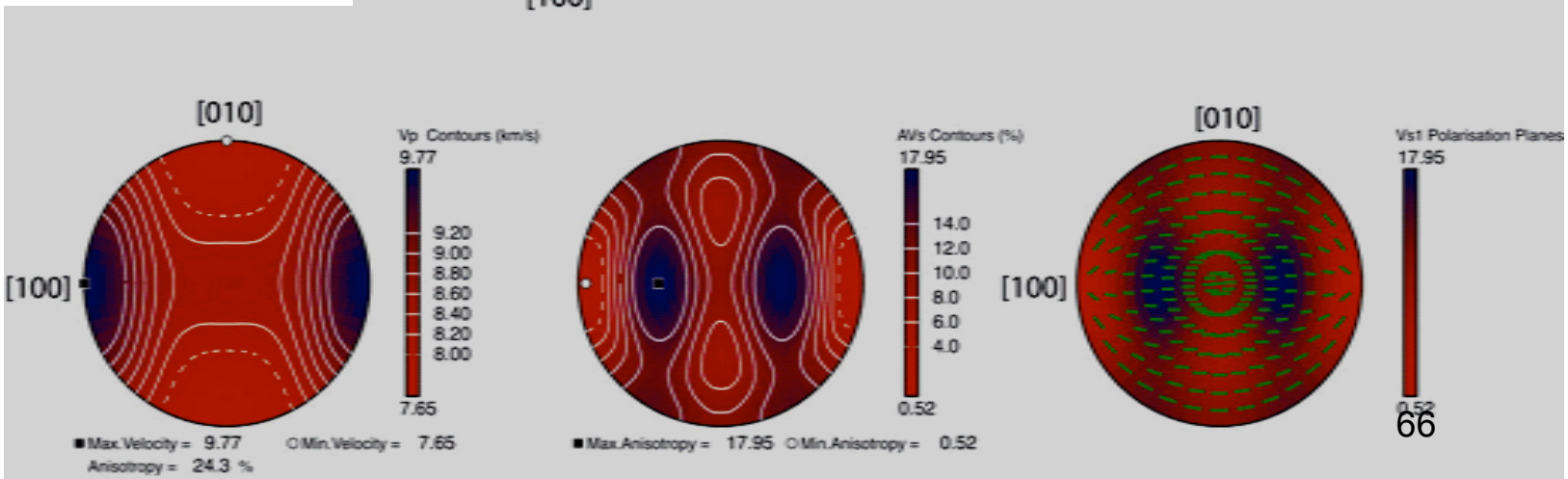

Upper Mantle (0- 410 km)

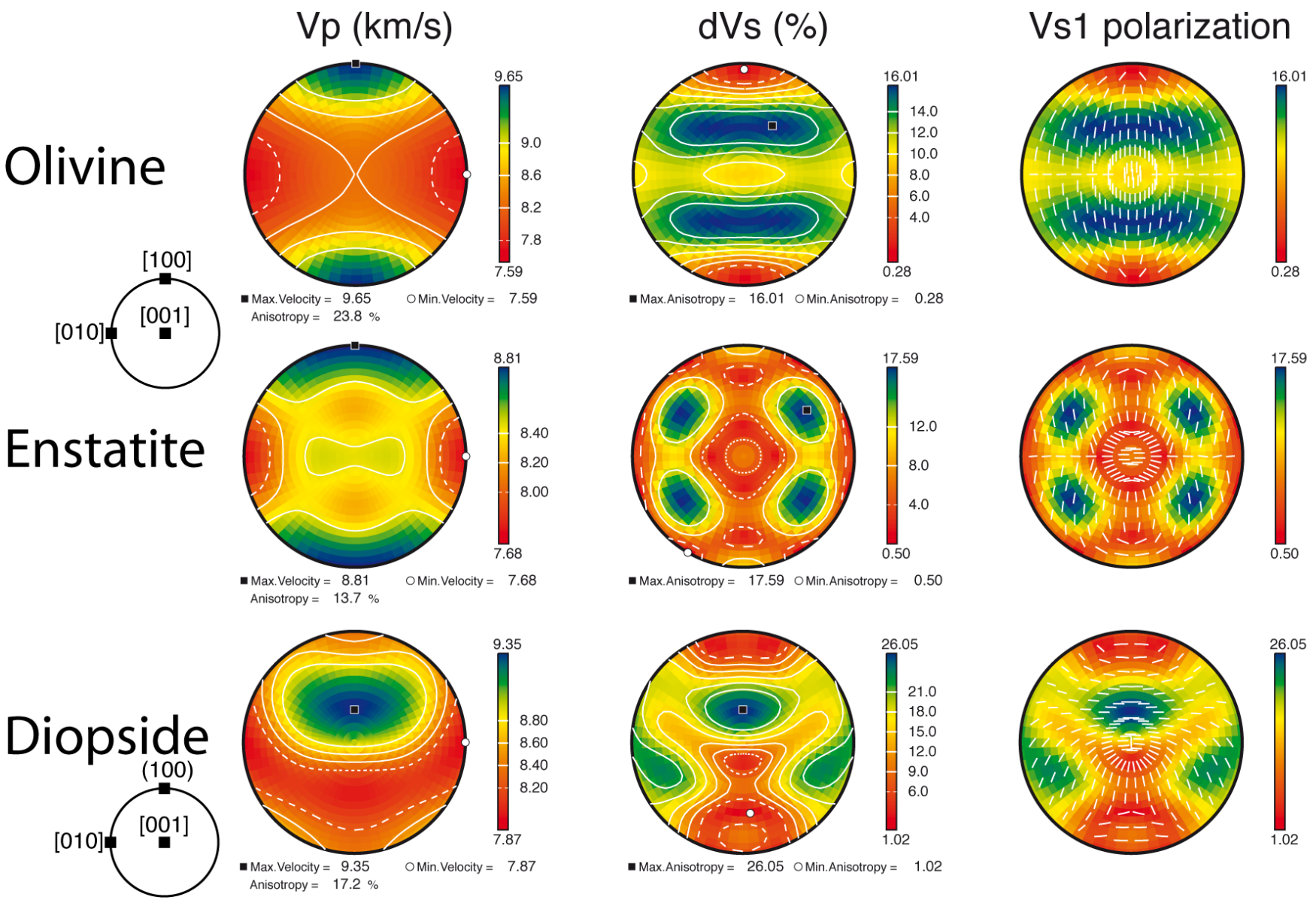

Transition zone (410-670 km)

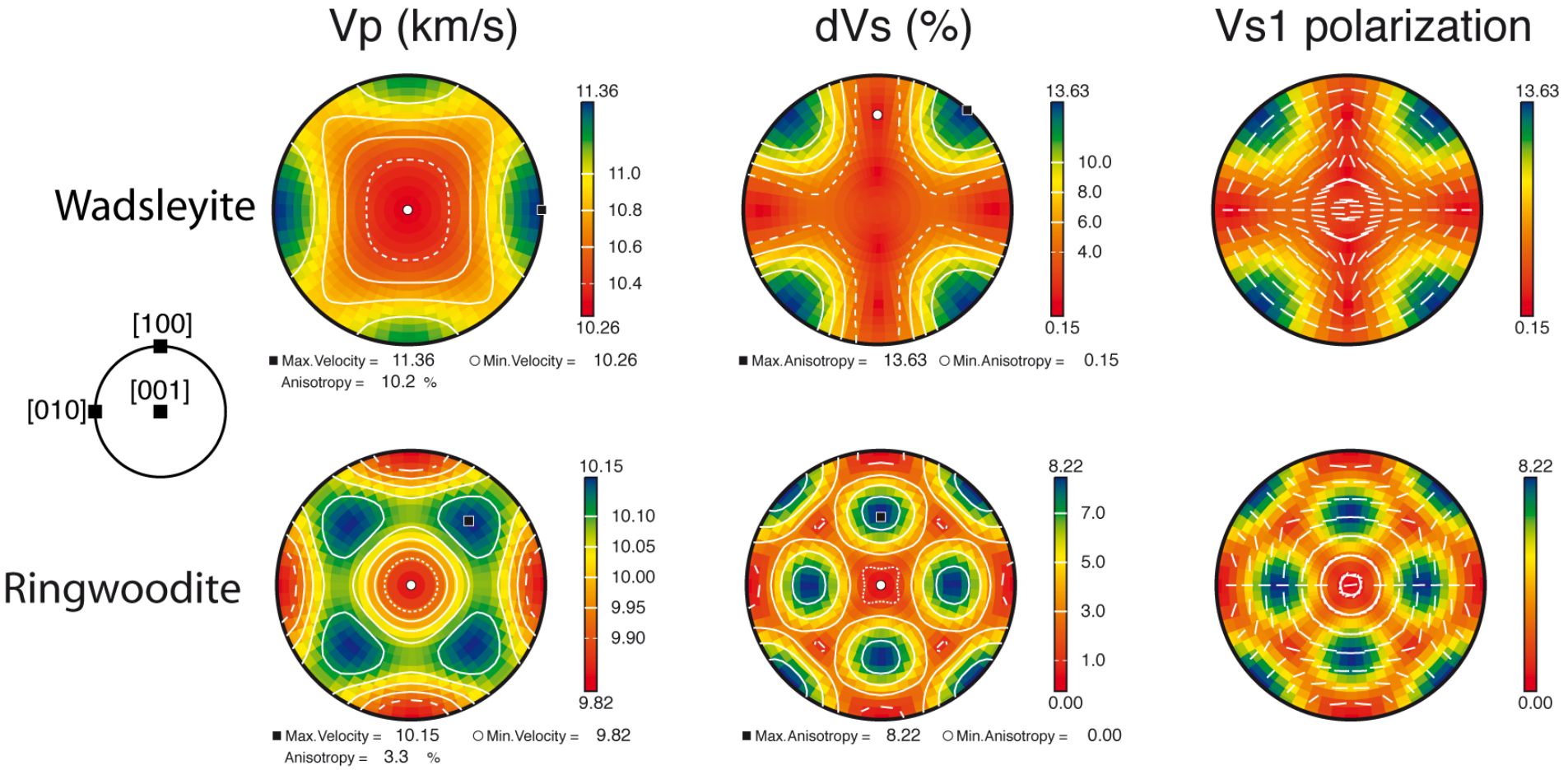

Lower Mantle (670-2800 km)

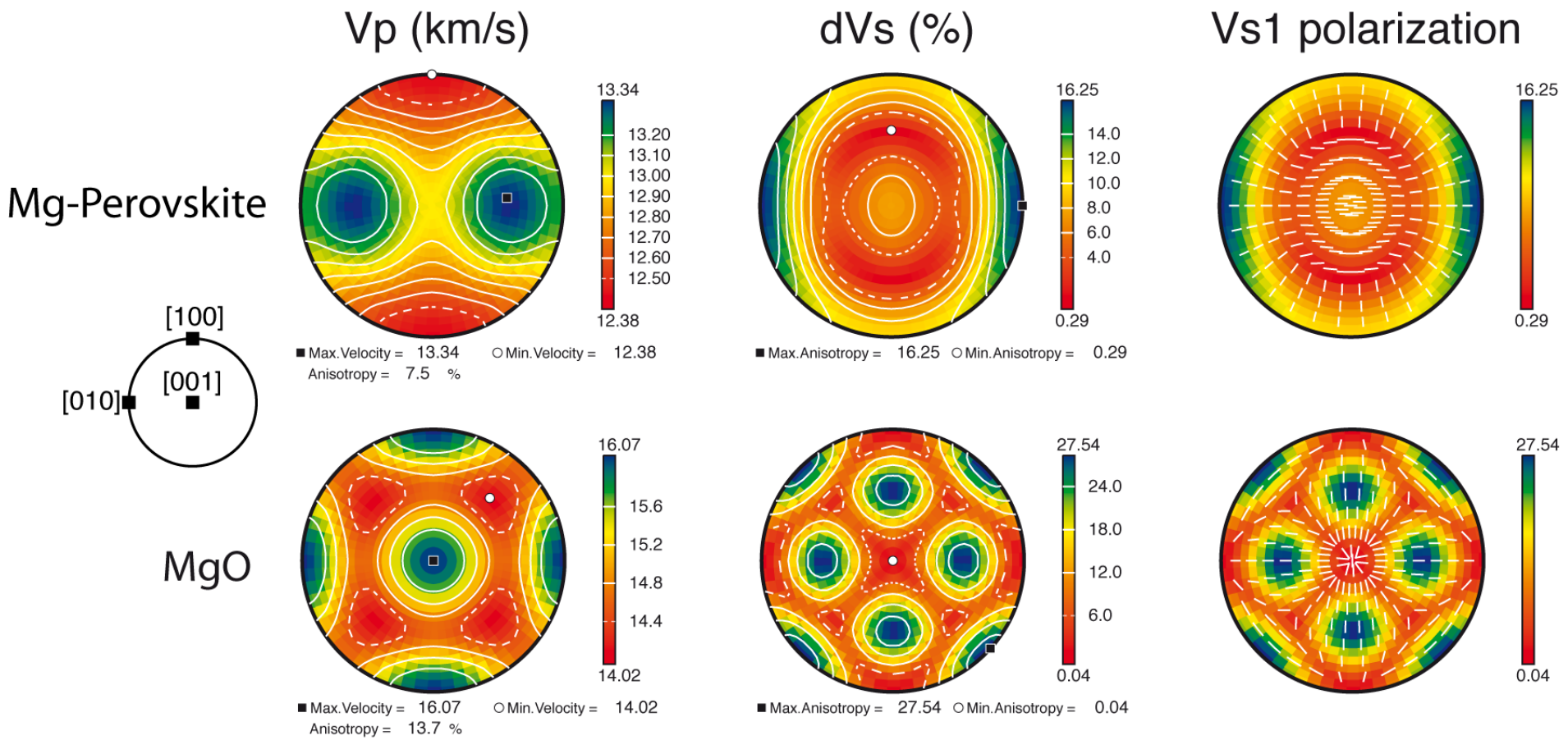

Trigonal/Rhombohedral C14

Single Crystal α-Quartz

C14 is negative
Standard value

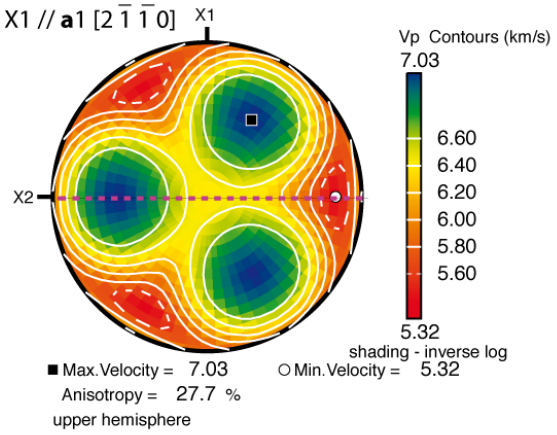

C14 is zero
Hexagonal elastic symmetry

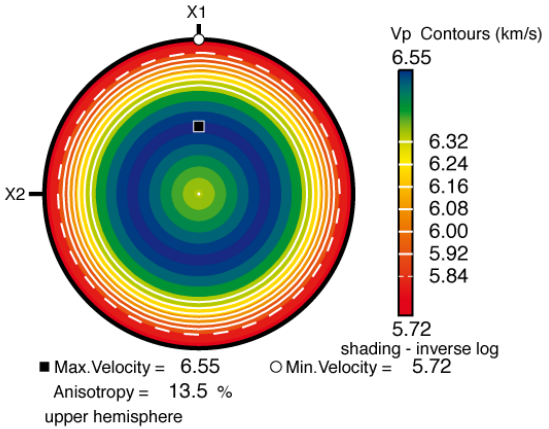

C14 is positive
60° or 180° rotation

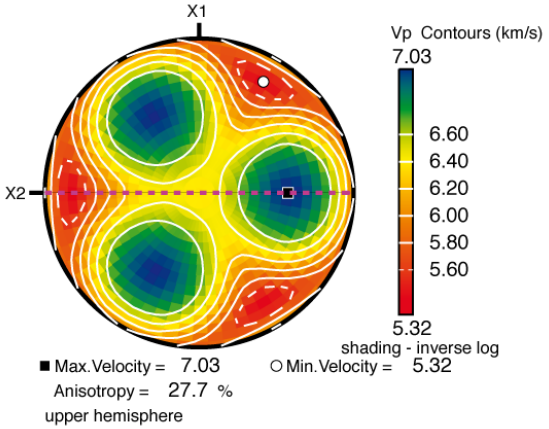

Single Crystal Calcite

C14 is negative
Not standard value
Reverse setting

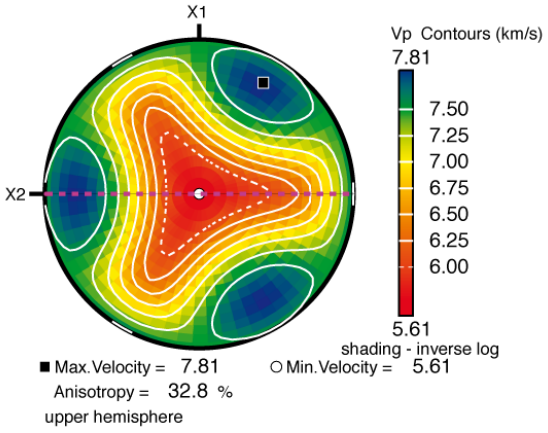

C14 is zero
Hexagonal elastic symmetry

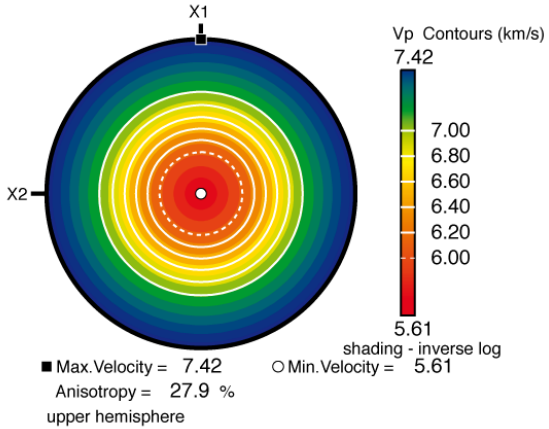

C14 is positive
60° or 180° rotation
Standard value
Obverse setting

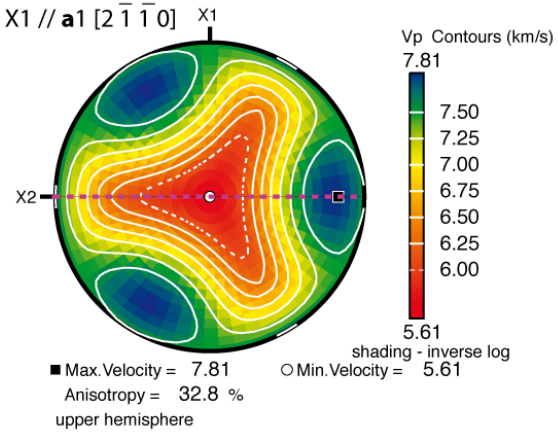

Background for calcite 1

Table

Computed and experimental stiffness coefficients for calcite. See Section 3.2 for the explanation of the different signs of C_{14}.

C_{11}	C_{12}	C_{13}	C_{14}	C_{33}	C_{44}	(GPa)
159	70	63	+20	98	39	calculated ab-initio with data in Table 3
144	54	51	−21	84	34	exptl. from Landoldt-Börnstein [16]

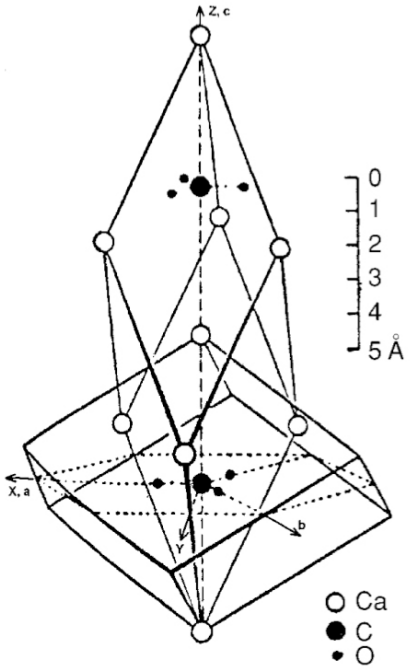

Composite of Fig. 1 from Kaga [18] and Fig. 140 p. 292 in [26]. In the axes shown on the Figure, the slender primitive rhombohedron indexes as form $\{01\bar{1}1\}$ rather than $\{10\bar{1}1\}$ as it should for an obverse setting of the rhombohedral lattice in the hexagonal axes. Kaga [18] (and therefore all other post-1949 authors who report a negative value for C_{14}) then used the reverse setting of the rhombohedral lattice

LePage et al (2002) phys. stat. sol. (b) 229, No. 3, 1155–1161

Background for calcite 2

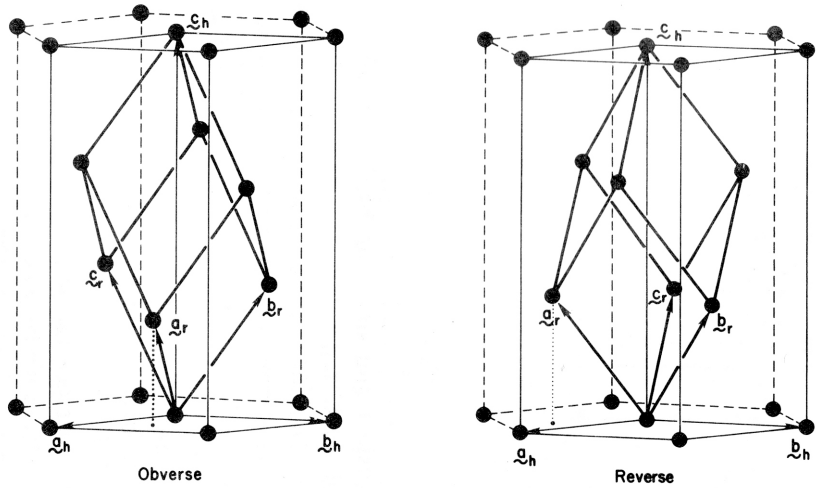

Obverse setting to Reverse is 180° rotation about the c-axis

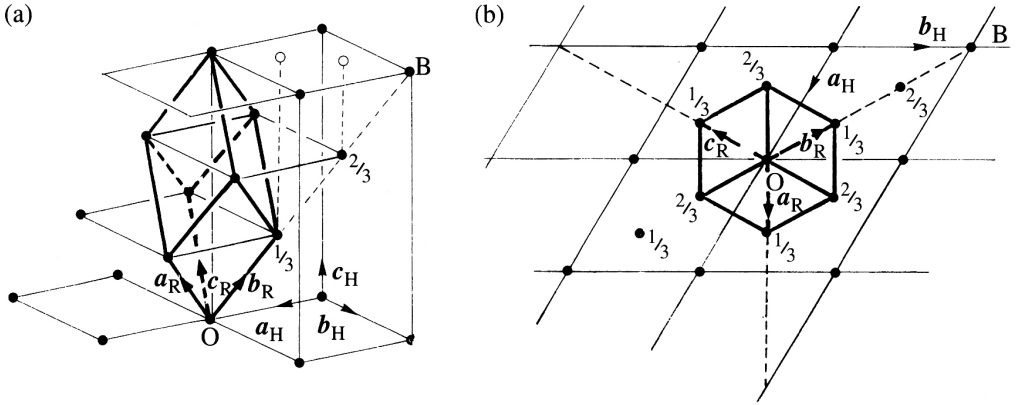

Rhombohedral lattice. The basis of the rhombohedral cell is labelled $\boldsymbol{a}_R$, $\boldsymbol{b}_R$, $\boldsymbol{c}_R$, the basis of the hexagonal centred cell is labelled $\boldsymbol{a}_H$, $\boldsymbol{b}_H$, $\boldsymbol{c}_H$ (numerical fractions are calculated in terms of the $\boldsymbol{c}_H$ axis). (a) Obverse setting; (b) the same figure as in (a) projected along $\boldsymbol{c}_H$.

References – Tensors and Crystal Physics

- Bhagavantam, S., Crystal Symmetry and Physical Properties , London, New York, Academic Press (1966)
- Cady, W. G. Piezoelectricity: An Introduction to the Theory and Applications of Electromechanical Phenomena in Crystals, New rev. ed., 2 vols. New York: Dover, 1964.
- Curie, P., Oeuvres , pp. 118, Paris, Société Français de Physique (1908)
- Hartmann,E. 1984, An Introduction to Crystal Physics, International Union of Crystallography Teaching Pamphlet 18
- http://www.iucr.org/iucr-top/comm/cteach/pamphlets.html
- D.R.Lovett Tensor properties of Crystals, Institute of Physics Publishing, Bristol and Philadelphia, 2nd Edition 1999
- **D.McKie and C.McKie Essentials of Crystallography, Blackwell Scientific Punlishing, 1986**
- **Mainprice, D. 2007 Seismic anisotropy of the deep Earth from a mineral and rock physics perspective. Schubert, G. 'Treatise in Geophysics' Volume 2 pp 437-492. Oxford: Elsevier.**
- **Nye, J. F., Physical Properties of Crystals , Oxford, Clarendon Press (1957)**
- **A.Putnis, 1992. Introduction to Mineral Sciences, Cambridge University Press (Chapter 2)**
- **Wenk, H.-R. and Bulakh,A., 2004. Minerals Their Constitution and Origin, Cambridge University Press. (Chapter 8)**

Useful web pages

- **AGU Bookshelf Reference Books**

http://www.agu.org/reference/minphys.html

- **Bilbao Crystallographic server (interactive)**

http://www.cryst.ehu.es/

- **American Mineralogist Table of Contents (old reference are free!)**

http://www.minsocam.org/MSA/AmMin/TOC/

- **American Mineralogist Crystal Structure Database (PDFs of publications are often associated with data files *.cif etc)**

http://rruff.geo.arizona.edu/AMS/amcsd.php

- **American Mineralogist Mineral PDFs**

http://rruff.geo.arizona.edu/doclib/hom/

- **Crystallography Open Database**

http://cod.crystallography.net/

- **Russian Crystallographic & chemical Database**

http://database.iem.ac.ru/mincryst/search.php?

- **Dictionary of Crystallography**

http://reference.iucr.org/dictionary/Main_Page

CAREWARE

- **Presently available Unicef CAREWARE programs**
- **For Mac and Windows :**
- **link ftp://www.gm.univ-montp2.fr/mainprice//CareWare_Unicef_Programs/**
- http://www.gm.univ-montp2.fr/PERSO/mainprice/
- **Pole Figures**
- **Inverse Pole Figures**
- **Anisotropic Elastic and Seismic properties**
- **Second Order Symmetric Tensor Properties**
- **Field work (az/inc) pole figures**
- All programs have a simple question and answer interface (no graphical interface with pull down menus) and are intended to produced publication or presentation ready graphics in Adobe Illustrator postscript.

Pole figure programs for data in Euler angle triplets

PF - general purpose program for Euler angle triplets
PFctf - for Channel 5 ASCII text export files (*.ctf)

Olivine pole figures

90OA65A

[100]

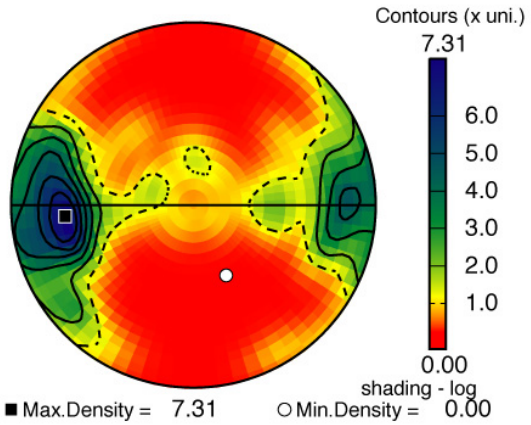

[010]

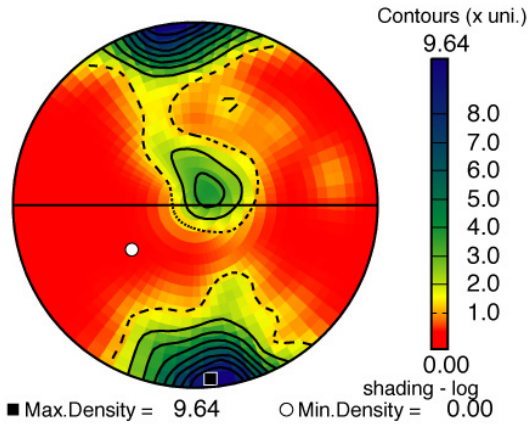

[001]

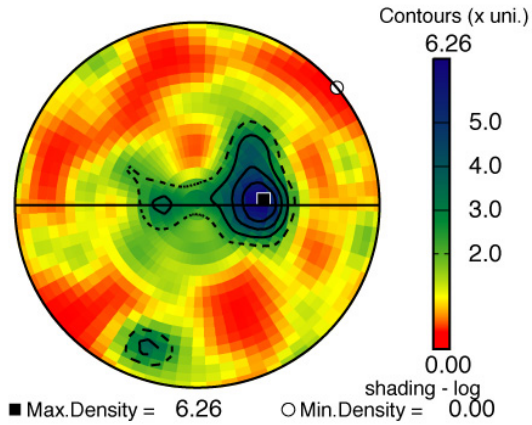

Seismic and elastic tensor properties for data in Euler angle triplets

Anis2k - data in Euler angle triplets

Anisctf - for Channel 5 ASCII text export file (*.ctf)

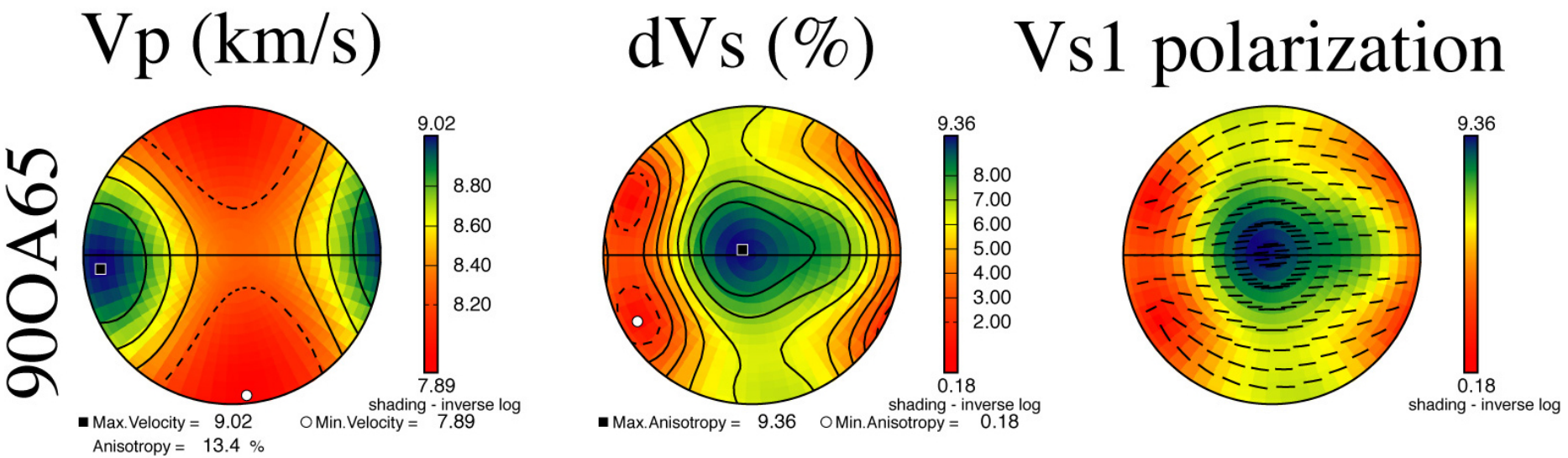

Anisotropic physical properties of rocks
Part II : Estimation of the anisotropic physical properties of rocks
2010

Introduction

Effective medium and anisotropy

Quantitative texture analysis and calculation of physical properties

Example : Olivine to Antigorite transformation

Introduction

- The calculation of the physical properties from microstructural information (crystal orientation, volume fraction, grain shape etc.) is important for rocks because it gives insight into the role of microstructure in determining the bulk properties.
- A calculation can be made for the in-situ state at high temperature and pressure for samples where the microstructure has been changed by subsequent chemical alteration (e.g. the transformation olivine to serpentine) or mechanically induced changes (e.g. fractures created by decompression). The in-situ temperatures and pressures can be simulated using the appropriate single crystal derivatives.
- Additional features not necessarily preserved in the recovered microstructure, such as the presence of fluids (e.g. magma) can be modeled.
- The effect of phase change on the physical properties can also be modeled using these methods.
- Modeling is essential for anisotropic properties as experimental measurements in the many directions necessary to fully characterize anisotropy is not currently feasible for the majority of the temperature and pressure conditions found in the deep Earth.

Effective medium and Anisotropy

Microscopic and Macroscopic

Microscopic

$C_i = \sigma_i \; e_i^{-1}$

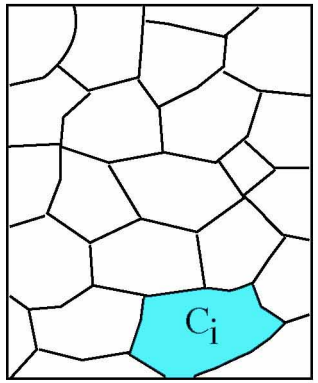

Macroscopic

$C^* = \langle \sigma \rangle \; \langle e \rangle^{-1}$

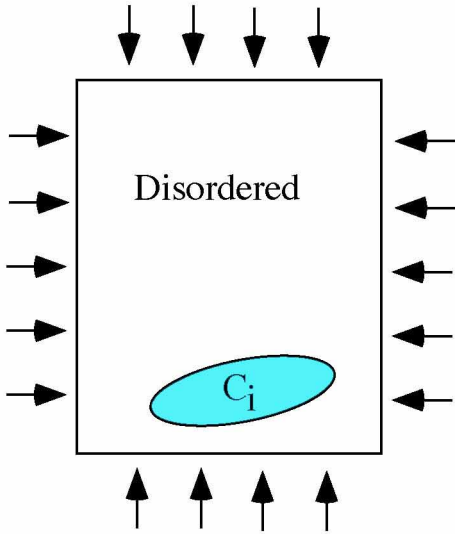

Homogeneous Effective Media (H.E.M.)

C^* = effective medium elastic constants

$\langle \sigma \rangle$ = volume averaged stress = $\Sigma V_i \sigma_i = \Sigma V_i (C_i e_i)$

$\langle e \rangle$ = volume averaged strain = $\Sigma V_i \; e_i$

Frequency, Wavelength and Representative Volume Element (RVE)

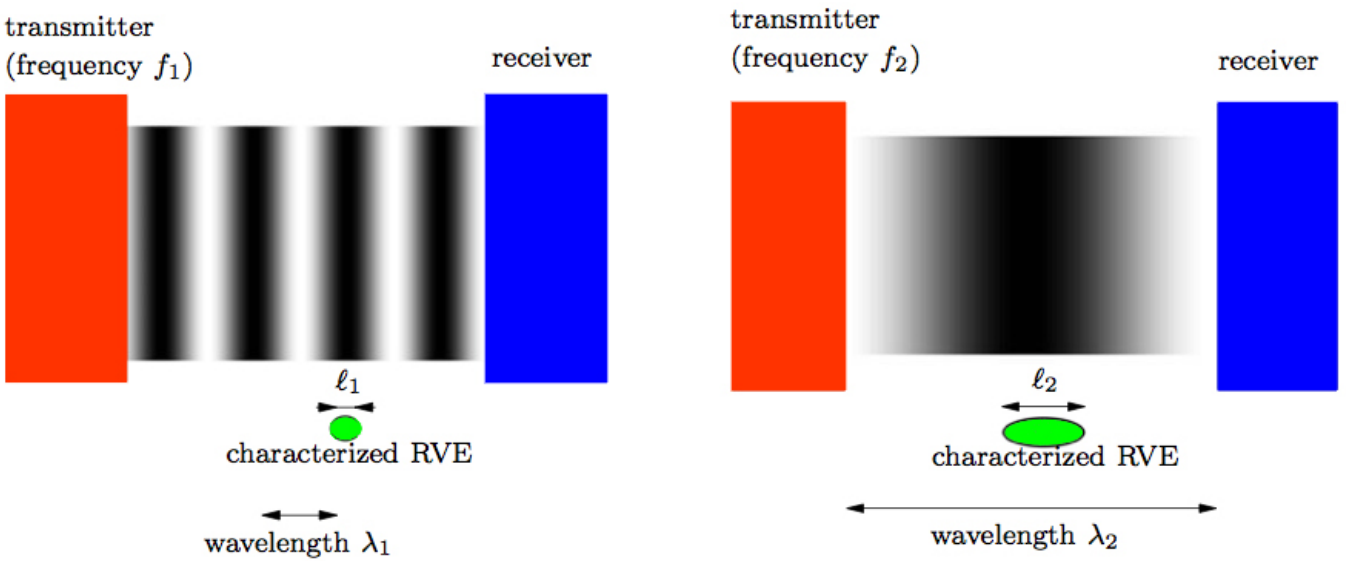

Schematic, grey-scale based illustration of stress magnitude in specimens tested ultrasonically with different frequencies ($f_1 > f_2$) (Fritsch and Hellmich 2007)

Length scale and effective medium

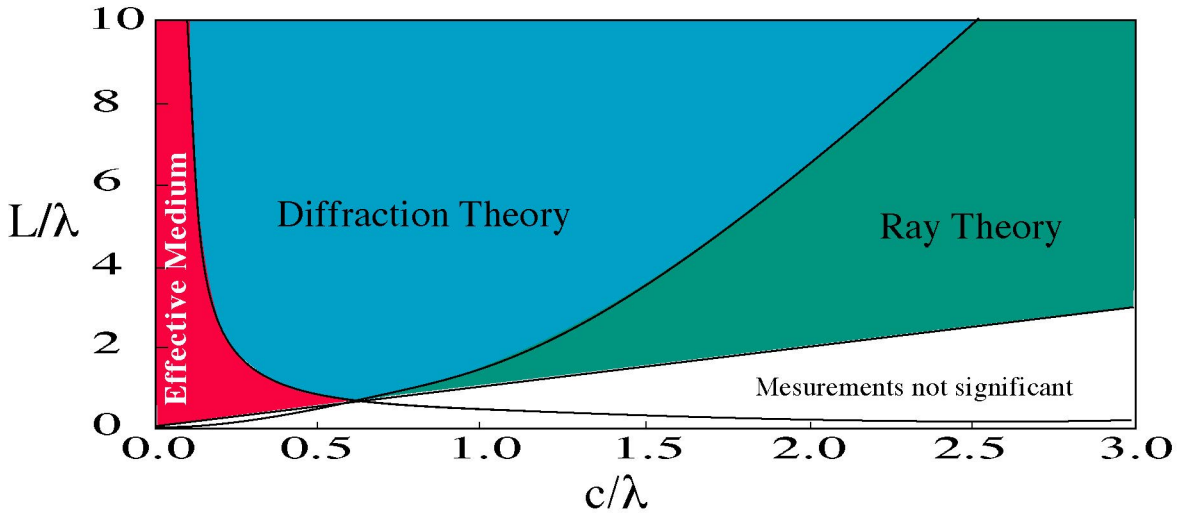

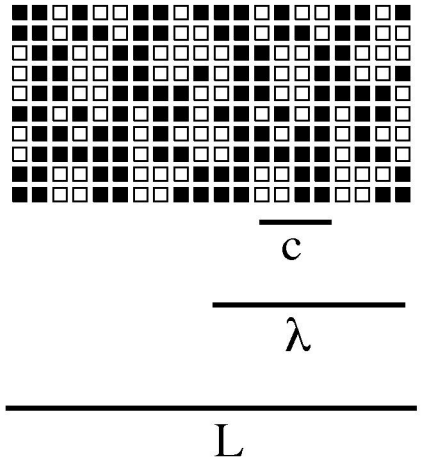

Effective medium $L > \lambda > c$

correlation length (motif)

dimension of physical phenomenon (e.g. seismic wavelength)

dimension of specimen (propagation distance)

Simple volume averages

Voigt Average

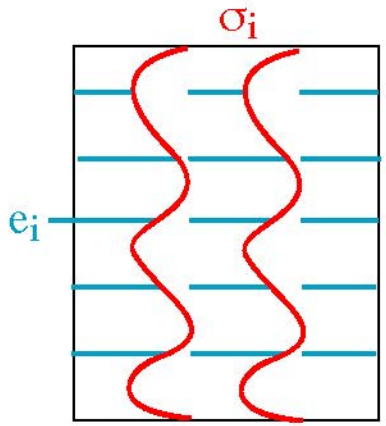

e_i = constant: $C^* \langle \sigma \rangle = \sum V_i (C_i \; e_i)$

$$C^* \approx C^{Voigt} = \sum V_i \, C_i$$

Reuss Average

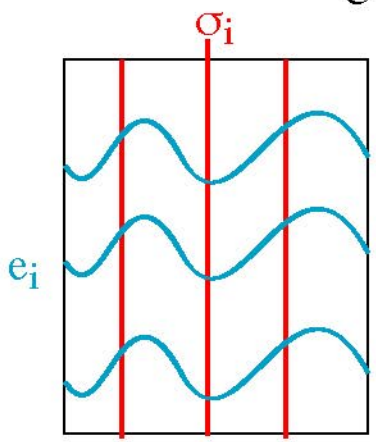

σ_i = constant: $C^* \; \langle e \rangle^{-1} = (\sum V_i \; e_i)^{-1} = (\sum V_i \; (S_i \; \sigma_i))^{-1}$

$$C^* \approx C^{Reuss} = (\sum V_i \; S_i)^{-1}$$

- easy to calculate
- widely separated bounds for strongly anisotropic minerals
- cannot introduce microstructure e.g. shape
- very poor bounds for mixtures with very different stiffnesses e.g. solids,liquids and voids

Relationships between Voigt and Reuss Averages

$$C^* \approx C^{\text{Voigt}} = \left[\sum_i V_i \; C(\mathbf{g_i})\right]$$

$$C^* \approx C^{\text{Reuss}} = \left[\sum_i V_i \; S(\mathbf{g_i})\right]^{-1}$$

$$S^* \approx S^{\text{Reuss}} = \left[\sum_i V_i \; S(\mathbf{g_i})\right]$$

$$C^{\text{Voigt}} \neq C^{\text{Reuss}} \quad \text{and} \quad C^{\text{Voigt}} \neq [S^{\text{Reuss}}]^{-1}$$

Voigt & Reuss micro-structural models

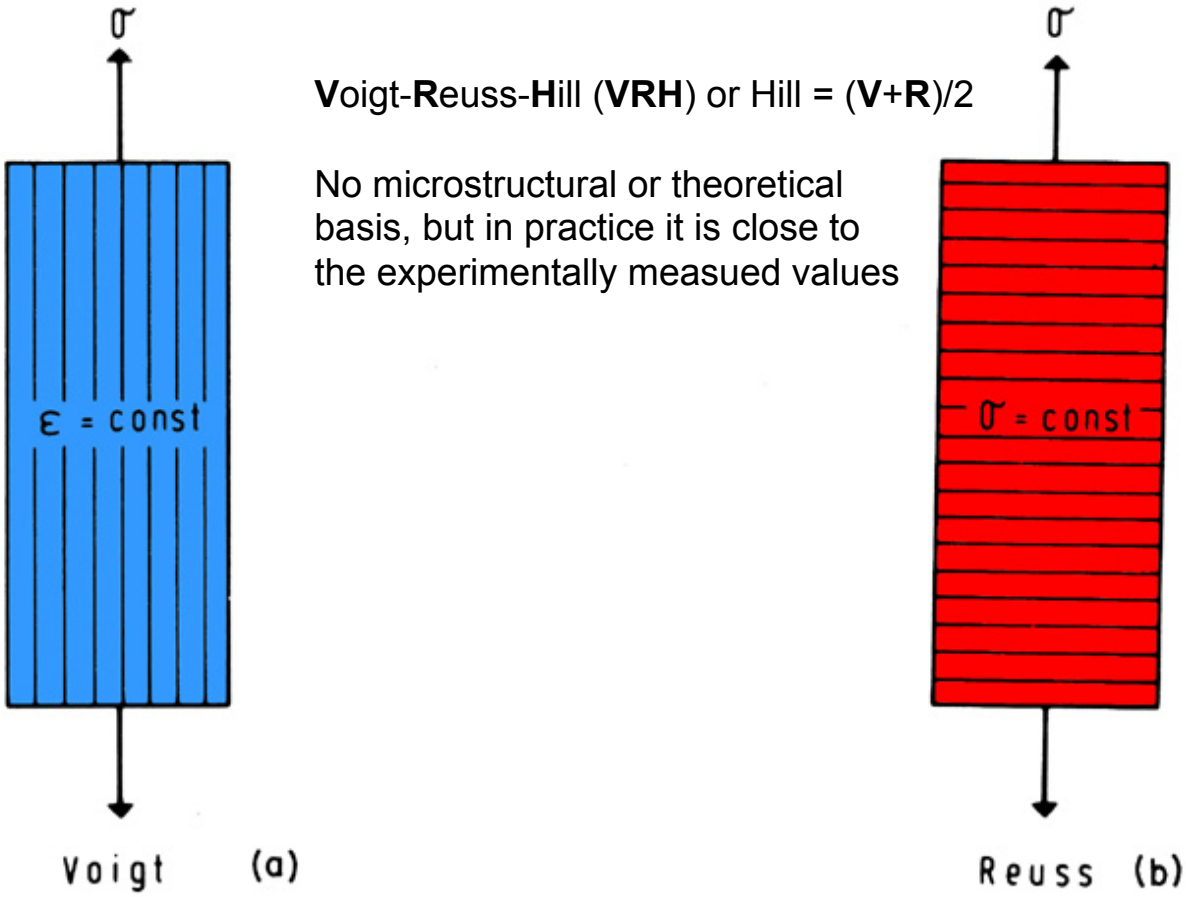

Voigt-**R**euss-**H**ill (**VRH**) or Hill = (**V**+**R**)/2

No microstructural or theoretical basis, but in practice it is close to the experimentally measued values

(a) Grain structure of a polycrystal for which Voigt's assumption is valid. (b) Grain structure of a polycrystal for which Reuss's assumption is valid.

Macromodel composite laminates

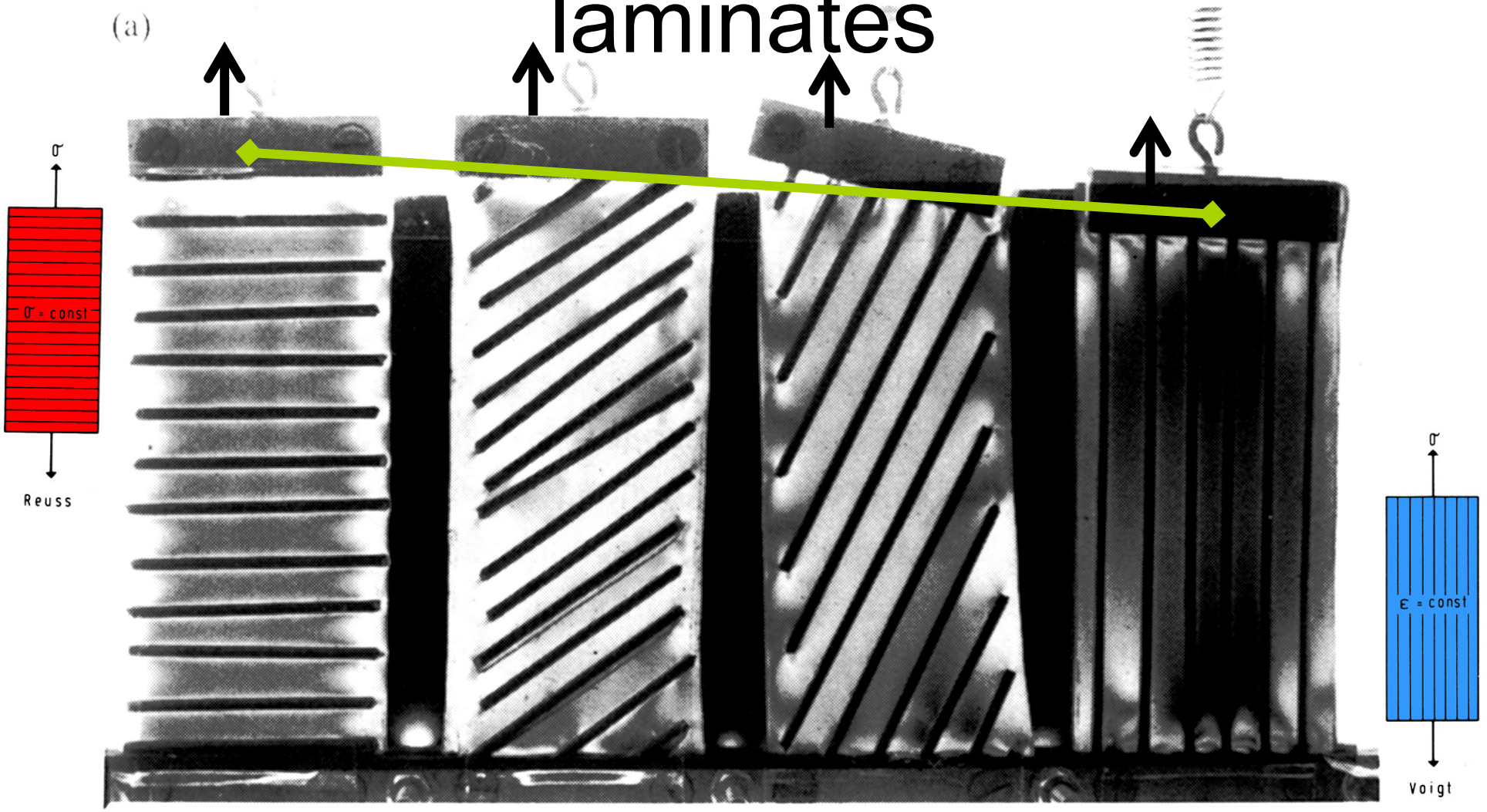

Aligned metal rods(black) in polyurethane matrix grey where lighter greys - larger shear strains

Vp Randomly Oriented Polycrystal Averages

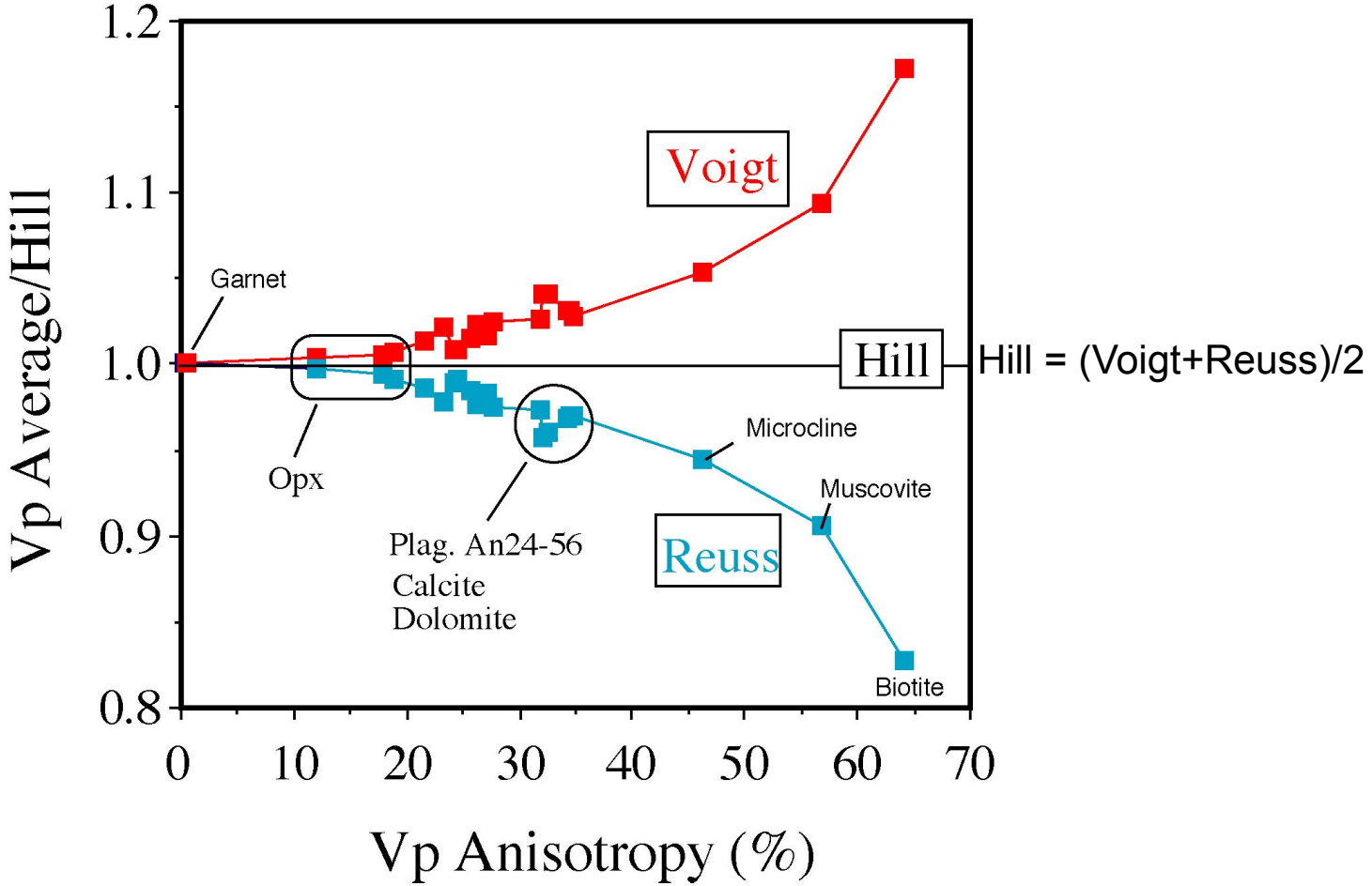

Mantle Minerals: Vp Anisotropy

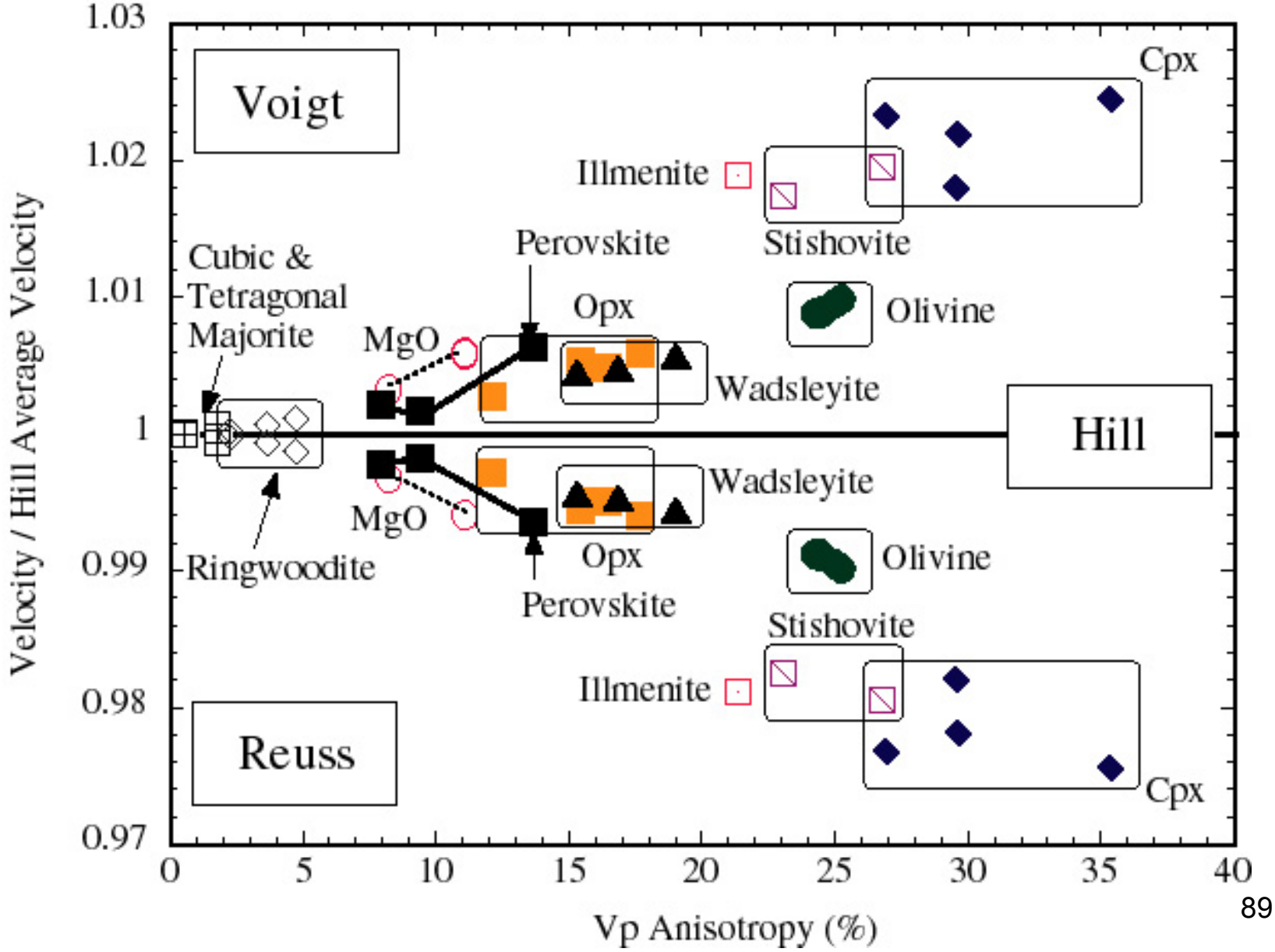

Mantle Minerals: Vs anisotropy

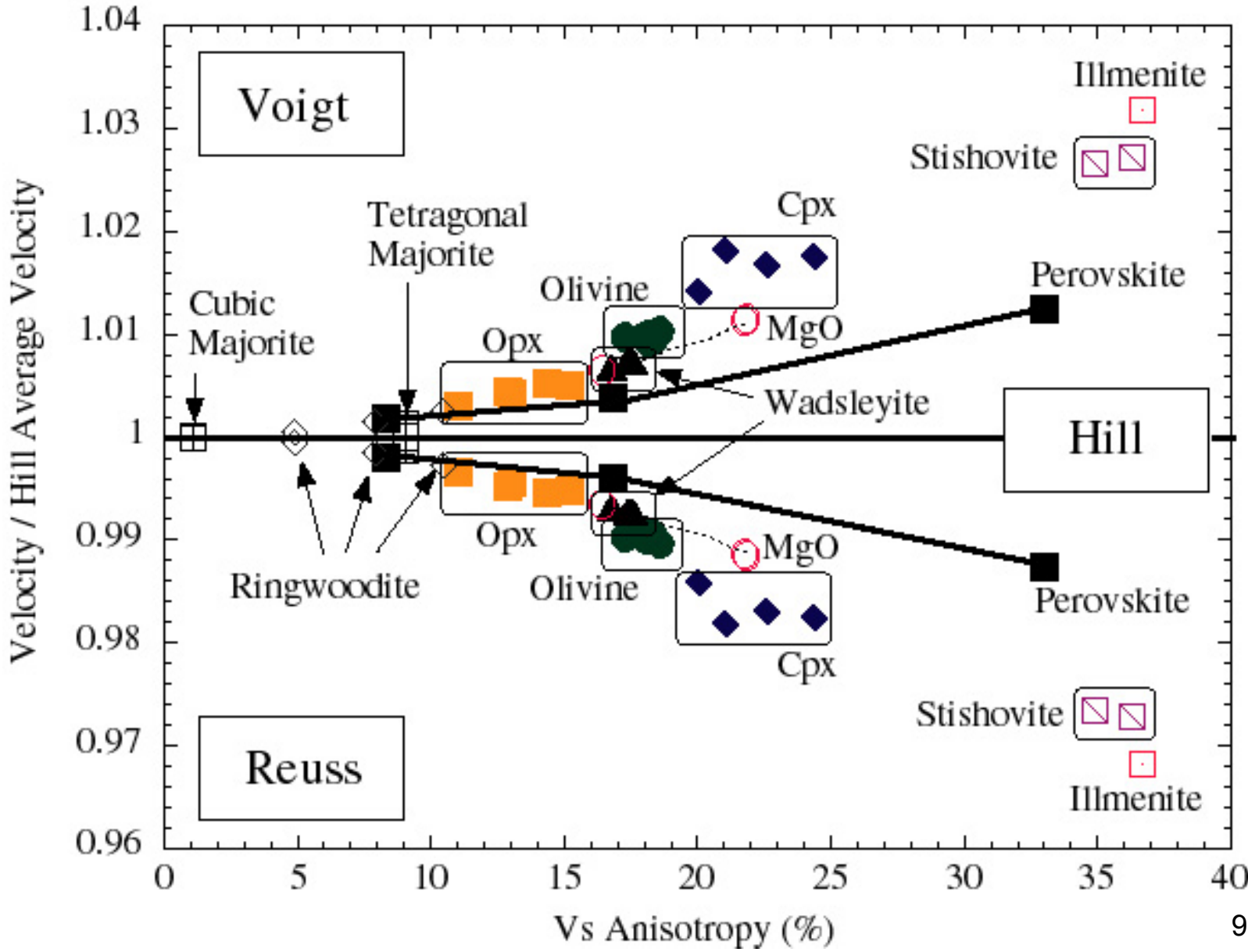

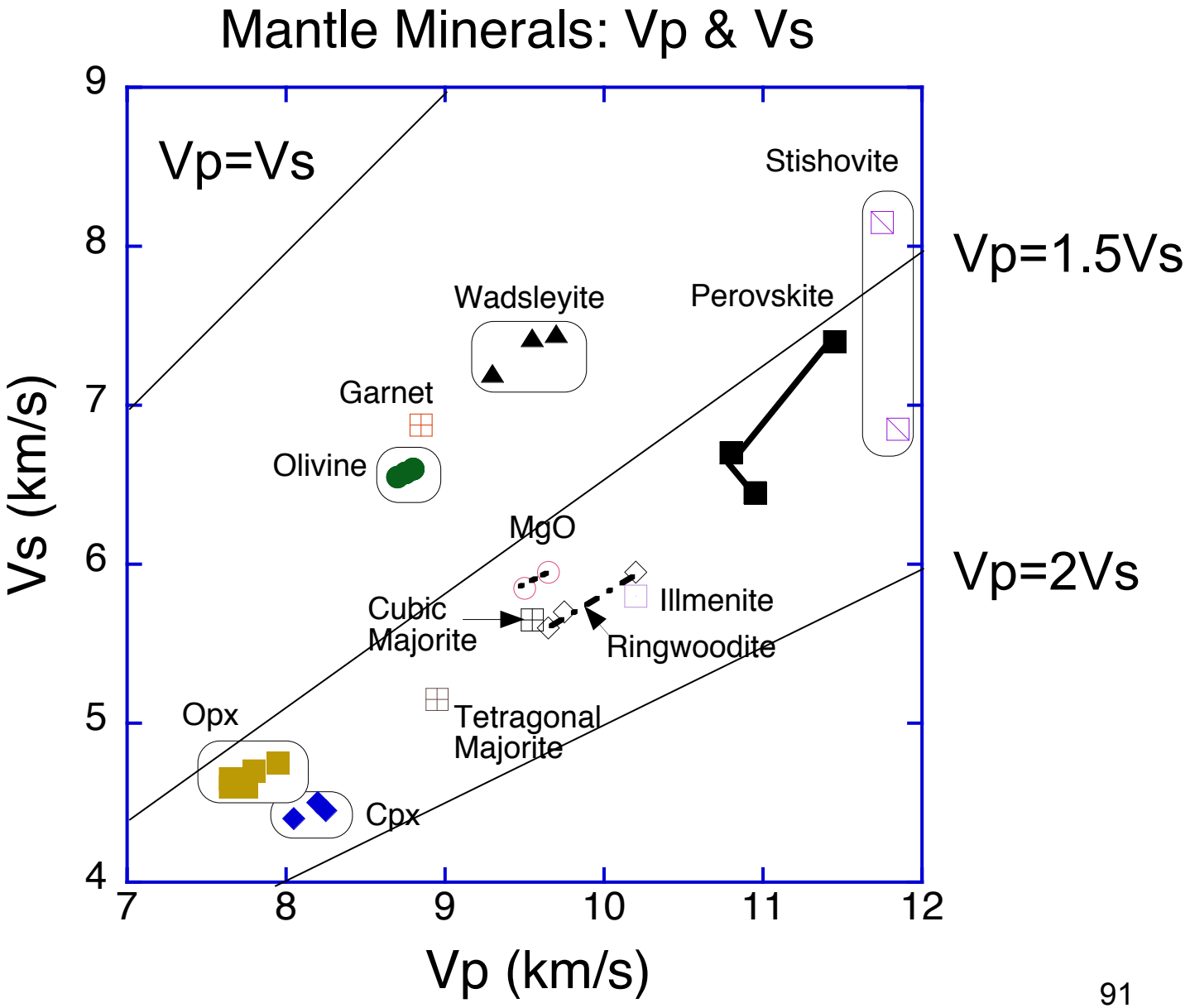
Mantle Minerals: Vp & Vs
Vp=Vs
Vp=1.5Vs
Vp=2Vs
Stishovite
Wadsleyite
Perovskite
Garnet
Olivine
MgO
Cubic
Majorite
Illmenite
Ringwoodite
Opx
Tetragonal
Majorite
Cpx
Vs (km/s)
Vp (km/s)
9
8
7
6
5
4
7
8
9
10
11
12

Mantle Minerals: Vp & Vs anisotropy

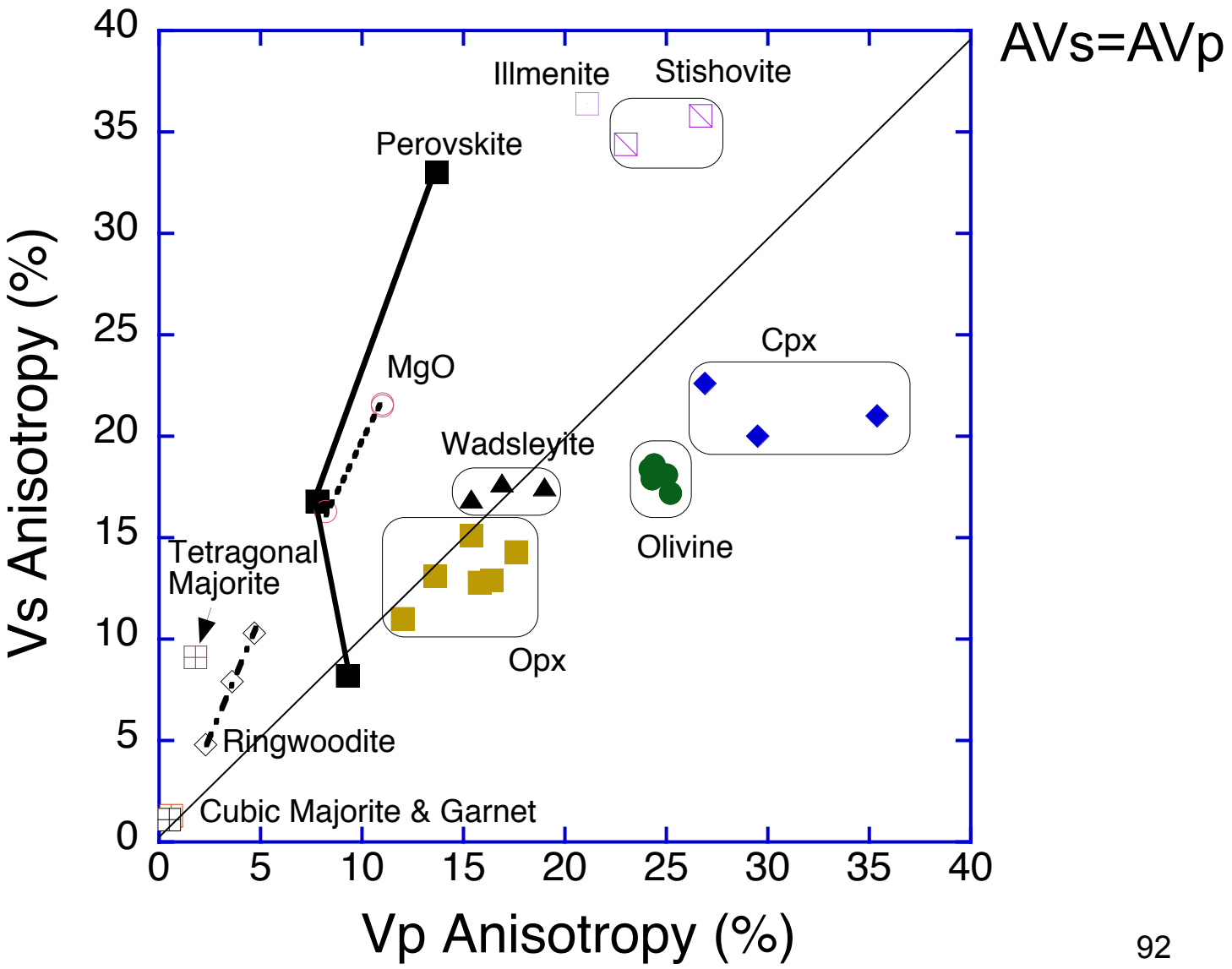

Oklahoma Gabbro
Stereo & Vp YZ profile

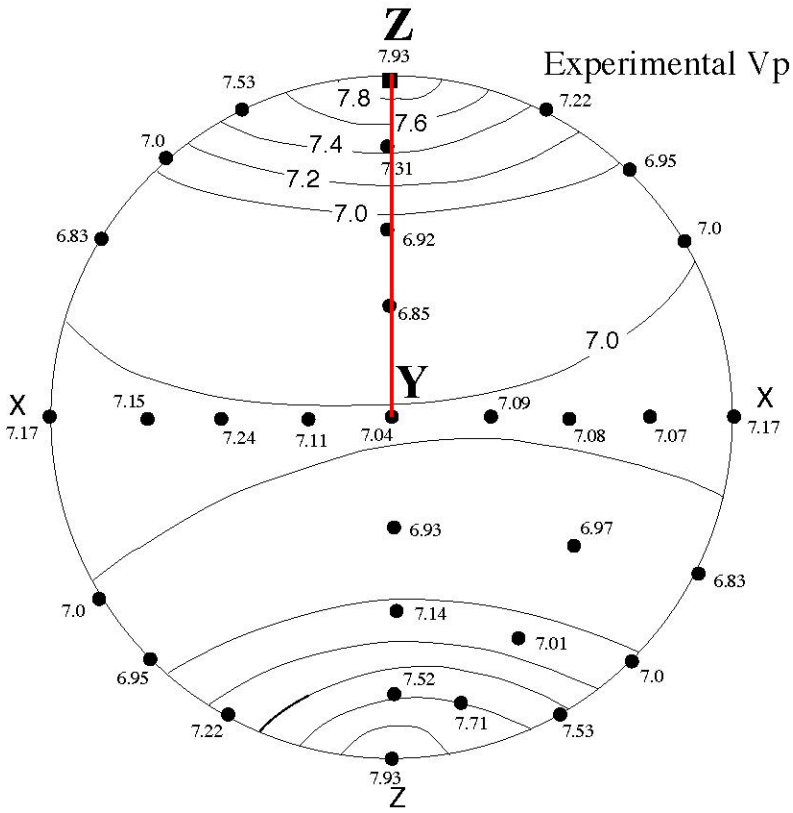

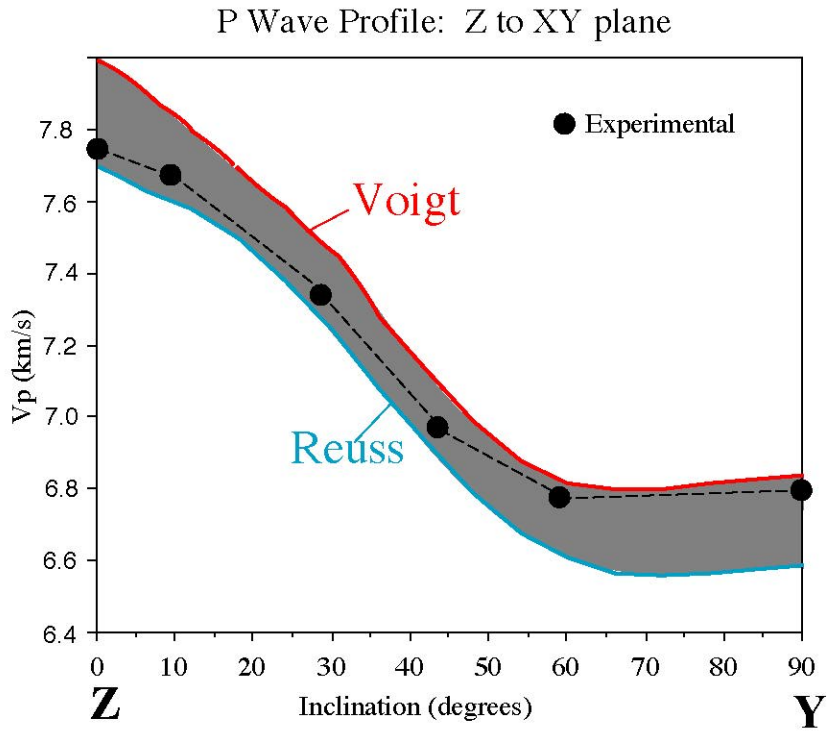

Confining pressure = 800 MPa

Physical Properties & Microstructure - Composite materials approach

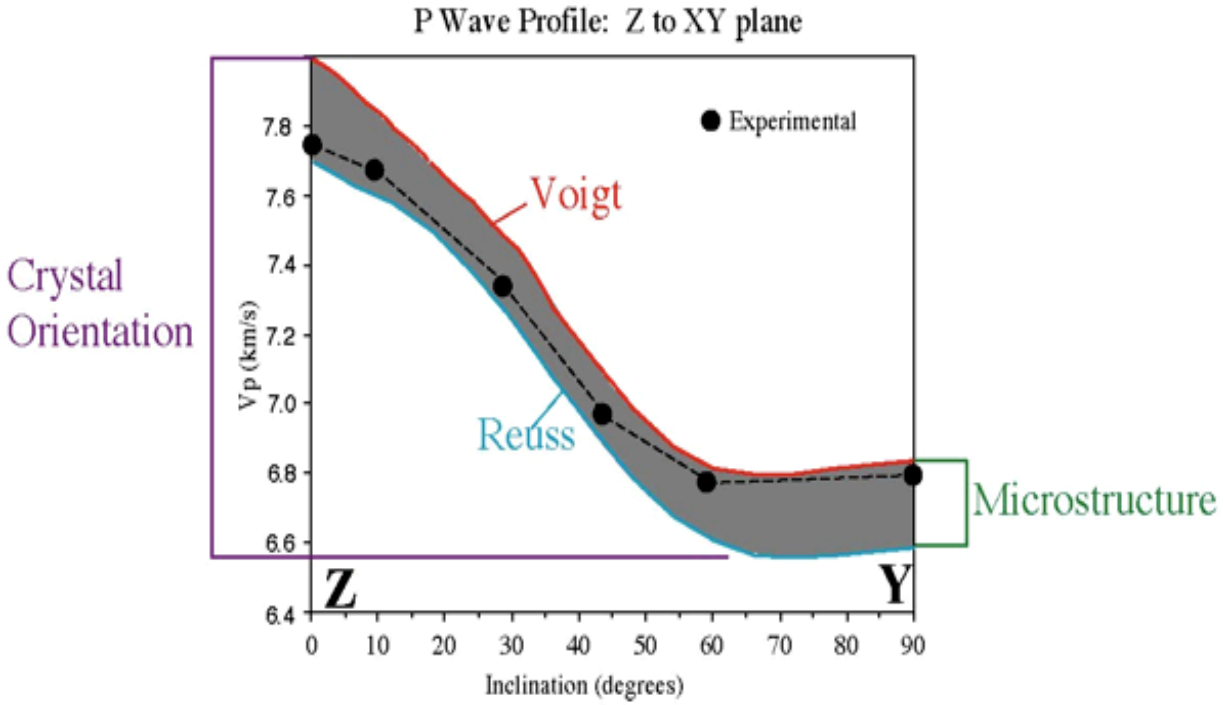

Crystal Orientation "signal" = 5 x Microstructure "signal"

Interaction between inclusions

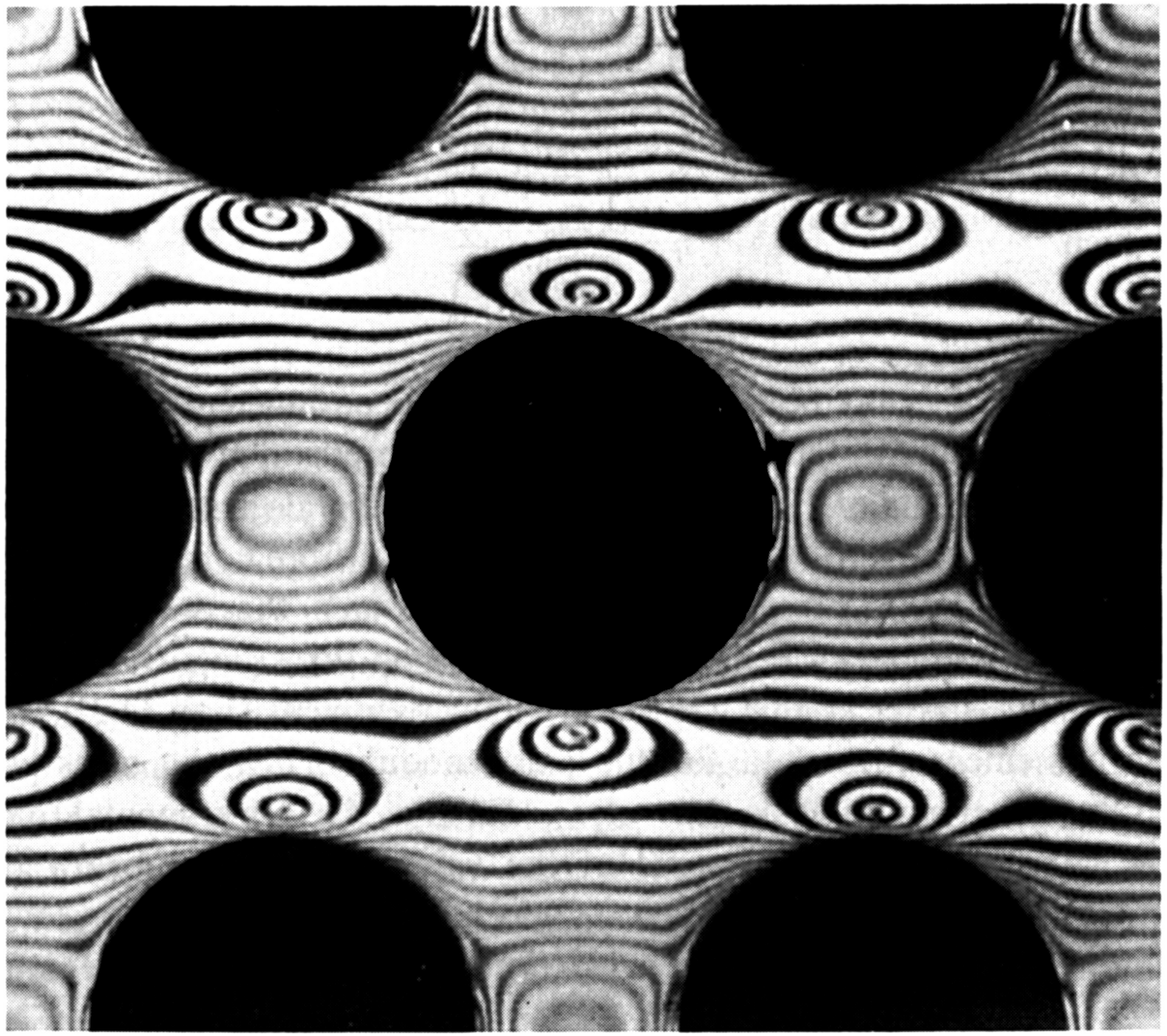

A photoelastic image (Puck 1967), showing isochromatic (equal birefringence) fringes for a macromodel composite loaded in transverse tension (vertical direction).

Ellipsoidal inclusion - special properties

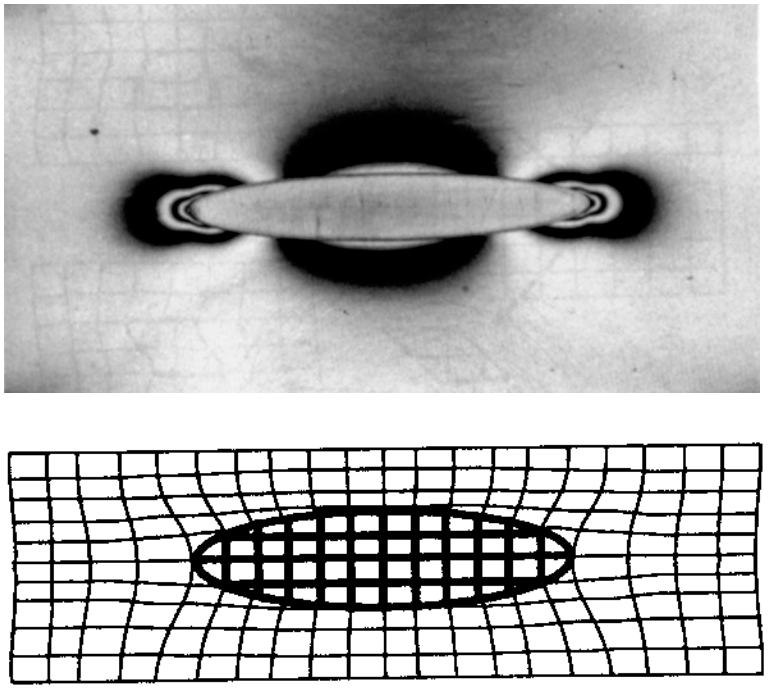

Uniform stress and strain field within the inclusion

Ellipsoid and Cylinder

homogeneous stress & strain fields

heterogeneous stress & strain fields

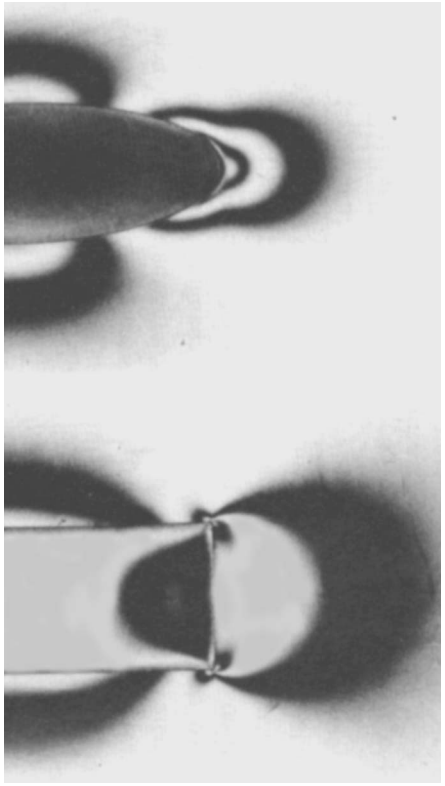

Self Consistent Method

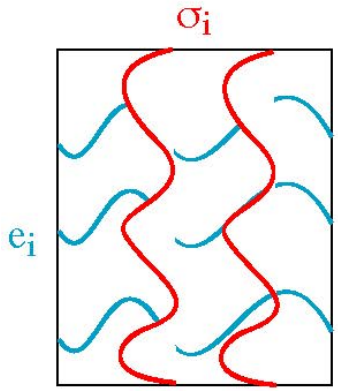

$e_i \neq$ constant $\sigma_i \neq$ constant : $C^* = <\sigma> <e>^{-1}$

$$C^* = <\sigma> <e>^{-1}$$

$$<\sigma> = \Sigma V_i (C_i e_i) \qquad <e> = \Sigma V_i e_i$$

$$C^* \approx C^{SC} = <\sigma> . <e>^{-1} = [\Sigma V_i (C_i e_i)] . [\Sigma V_i e_i]^{-1}$$

The value of e_i is found using a generalization of Eshelby's inclusion theory to anisotropic inclusions in anisotropic back ground media.

$$e_i = [\mathbf{I} + \mathbf{G} (C_i - C^*)]^{-1}$$

Where I is the 4^{th} rank idenity tensor and G is a Green's tensor involving ellipitical intergrals over the inclusion shape.

- much more complex to calculate
- "best" bounds for strongly anisotropic minerals
- can introduce microstructure e.g. shape via Green's tensor as ellipsiodal inclusion
- "best" bounds for mixtures with very different stiffnesses e.g. solids,liquids and voids
- treats every object (grain, void, fracture) in an identical manor
- further information about neighbour interaction could be introduced via two-point correlation functions

DEM Method

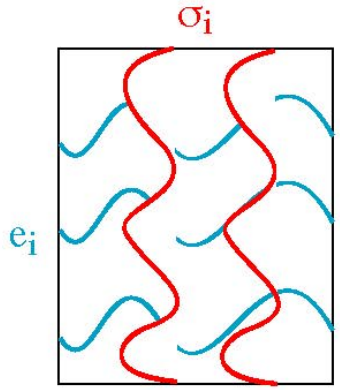

$e_i \neq$ constant $\sigma_i \neq$ constant : $C^* = <\sigma> <e>^{-1}$

$$C^* = <\sigma> <e>^{-1}$$

$$<\sigma> = \Sigma V_i (C_i e_i) \qquad <e> = \Sigma V_i e_i$$

$$dC^* \approx dC^{DEM} = \frac{dV_b}{(1-V_b)} (C_i - C^{DEM}) e_i$$

Developed for two phase aggregates type AB (McLaughlin,1977) where Vb = 1-Va. The phase B is the included phase and phase A is the host phase. Requires some inital value of C* at a compostion Vb - this may be a pure end member.The incremental nature of the differential approch preserves the percolating (connectivity) properties of the initial estimate. For example if starting from pure A, A will always be connnected. If starting from 50:50 A:B then both phases will be connected.

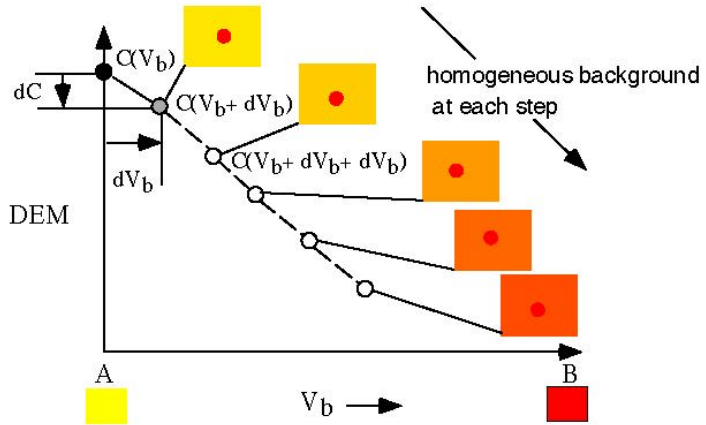

- now phases A and B are microstructurally different (A=Host, B= Inclusion)
- preserves connectivity of initial estimate

VpX and VpZ Gabbro - Basalt : Effect of Aspect Ratio

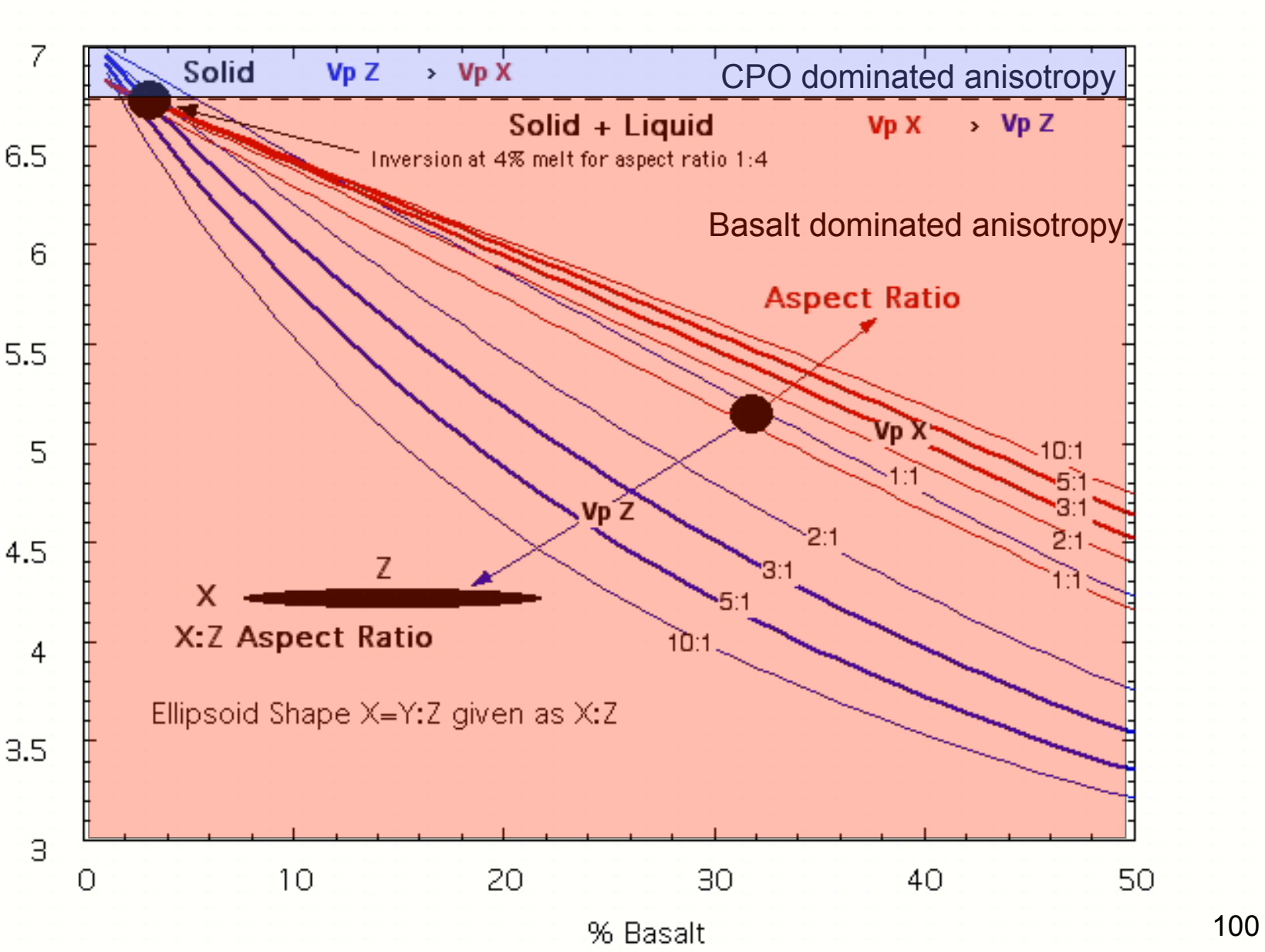

Hybrid Methods

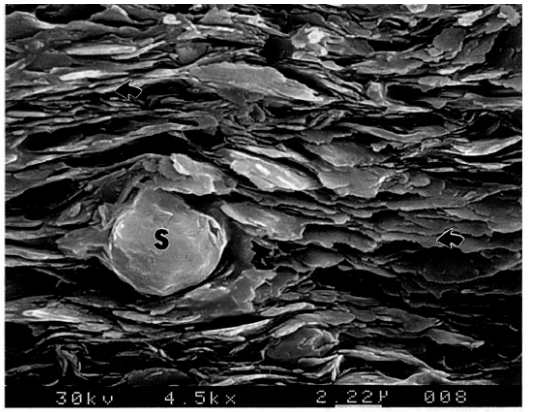

SEM photomicrographs of the fabric of the Williamson Shale- basinward facies graptolite black shale

Application of Combined SC and DEM : Percolating Fluid

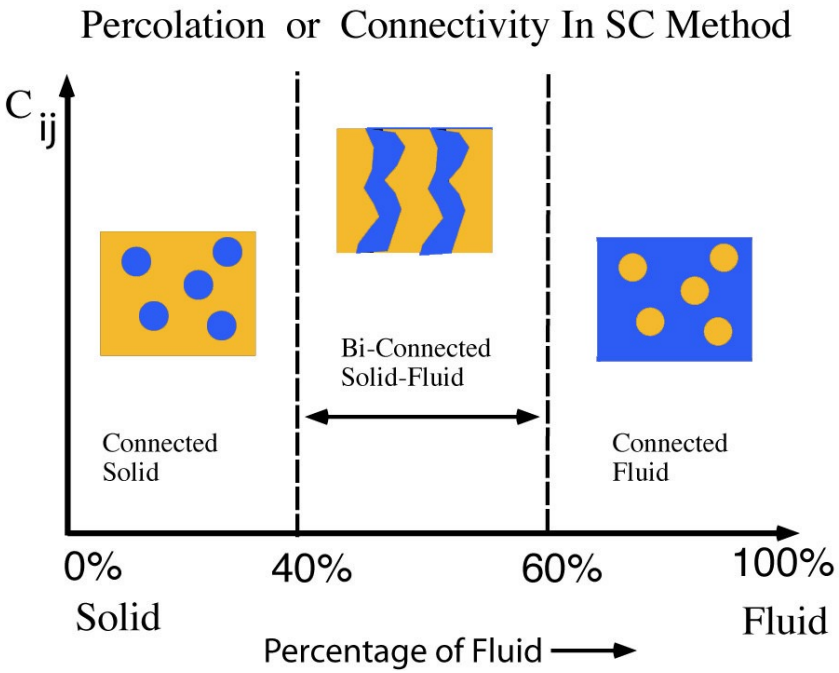

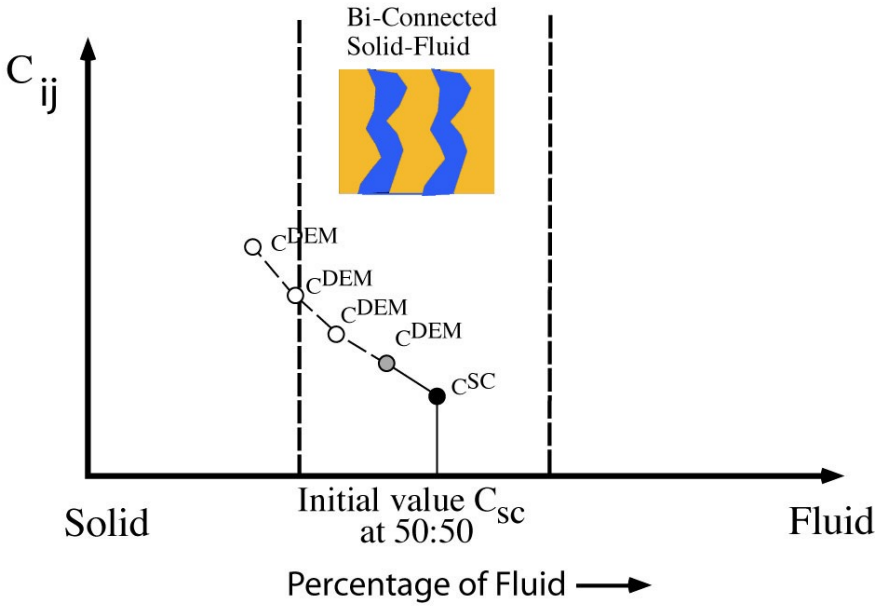

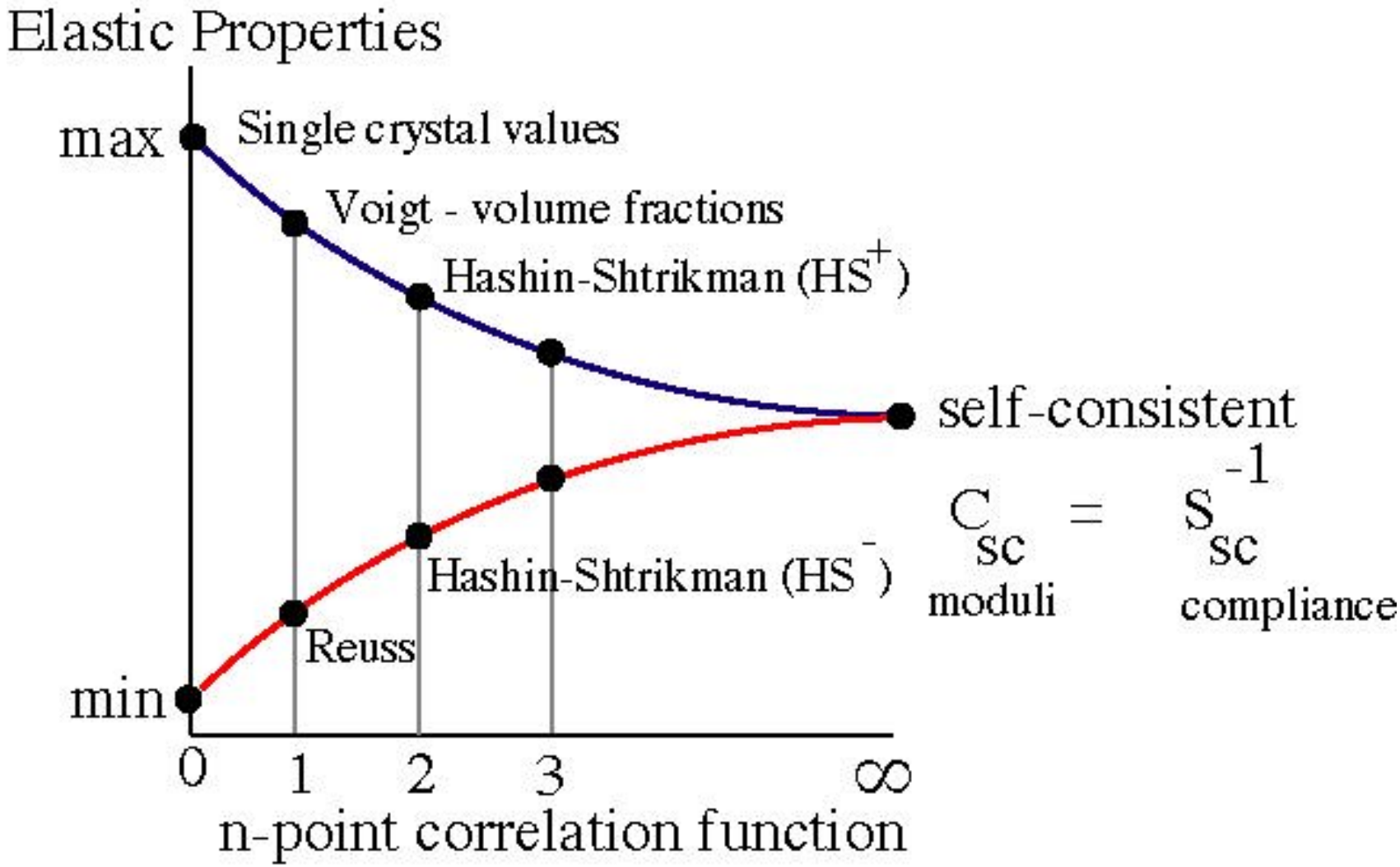
Elastic Properties
max
Single crystal values
Voigt - volume fractions
Hashin-Shtrikman (HS+)
self-consistent
C sc = S sc -1
moduli
compliance
Hashin-Shtrikman (HS-)
Reuss
min
0
1
2
3
∞
n-point correlation function

Cluster method

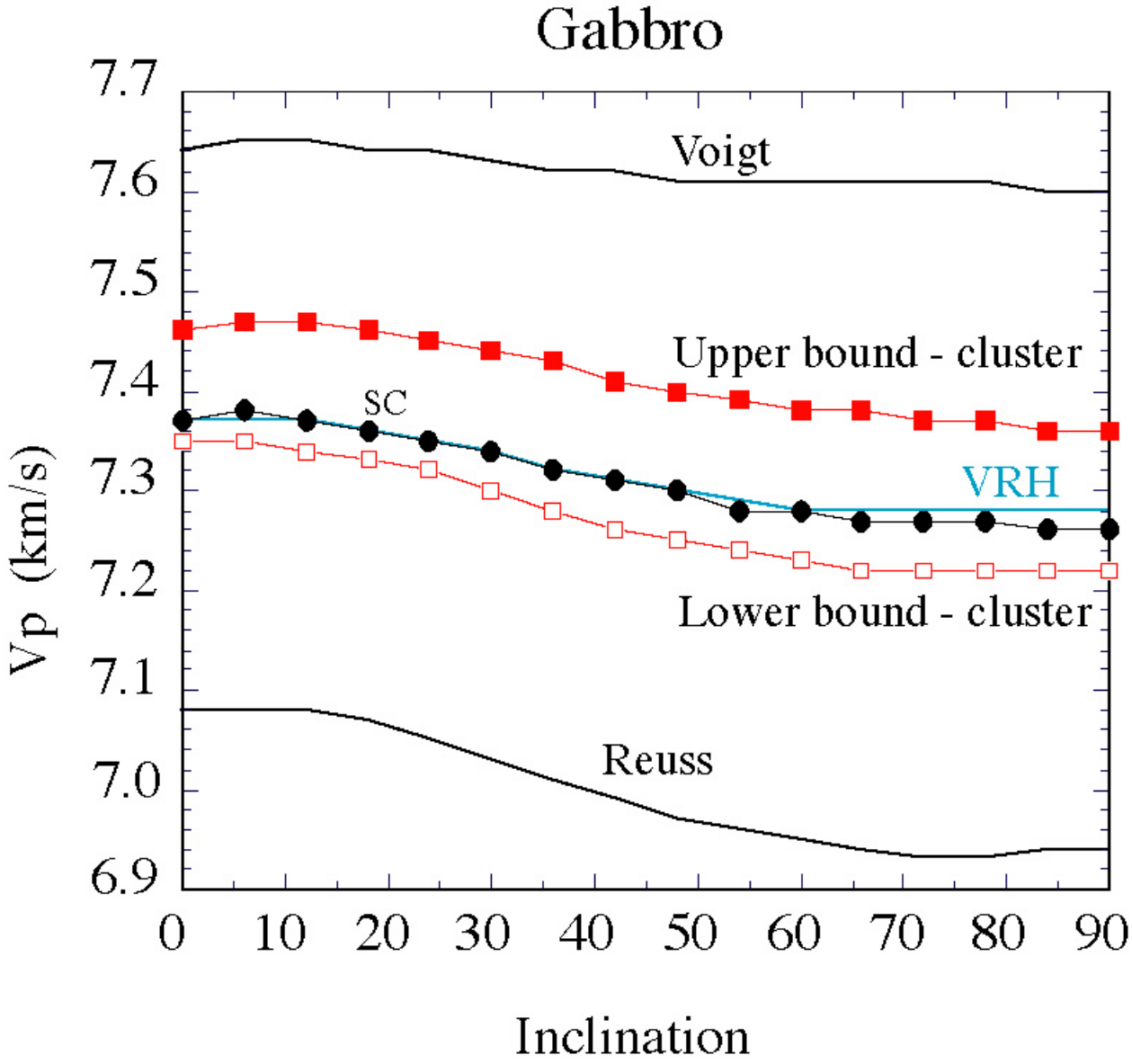

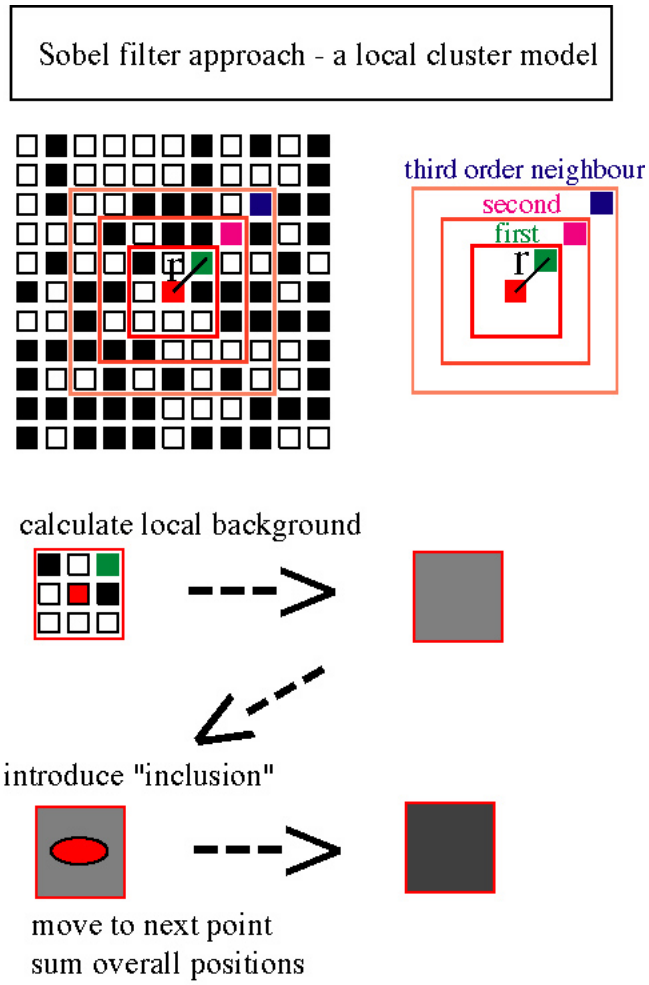

Quantitative texture analysis and calculation of physical properties

- Orientation **g**

- Orientation distribution function (O.D.F.)

- Elastic properties of aggregate

- Extrapolation of elastic constants to Pressure & Temperature

- Extrapolation of density to Pressure & Temperature

Orientation g

Orientation of crystals in a polycrystal can be measured by volume diffraction techniques (e.g. X-ray or neutron diffraction) or individual orientation measurements (e.g. U-stage & Optical microscope, electron channeling or EBSD).

An orientation, often given the letter **g** (gefüge = fabric or structure), of a grain or crystal in sample co-ordinates can be described by the rotation (or orientation) Matrix between crystal and sample co-ordinates. In practice it is convenient to describe the rotation by a triplet of Euler angles, for example $\mathbf{g} = \varphi 1 \phi \varphi 2$ used by Bunge (1982).

N.B. One should be aware there are many different definitions of Euler angles that are used in the physical sciences, here we will use the definition given by Bunge (1982).

Orientation of a crystal defined by 3 Euler angles

XYZ - Specimen Frame

X'Y'Z' - Crystal Frame

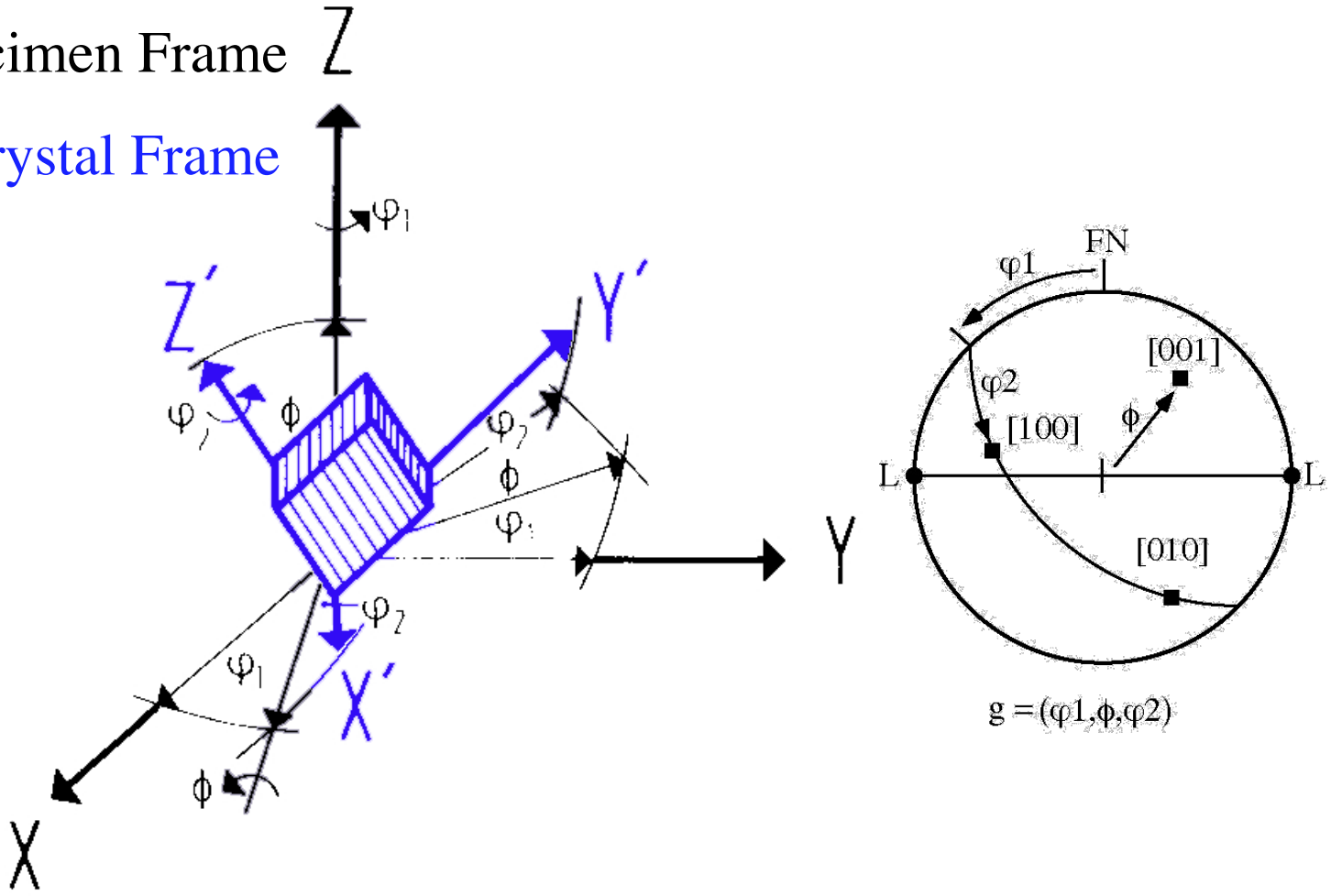

Beware there many different conventions - here the convention of Bunge (1982)

Orientation Distribution Function

The orientation distribution function (O.D.F.) f(**g**) is defined as the volume fraction of orientations with an orientation in the interval between **g** and **g**+d**g** in a space containing all possible orientations given by

$$\Delta V/V = \int f(\mathbf{g})\, d\mathbf{g}$$

where $\Delta V/V$ is the volume fraction of crystals with orientation **g**, f(**g**) is the texture function and $d\mathbf{g} = 1/8\pi^2 \sin\phi\, d\varphi 1 d\phi\, d\varphi 2$ is the volume of the region of integration in orientation space.

The function f(**g**) is given in terms of symmetrical generalized spherical harmonics (Bunge,1982) as

$$f(\mathbf{g}) = \sum_{l=0}^{Lmax} \sum_{m=l}^{M(l)} \sum_{n=-l}^{l} C_l^{mn}\, T_l^{mn}(\mathbf{g})$$

C_l^{mn} are the coefficients of the series development of the texture function f(**g**), $T_l^{mn}(\mathbf{g})$ are the generalised spherical harmonic functions, M(l) is the number of linearly independent harmonics and Lmax is the maximum degree used in the expansion. For tensor properties of rank 2 or 4 the maximum degree of expansion is Lmax=2 or Lmax=4 repectively.

X-ray analysis program !

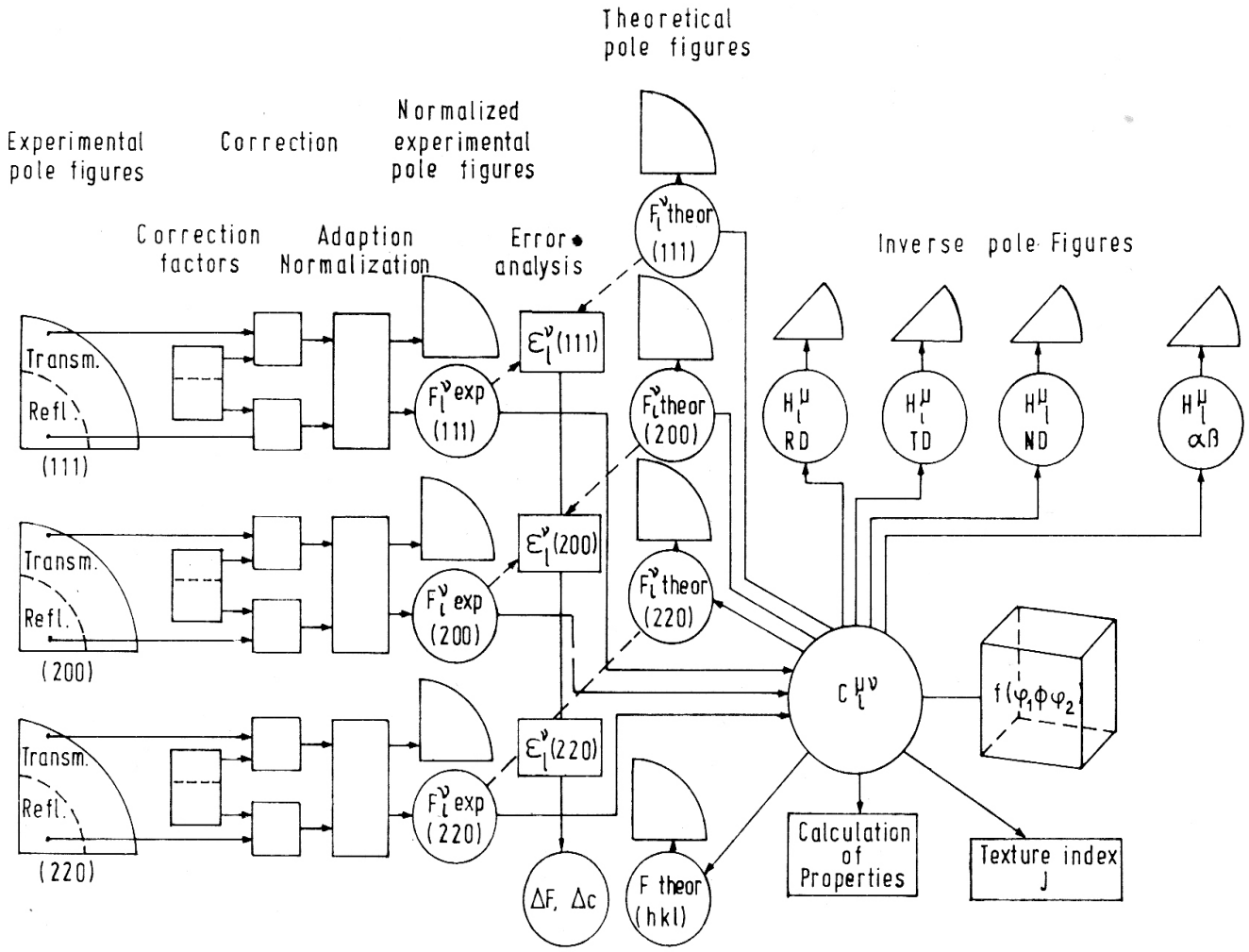

Figure 9.3 Structure of the texture analysis program system[171]

Harmonic Method

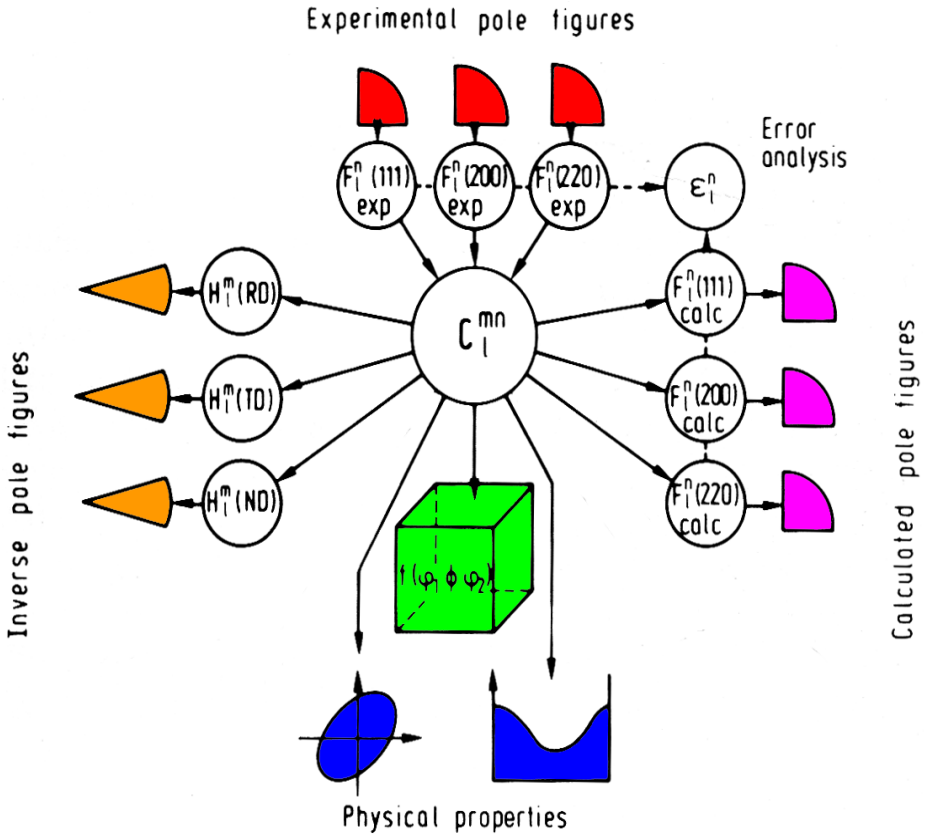

The general scheme of harmonic texture analysis.

Pole figure comparison : FB085 Olivine100 grains (U-stage)

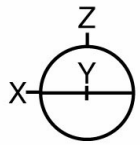

(100) (010) (001)

PF2k
(box counting with
gaussian half-width = 8.5°)

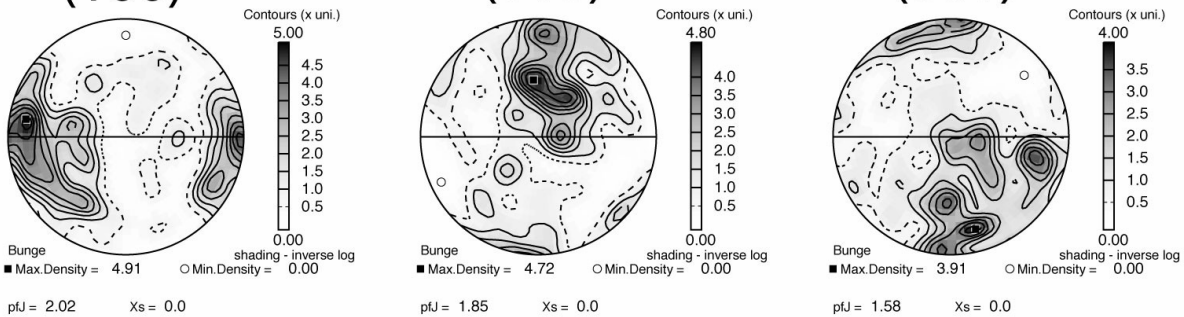

CGRAIN
(SH Even Coeffs Lmax=22
by F.Wagner Metz
gaussian half-width =10°)

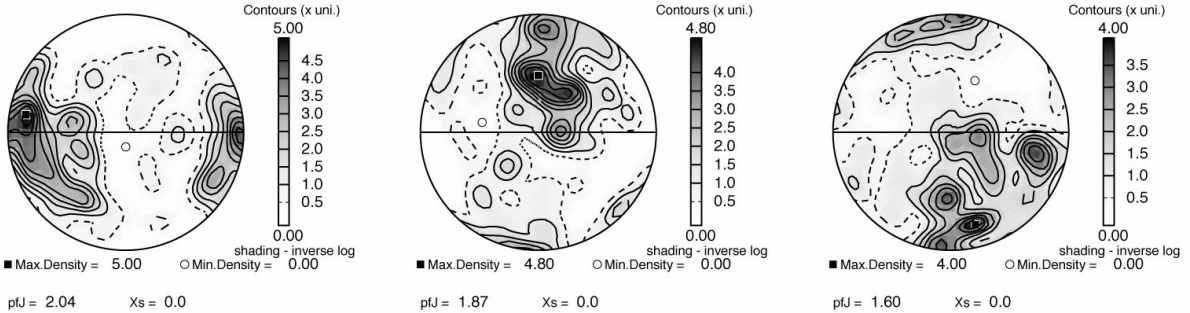

CGRAIN
(SH Even Coeffs Lmax=4
by F.Wagner Metz
gaussian half-width =10°)

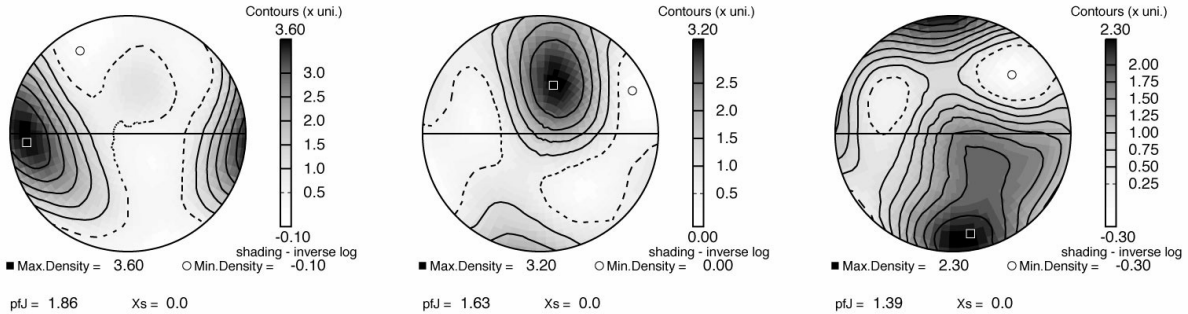

CGRAIN
(SH Even Coeffs Lmax=2
by F.Wagner Metz
gaussian half-width =10°)

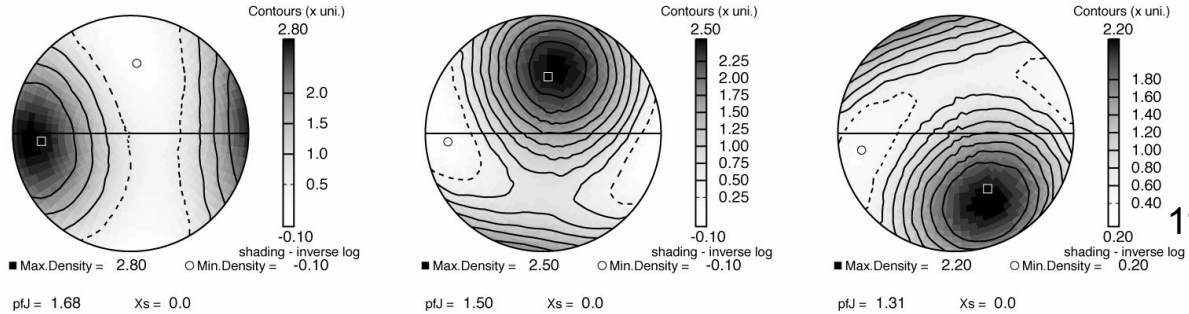

Cartesian references frames: Euler and Tensor 1

A potential complication is the fact that the Cartiesan frame defined by orthogonal crystallographic directions used report elastic tensor of the single crystal many not be the same as those used for Euler angle reference frame used in texture analysis (e.g. MTEX, BearTex ...) or measurement (e.g. EBSD) packages. To account for this difference a rotation may be required to bring the crystallographic frame of tensor into coincidence with the Euler angle frame,

$$C_{ijkl}(\mathbf{g}^E)=T_{ip}.T_{jq}.T_{kr}.T_{lt}\ C_{pqrt}(\mathbf{g}^T)$$

where $C_{ijkl}(\mathbf{g}^E)$ is the elastic property in the Euler reference and $C_{pqrt}(\mathbf{g}^T)$ is the elastic property in the original tensor reference frame, BOTH frames are in crystal co-ordinates.

Cartesian references frames: Euler and Tensor 2

The orthogonal transformation (or rotation) matrix T_{ij} is constructed from the angles between the two sets perpendicular crystallographic axes, forming rows and columns of the matrix (see Nye, 1957).

		Tensor Axes		
		Tx	Ty	Tz
Euler Axes	Ex	T_{11}	T_{12}	T_{13}
	Ey	T_{21}	T_{22}	T_{23}
	Ez	T_{31}	T_{32}	T_{33}

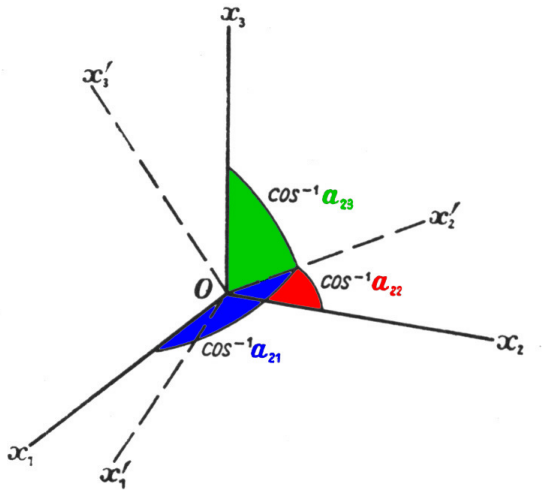

Transformation of axes.

Rotation into specimen co-ordinates

To calculate the seismic properties of a polycrystal, one must evaluate the elastic properties of the aggregate. In the case of an aggregate with a crystallographic fabric, the anisotropy of the elastic properties of the single crystal must be taken into account. For each orientation **g,** the single crystal properties have to be rotated into the specimen co-ordinate frame using the orientation or rotation matrix g_{ij},

$$C_{ijkl}(\mathbf{g}) = g_{ip} . g_{jq} . g_{kr} . g_{lt}\ C_{pqrt}(\mathbf{g}^E)$$

where $C_{ijkl}(\mathbf{g})$ is the elastic property in sample co-ordinates,
$g_{ij} = g(\varphi 1 \phi\ \varphi 2)$ the measured orientation in sample co-ordinates
and Cpqrt($\mathbf{g}^E$) is the elastic property in crystal co-ordinates of the Euler frame (E).

Elastic properties of aggregate

The elastic properties of the polycrystal may be calculated by integration over all possible orientations of the ODF. Bunge (1985) has shown that integration is given as:

$$\langle C_{ijkl} \rangle^m = \int g_{ip} . g_{jq} . g_{kr} . g_{lt} . C_{pqrt}^m(\mathbf{g}^E) . f(\mathbf{g})\, dg = \int C_{ijkl}^m(\mathbf{g}) . f(\mathbf{g})\, dg$$

where $\langle C_{ijkl} \rangle^m$ is the elastic properties of the aggregate of mineral m.

Alternatively it may be determined by simple summation of individual orientation measurements (e.g. U-stage or EBSD),

$$\langle C_{ijkl} \rangle^m = \sum g_{ip} . g_{jq} . g_{kr} . g_{lt} . C_{pqrt}^m(\mathbf{g}^E) . V(\mathbf{g}) = \sum C_{ijkl}^m(\mathbf{g}) . V(\mathbf{g})$$

Where $V(\mathbf{g})$ is the volume fraction of the grain in orientation **g.**

Christoffel equation & Tensor

The final step is the calculation of the three seismic phase velocities by the solution of the Christoffel equation,

$$\left| \langle C_{ijkl} \rangle^{Voigt} n_j n_l - \rho V^2 \delta_{ik} \right| = \left| T_{ik} - \rho V^2 \delta_{ik} \right| = 0$$

where n is the plane wave propagation direction,
T_{ik} is the Christoffel tensor
ρ is the density of the rock,
δ_{ik} is the Kronecker delta and
the three values of V are the three seismic phase velocities.

The calculation is of the three seismic phase velocities from the Christoffel tensor

$$T_{ik} = \langle C_{ijkl} \rangle^{Voigt} n_j n_l$$

where the three eigenvalues E_i of the symmetric Christoffel tensor (T_{ik}) are related to three seismic phase velocities V_i (qP,qS1,qS2) by $V_i = (E_i/\varrho)^{1/2}$, and qS1 > qS2.

Extrapolation elastic constants to PT

To calculate the elastic constants at pressures and temperatures of Earth's interior the single crystal elastic constants are extrapolated to pressure and temperature using the following relationship:

$$C_{ij}(PT) = C_{ij}(P_oT_o) + (dC_{ij}/dP) \,.\, (P-P_o) + 1/2\, (d^2C_{ij}/dP^2) \,.\, (P-P_o)^2 + (dC_{ij}/dT) \,.\, (T-T_o)$$

where Cij (PT) are the elastic constants at pressure P and temperature T,
$Cij(P_oT_o)$ the elastic constants at reference pressure P_o = 0.1 MPa and temperature T_o= 25 °C;
dCij/dP is the first order pressure derivative
and dCij/dT is the first order temperature derivative.

The second order pressure derivatives d^2Cij/dP^2 are available for an increasing number of mantle minerals and first order temperature derivatives seem to adequately describe the temperature dependence of most minerals.

Mg-Perovskite Cij at lower mantle PT

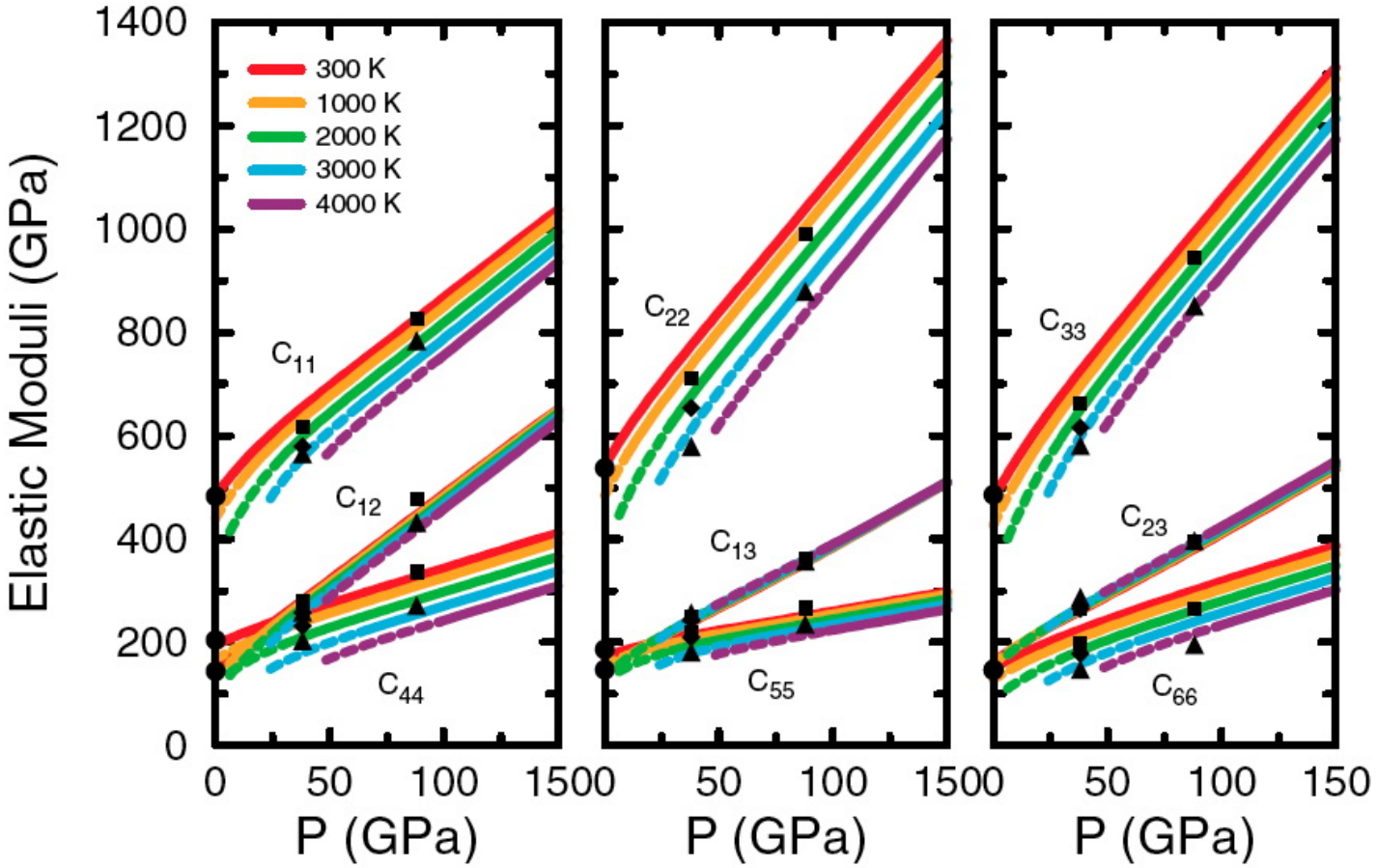

FIG. 1 (color). Pressure dependence of the adiabatic elastic constants of $MgSiO_3$. The line's thickness represents uncertainties caused mainly by the use of the local density approximation (LDA) (see [11]). Full (dashed) lines correspond to results within (outside) the (P, T) regime of validity of the QHA. Measurements are represented by full circles at 0 GPa [5]. Full symbols at $P > 0$ GPa are the results of Oganov *et al.* [4] at 38 and 88 GPa (squares: 1500 K, diamonds: 2500 K, up triangles: 3500 K).

Wentzcovitch_et_al 2004

Extrapolation of density to PT

The seismic velocities also depend on the density of the minerals at pressure and temperature which can be calculated using an appropriate equation of state. The Murnaghan equation of state derived from finite strain is sufficiently accurate at moderate compression (Knittle, 1995) of the upper mantle and leads to the following expression for density as a function of pressure,

$$\rho(P) = \rho_o(1+(K'/K).(P-P_o))^{1/K'}$$

where K is bulk modulus, K' = dK/dP the pressure derivative of K, ρ_o is the density at reference pressure P_o and temperature T_o.

For temperature the density varies as

$$\rho(T) = \rho_o[1-\int \alpha_v(T)\, dT] = \rho_o[1 - \alpha_{av}\,(T-To)]$$

where $\alpha_v(T) = 1/V(\partial V/\partial T)$ is the volume thermal expansion coefficient as a function of temperature and α_{av} is an average value of thermal expansion which is constant over the temperature range (Fei, 1995). According to Watt (1988) an error of less 0.4% on the P and S velocity results from using α_{av} to 1100K for MgO. For temperatures and pressures of the mantle, the density can be described by,

$$(P,T) = \rho_o\{(1+(K'/K).(P-P_o))^{1/K'}[1 - \alpha_{av}\,(T-To)]\ \}$$

Topotactic relationships between olivine and antigorite: Implications for subduction zone seismology and geodynamics

David Mainprice, **Francoise Boudier, Alain Baronnet and Roland Pellenq**

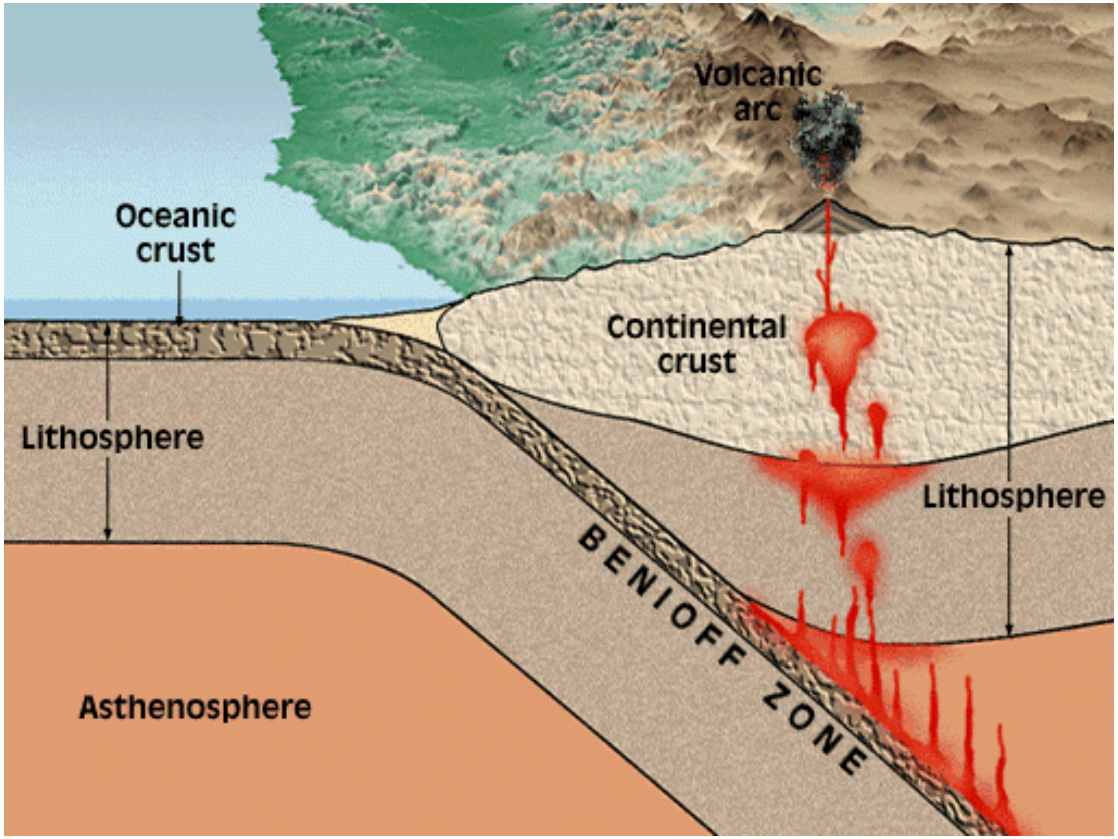

Moses Rock Utah – Farallon plate subduction

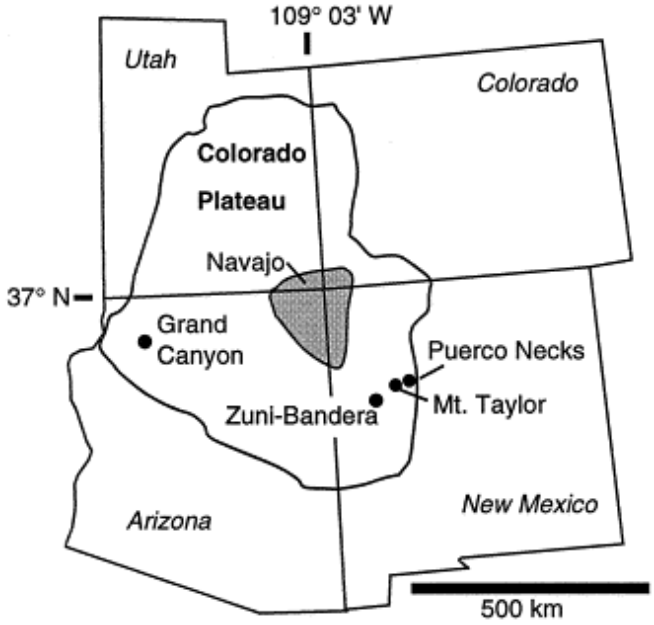

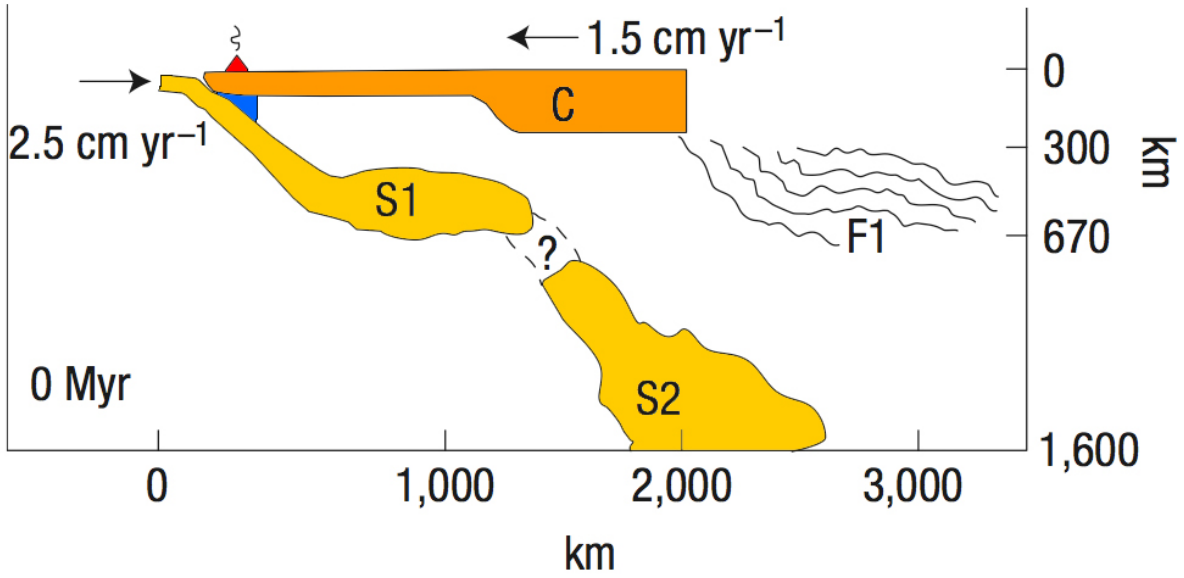

Sigloch et al.08 Nature Geosciences

A sample from a subduction zone

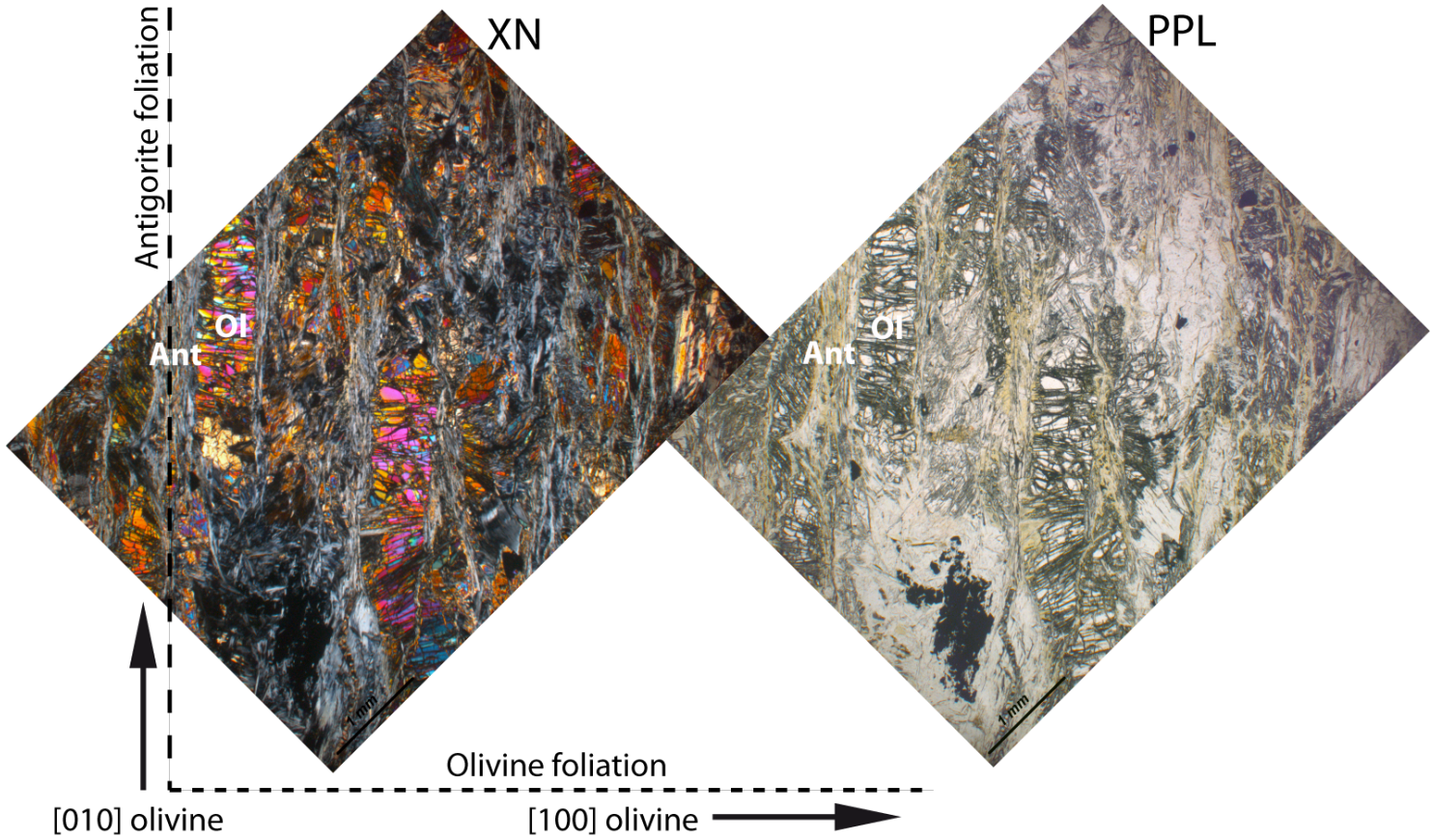

Olivine – Antigorite Schist from Moses Rock, Utah

Phase diagram & Geotherm

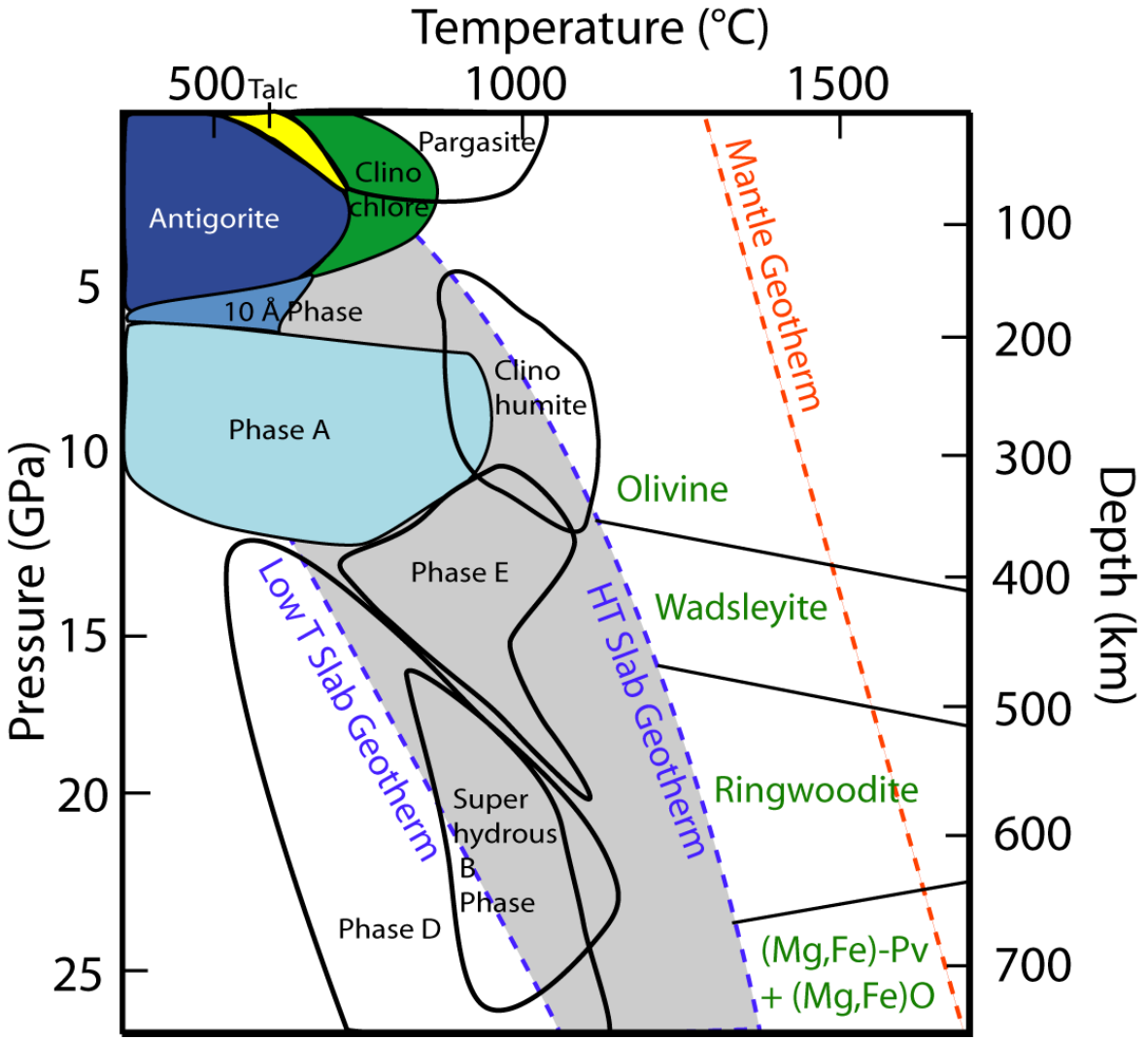

Mainprice and Ildefonse (2009)

Relationship olivine microstructure & CPO

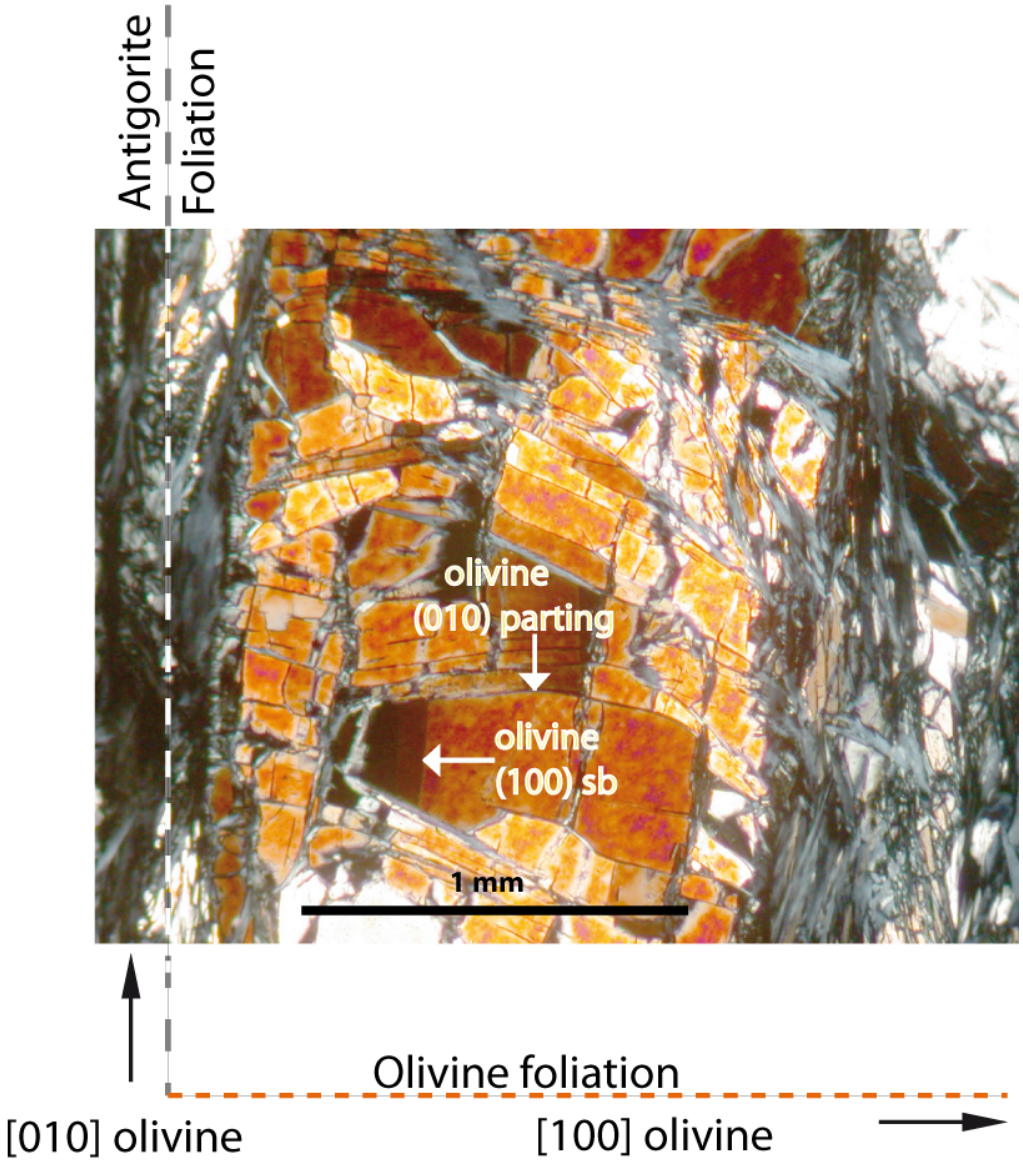

EBSD data

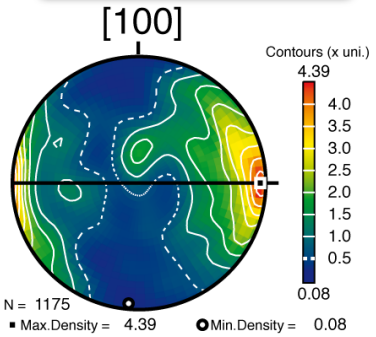

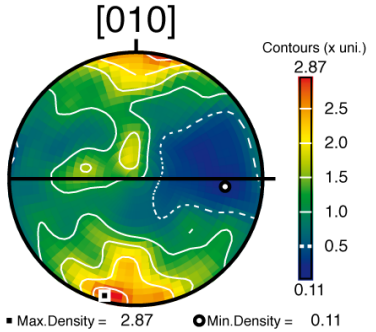

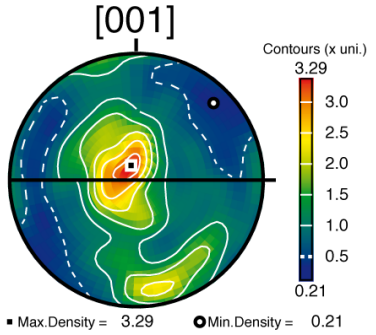

HRTEM
View along [010]atg

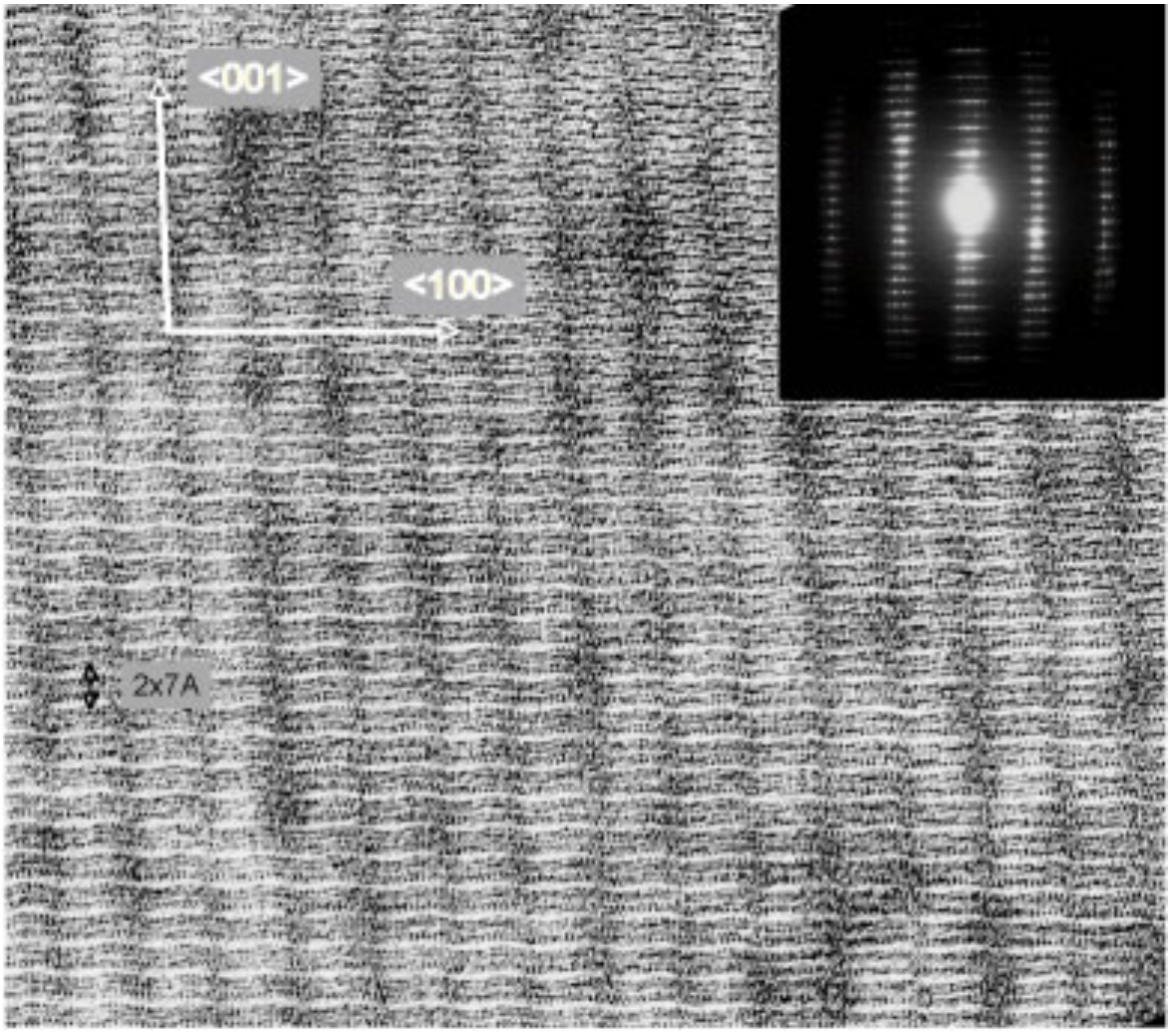

CTEM data

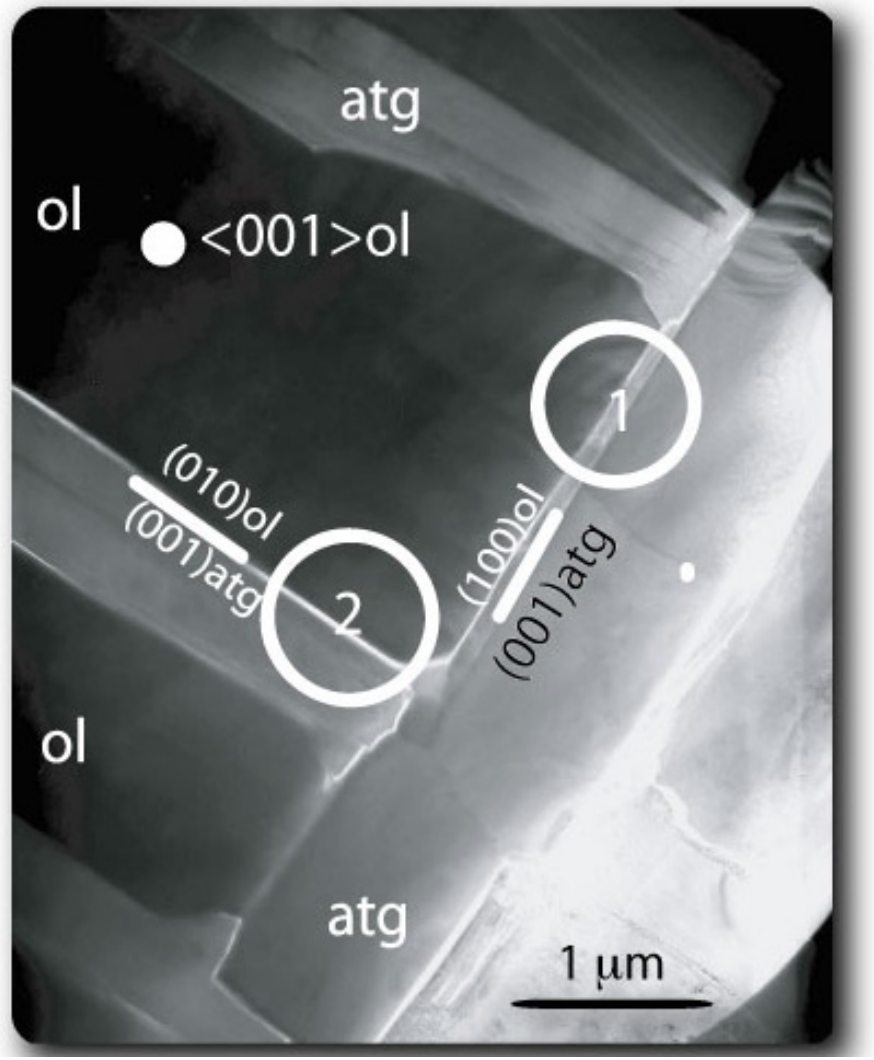

relation 1

$(100)_{Olivine}$ || $(001)_{Antigorite}$

$[001]_{Olivine}$ || $[010]_{Antigorite}$

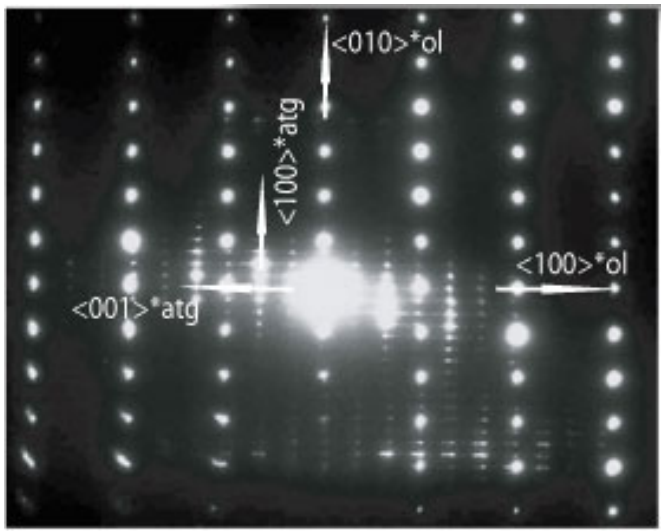

relation 2

$(010)_{Olivine}$ || $(001)_{Antigorite}$

$[001]_{Olivine}$ || $[010]_{Antigorite}$

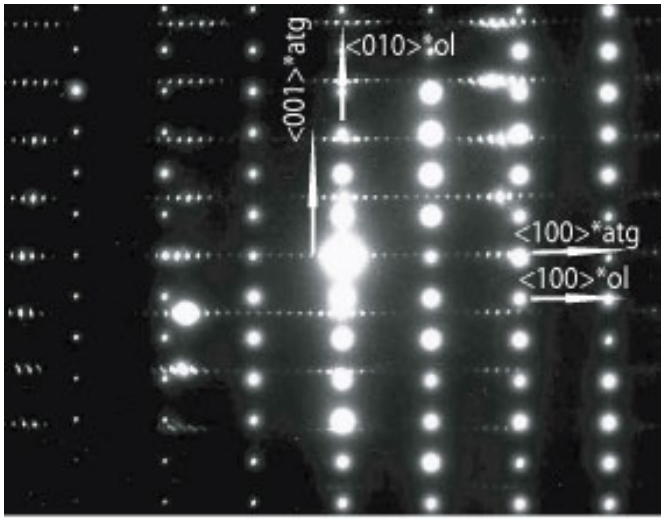

Summary of Olivine – Antigorite Schist

•Hydrated Moses Rock peridotite has classical "A-type" olivine CPO, typical of "dry" olivine, but sample contains hydrated minerals antigorite, chlorite ... Do we need "wet" olivine to explain the subduction zone dynamics ?

•Antigorite has topotactic relationships with olivine,
two types of relations are observed:
(1) (100)ol ll (001)atg with [001]ol ll [010]atg
and (2) (010)ol ll (001)atg with [001]ol ll [010]atg

•Dominant antigorite orientation (1) develops a schistosity perpendicular to the mantle flow fabric of the olivine aggregate

•Develops coeval with hydrous fluid induced micro-cracking controlled by the olivine crystallography:
(010) parting, (100) dislocation walls, fast hydrogen diffusion ll [100]

Crystallographic relationships

Misorientation Δ g between lattices : olivine - antigorite

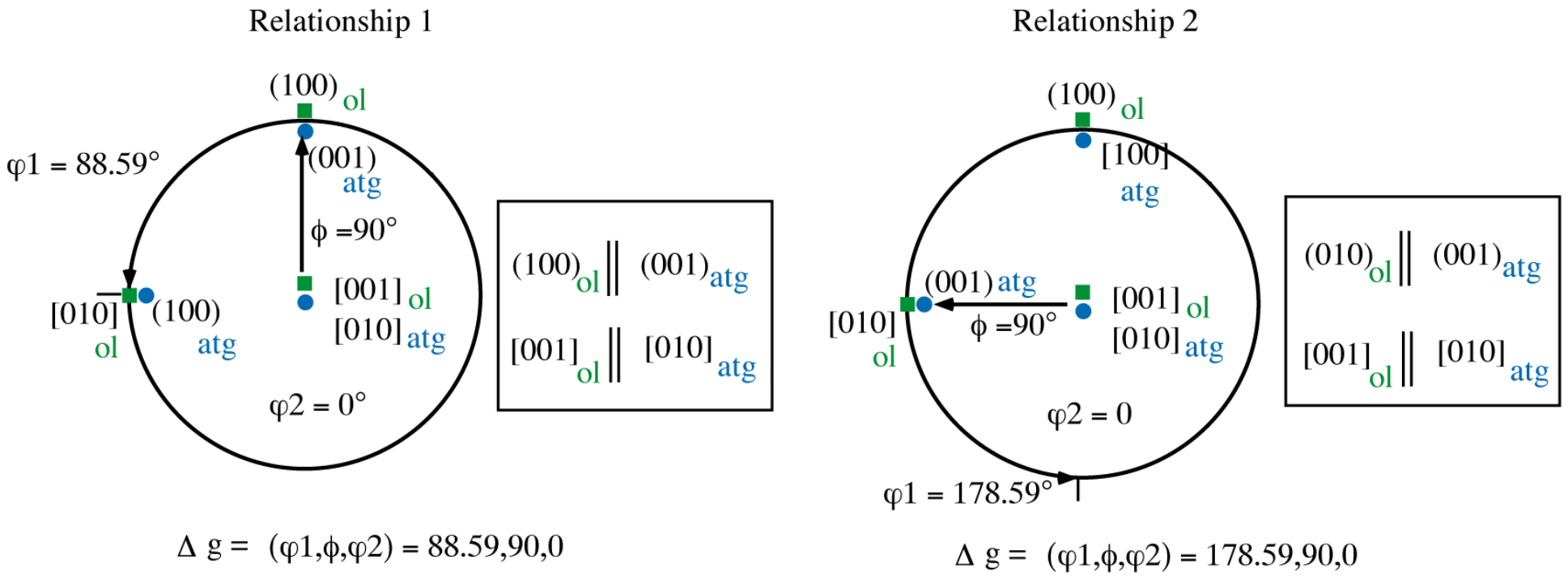

Antigorite has topotactic relationships with olivine, two types of relations are observed:

(1) (100)ol ll (001)atg with [001]ol ll [010]atg

and (2) (010)ol ll (001)atg with [001]ol ll [010]atg

Calculate antigorite orientation from olivine

$$g_{n=1\text{ to }4}^{Antigorite} = \Delta g \bullet S_n^{Olivine} \bullet g^{Olivine}$$

SEISMIC

IMPLICATIONS

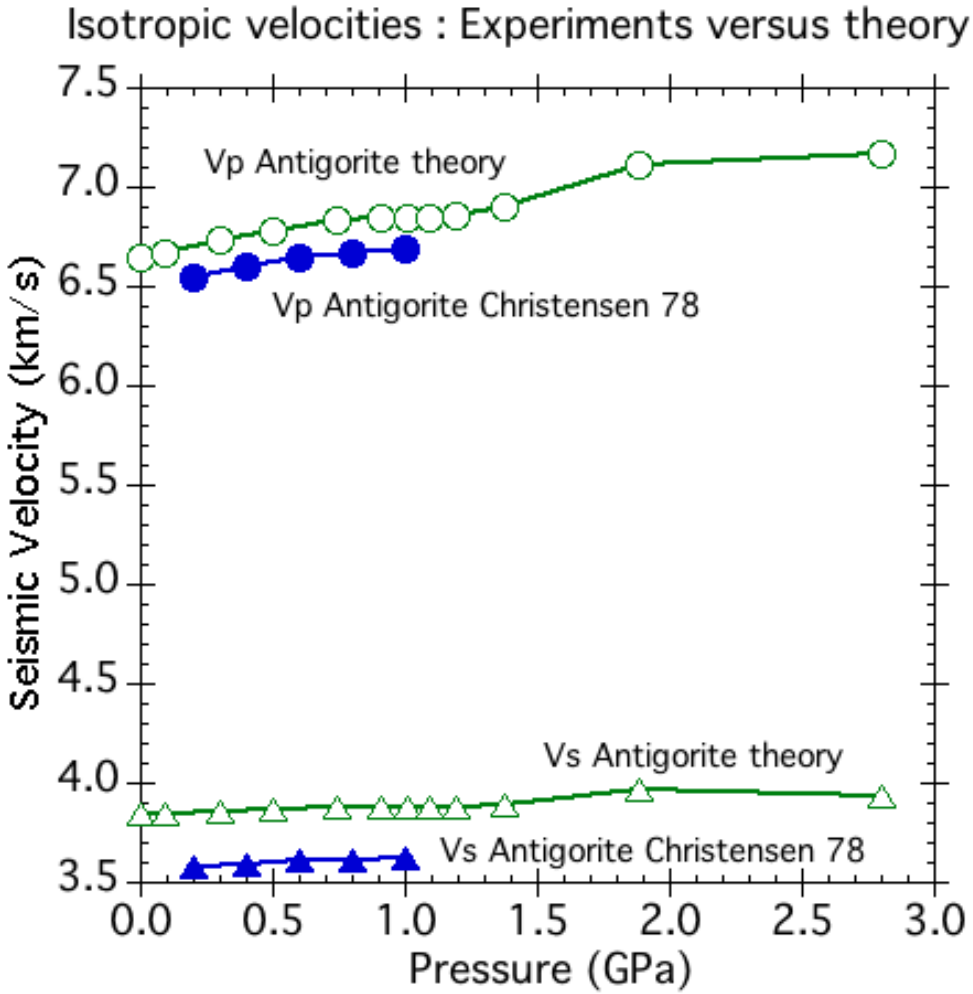

a) Experimentally Lizardite and Antigorite have different velocities (Christensen,2004,1978,1966).

b) Agreement of Antigorite elastic contants of Pellenq et al. (GULP) with experimental data is good.

Shear Wave Splitting

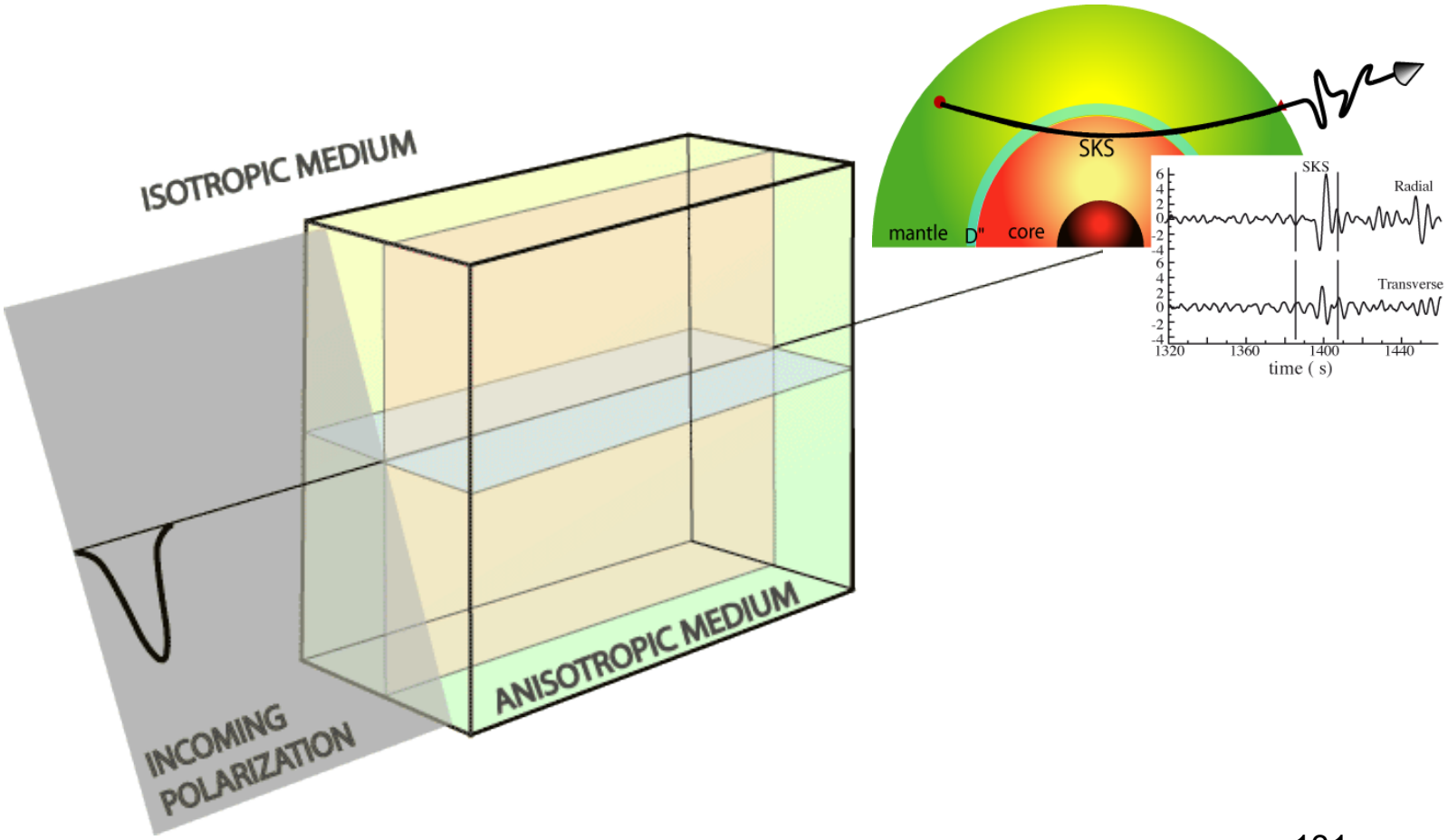

http://garnero.asu.edu

ANTIGORITE MODEL for Moses rock schist

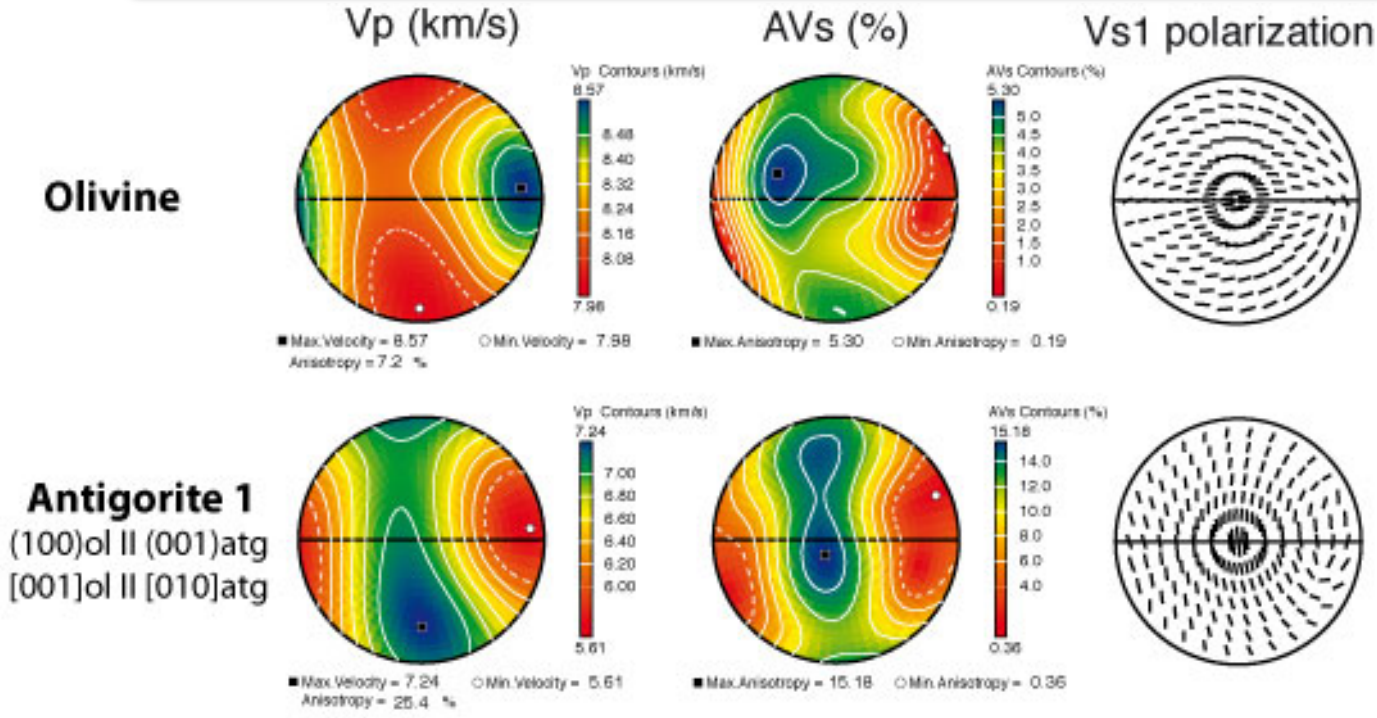

Thickness=100.dt.<Vs>/Avs

dt=0.25 - 1.0s
<Vs>=4.19 km/s
AVs=10%
Thickness (dt 1.0s)=41.9 km
(dt=0.25s)=10.5 km

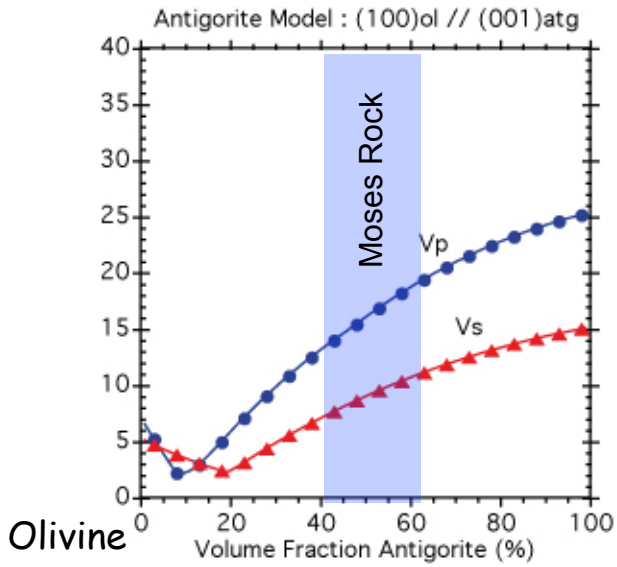

Overview of Serpentine contribution to anisotropy

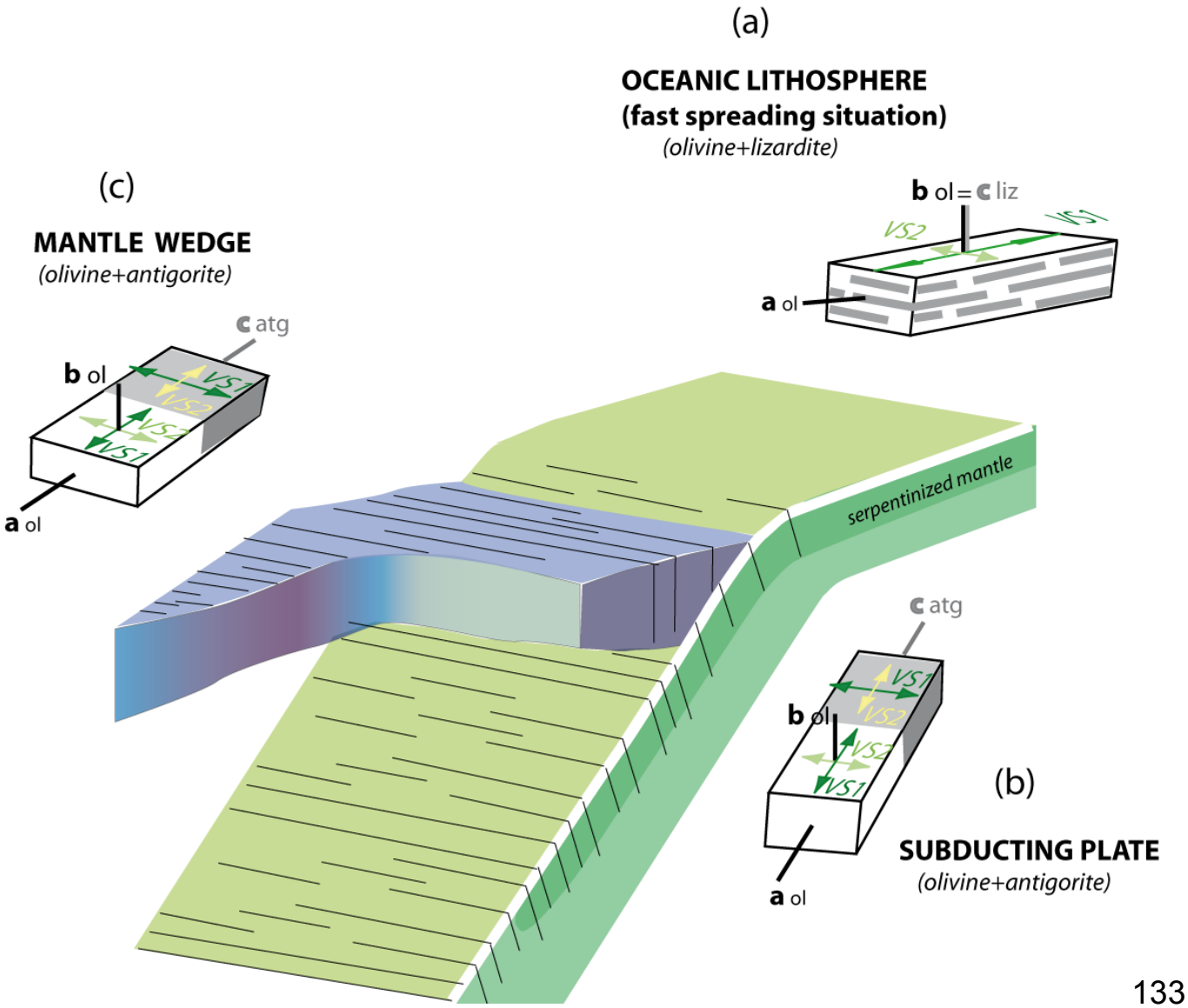

ANTIGORITE MODEL : mixture of Antigorite 1 & 2 (100% antigorite)

Z – vertical S-waves
X & Y in horizontal plane

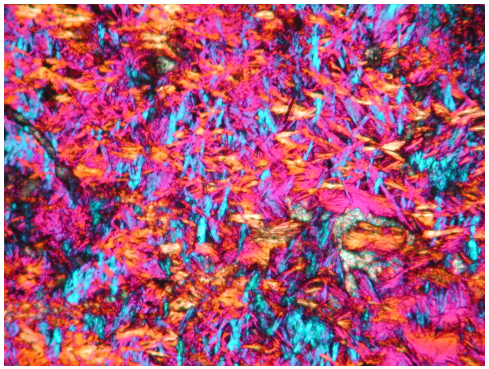

Orange – Atg(001) EW
Blue – Atg(001) NS

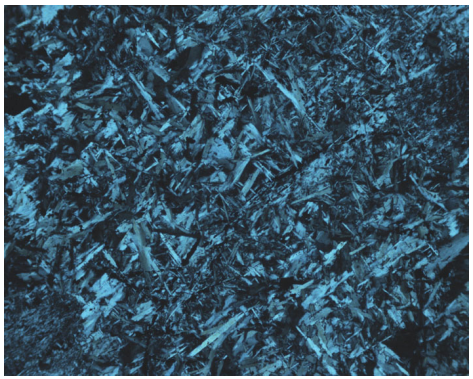

N.I. Christensen (per.comm.)

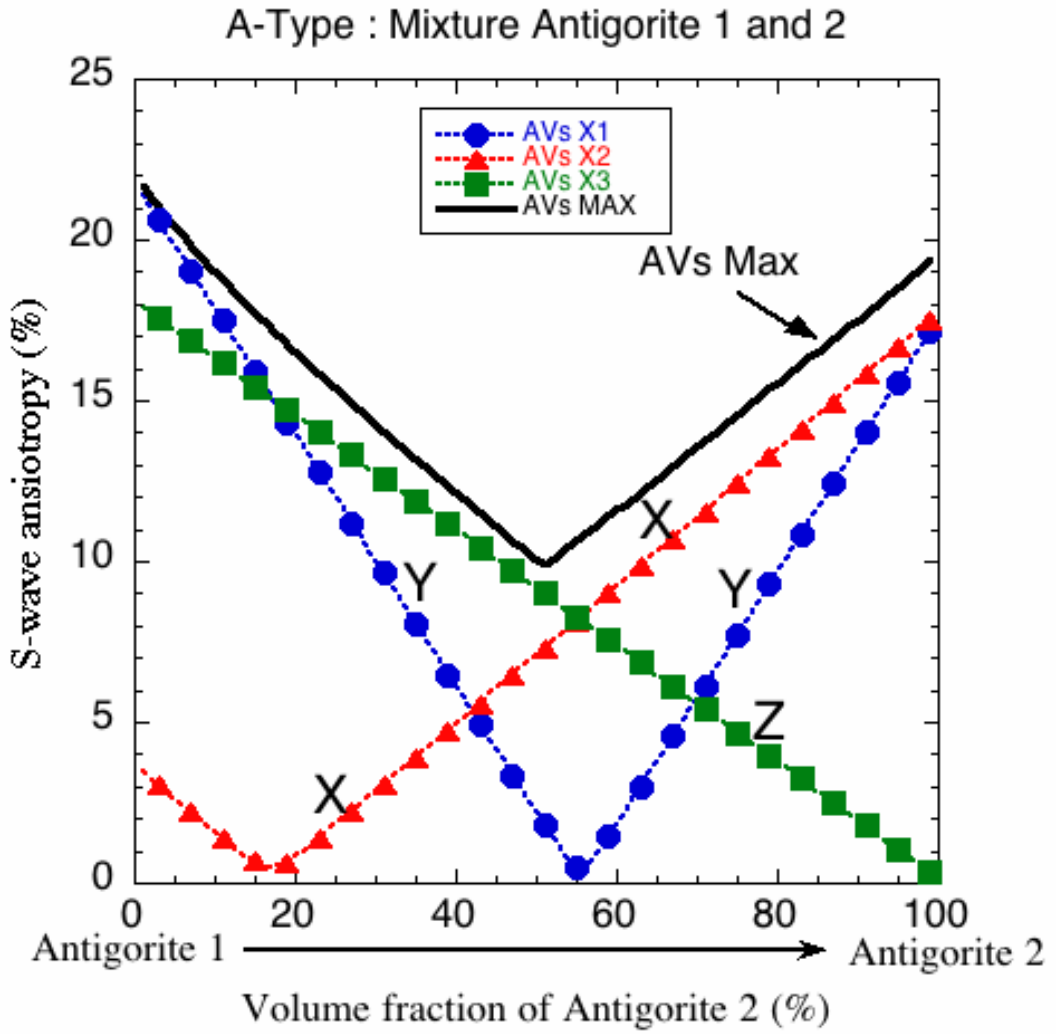

100% Antigorite type 2 (100)ol ll (001)atg would result in ZERO vertical (Z direction) anisotropy

Mantle wedge S-wave anisotropy

a) Trench parallel in western Pacific (Japan, Ryuku, Marianas & Tonga).

b) Trench normal in northern Pacific (Kamchatka & Alaska).

c) *Low or no anisotropy in Aleutians, Central and South America = warm lithosphere*

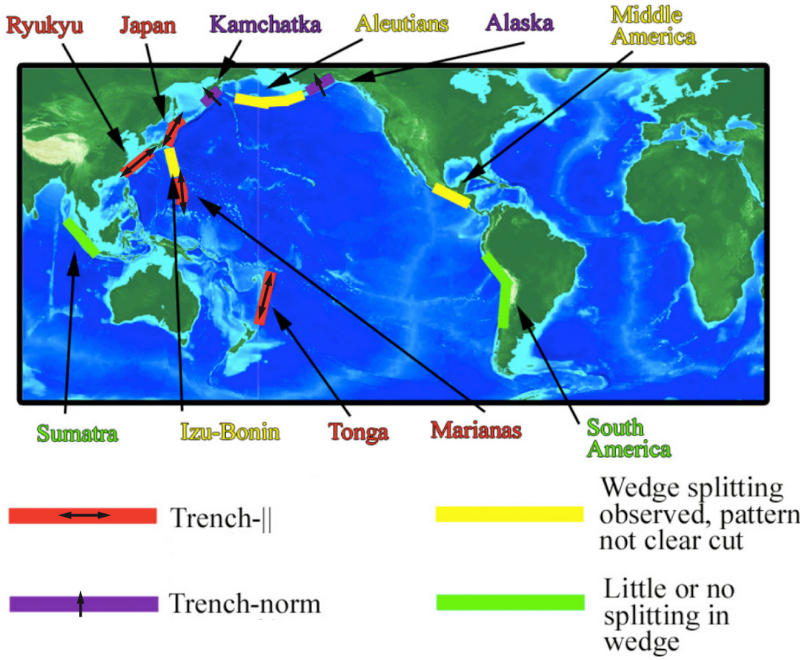

After Long & Silver (2008) Science

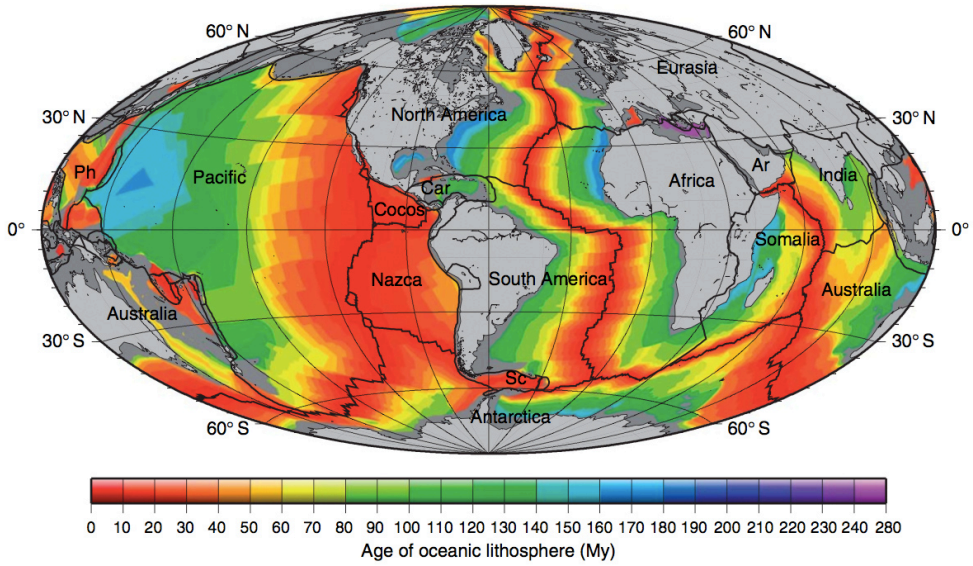

Müller et al (1997)

Summary of Seismic results

•Using type (1) (100)ol ll (001)atg antigorite topotactic relationships with olivine produces TRENCH PARALLEL anisotropy for "A-type" olivine CPO, (as suggested by Moses Rock sample), with the correct order of magnitude to explain seismic delay times of 1s in the Mantle wedge.

•Using type (2) (010)ol ll (001)atg antigorite topotactic relationships with olivine produces ZERO vertical anisotropy for "A-type" olivine at 100% antigorite, which may explain subduction of young (warm) slabs on western Mexico and South America with no clear anisotropy and probably high Antigorite volume fractions.

•Why type (1) or type (2) may be favoured is not yet determined... But you can have both !